1988

The Parabrachial Nucleus in the Rat: An Immunhistochemical Study of Its Forebrain Neural Input

Margaret M. Moga
Loyola University Chicago

THE PARABRACHIAL NUCLEUS IN THE RAT:

AN IMMUNHISTOCHEMICAL STUDY OF ITS FOREBRAIN NEURAL INPUT

By

Margaret M. Moga

A Dissertation Submitted to the Faculty of the Graduate School

of Loyola University of Chicago in Partial Fulfillment

of the Requirements for the Degree of

Doctor of Philosophy

May

1988

ACKNOWLEDGEMENTS

I would like to thank my family, especially my mother, for their tremendous support during this venture; my advisor, Dr. Thackery S. Gray, for his support and advice; my co-workers, Andrea Zardetto-Smith and Debra Magnuson, for their help, and my lab-mates at the University of Chicago, Karen Hurley, Rodney Holmes, Horst Herbert, Quan Ha and Chris Breder, for their friendship and interest.

I would also like to thank my committee members, Dr. Castro, Dr. Neafsey, Dr. Wurster and Dr. Saper; their comments and criticisms were extremely helpful and much appreciated and it was a pleasure working with them. I am especially grateful to Dr. Saper for the opportunity to work in his lab, and to my advisor, Dr. Gray, for giving me the opportunity to do so.

Many other members of the Anatomy Department provided me with technical and secretarial assistance and/or moral support. Though too many to name, I'd like to thank in particular: Genevieve Fitzgibbon, Rosemarie Sarno, Linda Fox, Judy Maples, Carl Sievert and Hisham Mostafa.

VITA

The author, Margaret M. Moga, was born on October 4, 1955 in Evanston, Illinois.

Her secondary education was received at Lake Forest High School in Lake Forest, Illinois, from which she graduated in June of 1973. In September of that year she entered Knox College in Galesburg, Illinois and graduated with a Bachelor of Arts degree in June of 1977. Following graduation, she was employed as a Systems Engineer at the IBM Corporation for five years. In August of 1982, she entered the Department of Anatomy at Loyola University of Chicago in Maywood, Illinois. While in the Department of Anatomy, she received a Basic Science Fellowship and taught in the gross anatomy and neuroscience courses. At Loyola, she has been active on the Graduate Student Council and the Committee on Student Life. She is a member of the Society for Neuroscience, the American Association of Anatomists and the Society of Sigma Xi.

TABLE OF CONTENTS

LIST OF TABLES

LIST OF FIGURES

ABBREVIATIONS

ac	anterior commissure
ACTH-ir	adrenocorticotropin-immunoreactivity
AII-ir	angiotensin II-immunoreactivity
ARC	arcuate nucleus
AVP-ir	vasopressin-immunoreactivity
AVPV	anteroventral periventricular nucleus
B	basal nucleus of Meynert
BAC	bed nucleus of the anterior commissure
BL	basolateral nucleus of the amygdala
BST	Bed nucleus of the stria terminalis and subnuclei
	AL anterior lateral subnucleus
	AM anterior medial subnucleus
	DL dorsal lateral subnucleus
	IM intermediate subnucleus
	JXC juxtacapsular subnucleus
	PI posterior intermediate subnucleus
	PL posterior lateral subnucleus
	PM posterior medial subnucleus
	PO preoptic subnucleus
	SC supracapsular subnucleus
	VL ventral lateral subnucleus
	VM ventral medial subnucleus
BSTL	bed nucleus of the stria terminalis, lateral subdivision

CCK-ir	cholecystokinin-immunoreactivity
Ce	central nucleus of the amygdala
CeL	central nucleus of the amygdala, lateral subdivision
CeM	central nucleus of the amygdala, medial subdivision
CRF-ir	corticotropin releasing factor-immunoreactivity
DB	horizontal nucleus of the diagonal band
DMH	dorsomedial hypothalamus
DVC	dorsal vagal complex
DYN-ir	dynorphin-immunoreactivity
ec	external capsule
ENK-ir	enkephalin-immunoreactivity
f	fornix
FStr	fundus striati
fx	fornix
GAL-ir	galanin-immunoreactivity
GP	globus pallidus
I	intercalated nuclei of the amygdala
ic	internal capsule
KF	Kolliker-Fuse nucleus
La	lateral nucleus of the amygdala
LH	lateral hypothalamus
LoC	locus coeruleus
LPO	lateral preoptic area
Me	medial nucleus of the amygdala
MgPO	magnocellular preoptic nucleus
MnPO	median preoptic nucleus

mnt	mesencephalic nucleus and tract of the trigeminal nerve
MPO	medial preoptic nucleus
MS	medial septal nucleus
MSH-ir	alpha-melanocyte stimulating hormone-immunoreactivity
mt	mammillothalamic tract
NT-ir	neurotensin-immunoreactivity
NTS	nucleus of the solitary tract
oc	optic chiasm
ot	optic tract
OXY-ir	oxytocin-immunoreactivity
PB	parabrachial nucleus
PBl	lateral parabrachial nucleus
PBm	medial parabrachial nucleus
PH	posterior hypothalamus
POMC	proopiomelanocortin
PS	parastrial nucleus
PVH	paraventricular hypothalamus and subnuclei
	dp dorsal parvocellular subnucleus
	lp lateral parvocellular subnucleus
	mp medial parvocellular subnucleus
	pm posterior magnocellular subnucleus
	pv periventricular subnucleus
RCh	retrochiasmatic area of the hypothalamus
Rt	reticular nucleus of the thalamus
scp	superior cerebellar peduncle
SHy	septohippocampal nucleus

SI	substantia innominata
SO	supraoptic nucleus of the hypothalamus
SP-ir	substance P-immunoreactivity
SS-ir	somatostatin-immunoreactivity
st	stria terminalis
VMH	ventromedial hypothalamus
VMT	ventromedial nucleus of the thalamus
vst	ventral spinocerebellar tract
ZI	zona incerta

CHAPTER I

INTRODUCTION

The parabrachial nucleus (PB), located in the pontine region of the brainstem, has historically been associated with taste and feeding. Recently, physiological studies have implicated the PB in a number of other visceral/autonomic functions, including: pain, bladder control, thirst, and cardiovascular and respiratory responses. Anatomical studies have demonstrated that the PB is extensively connected with autonomic nuclei in both the forebrain and lower brainstem. Based on these responses and connections, investigators have proposed a pivotal role for the PB in the central regulation of autonomic function.

Like other central autonomic nuclei, the PB contains a high density of neuropeptide-immunoreactive cells and fibers. Microinjections of neuropeptides into autonomic nuclei, such as the PB, produce a variety of visceral effects. Possibly the neuropeptides present in the PB may be important in mediating its visceral responses. As a first step to understanding the role of neuropeptides in the PB, this dissertation sought to determine the sources of peptidergic input to the PB using the combined retrograde tracer-immunohistochemical method.

As the number of neuropeptides and the number of PB pathways is quite large, the scope of this dissertation is limited to an examination of the neuropeptides in forebrain afferents of the PB. The

peptidergic content of these afferents is almost entirely unknown. Furthermore, these forebrain projections to the PB and their intrinsic neuropeptides have been implicated in the control of visceral functions, such as respiratory and cardiovascular responses (e.g., Harper et al., '84).

The PB receives input from four major areas in the forebrain: the central nucleus of the amygdala (CeA), the bed nucleus of the stria terminalis (BST), the hypothalamus and the cortex. All of these areas contain neuropeptide-like immunoreactive cells and fibers. However, in preliminary experiments, neuropeptide-immunoreactive cells in the cortex were not found to contribute to the cortical-PB pathway. Many of the immunoreactive neurons in the insular and infralimbic cortices did not have the appearance of pyramidal cells (i.e., PB projecting cells); these cells may instead represent local projection neurons. Thus, this dissertation specifically examines, in three series of experiments, the peptidergic pathways from the CeA, BST and hypothalamus to the PB. In all experiments, the combined retrograde fluorescence-immunofluorescence method was used (Sawchenko and Swanson, '81).

Antisera to the neuropeptides were chosen based on the following criteria: one, the abundance of the antisera-stained cells in the nucleus projecting to the PB; two, the staining quality of the antisera; and three, the presence of antisera-stained fibers in the PB. Neuropeptides previously described in a forebrain pathway to the PB were not re-examined. As a control for antisera specificity, antisera were preincubated with their respective, synthetic neuropeptides, and

the sections processed as usual to determine whether any residual staining remained. Although immunohistochemical staining was eliminated in these controls, it is possible that these antisera may recognize unidentified neuropeptides containing similar amino acid sequences. Therefore, the neuropeptide immunoreactivity described in the following experiments is more accurately described as neuropeptide-like immunoreactivity (-ir), reflecting our uncertainty as to the precise targets of the antisera.

In the first series of experiments (Chapter III), neurons in the central nucleus of the amygdala that project to the PB were examined for their peptide content using antisera to the neuropeptides, corticotropin releasing factor (CRF), neurotensin (NT), somatostatin (SS) and proenkephalin (ENK). These antisera were chosen because neurons which stain for these antisera are particularly numerous in the CeA. Substance P-like immunoreactive neurons are also abundant in the CeA but their contribution to the CeA-PB pathway has been previously reported (Milner and Pickel, '86b).

In the second series of experiments (Chapter IV), neurons in the bed nucleus of the stria terminalis that project to the PB were examined for their peptide content. The BST and CeA are considered by some investigators to be one anatomical entity (e.g., DeOlmos et al., '85). To compare the peptidergic projections of the BST and CeA, I used similar antisera in both experiments. Like the CeA, CRF-ir, NT-ir, SS-ir and ENK-ir neurons are the most numerous of the neuropeptide-like immunoreactive neurons in areas of the BST which project to the PB.

In the third series of experiments (Chapter V), I examined the projection from the hypothalamus to the PB for its peptide content using antisera to a wide variety of neuropeptides: CRF, NT, SS, dynorphin, met-enkephalin, oxytocin, vasopressin, angiotensin II, galanin, alpha-melanocyte stimulating hormone, and adrenal corticotropin hormone. This large number of antisera was used in the hopes of finding a "major" (i.e., predominant) putative neurotransmitter in the hypothalamic projection to the PB, and also, of determining any differences in the peptidergic projections from different hypothalamic nuclei.

Modifications to the combined retrograde fluorescence-immunofluorescence technique were made during the course of these experiments. Preincubation with either Triton-X and/or normal goat serum prior to the incubation with the primary antibody was found not to be necessary and so, was excluded in the later experiments. Early experiments used a rhodamine-conjugated secondary antibody, whereas later experiments used a biotinylated secondary antibody followed by Texas Red-conjugated avidin. This was done for two reasons: one, subsequent lots of the rhodamine-conjugated antibody were not as brightly staining or as reliable, and the avidin-biotin-Texas Red complex produced a consistent, brightly-stained material which was more resistant to fading. In addition, the anesthetic was changed from sodium pentobarbital to chloral hydrate because increments of chloral hydrate could be added as needed with little risk to the survival of the animal. Fluoro-gold, a retrograde fluorescent tracer, became available during the course of these experiments and was used in a few

animals. During the BST and hypothalamus experiments, a fluorescent plotting system became available. With this system, multiple, actual sections could be and were easily plotted.

CHAPTER II

REVIEW OF RELATED LITERATURE

Historical perspective. A structure homologous to the parabrachial nucleus in mammals was first described in cyprinoid and siluroid fishes by Herrick ('05). He termed this homologous structure the superior secondary gustatory nucleus (SSGN), thus recognizing its importance in the central gustatory pathways. In cyprinoids and siluroids, the central gustatory pathways are particularly well developed and yet, are uncomplicated by the development of other systems; hence, they provide a model for the study of the gustatory pathways, and in particular the parabrachial nucleus, in higher vertebrates. In the fish, Herrick ('05) found that gustatory afferents reach the brain over the facial, glossopharyngeal and vagus nerves and that these afferents terminate in the nucleus of the solitary tract (NTS). From the NTS, secondary gustatory fibers ascend ipsilaterally to the SSGN in the dorsal isthmus region. The SSGN in fish is a circular structure encapsulated by a dense layer of heavily myelinated fibers passing downward from the cerebellum, and shows little intrinsic organization. Herrick ('05) noted two types of cells within the SSGN: the 'intrinsic' neuron, located in the center of SSGN and projecting to the contralateral SSGN; and the tertiary gustatory neuron, located along the perimeter of SSGN and projecting to the ventral diencephalon.

This pattern of gustatory connections (i.e., periphery to NTS to SSGN/PB to ventral diencephalon) is apparently maintained in amphibians and reptiles (Barnard, '36; Herrick, '44, '48). Early studies in mammals (Allen, '23; Barnard, '36) were unsuccessful in detecting similar gustatory pathways. Using the Marchi degeneration method after lesions of the NTS and/or neighboring nuclei gracilis and cuneatus in the guinea pig, Allen ('23) noted degenerating fibers coursing ventromedially in an arc to the medial lemniscus of the opposite side. These degenerating fibers were seen to terminate in the ventral portion of the dorsal thalamus. Similarly in the mouse, Barnard ('36) also noted fibers solely in the medial lemniscus after NTS lesions. Furthermore, he could find no evidence for a secondary visceral or gustatory nucleus. He supposed that the reduction in a synapse in the central gustatory pathways in mammals was due to 'the general process of greater cephalization'. Consequently, for over half a century, it was assumed that in mammals secondary gustatory fibers ascended with somatic fibers in the medial lemniscus to the thalamic 'taste area' (Ranson, '36; Zeman and Innes, '63; Burton and Benjamin, '71).

Beginning in 1971, Norgren and his colleagues reevaluated the central gustatory pathways in mammals using a more sensitive anterograde degeneration technique. After lesions in the rostral NTS, Norgen and Leonard ('71) found a concentration of degenerating fibers in the pontine tegmentum surrounding the superior cerebellar peduncle. Electrical recording from neurons in this area demonstrated that they receive gustatory input from both the anterior and posterior portions

of the tongue (Norgren and Pfaffmann, '75). Lesions of this 'pontine taste area' produced degenerating fibers in the previously identified lingual-taste area in the ventrobasal thalamus (Norgren and Leonard, '71). Later studies, using the tracers horseradish peroxidase (HRP) and tritiated amino acids, showed that neurons in PB project not only to the taste area of the thalamus but also to the caudal lateral hypothalamus, substantia innominata, central nucleus of the amygdala and bed nucleus of the stria terminalis (Norgren and Leonard, '73; Norgren, '74; Norgren, '76; Saper and Loewy, '80). Furthermore, physiological studies have found that many of these PB projections to the forebrain contain gustatory information (Norgren, '74,'76). From these studies, the central organization of the mammalian gustatory system was found to closely resemble the gustatory system first described by Herrick in the fish.

Anatomical relations. A number of anatomical studies of the mammalian PB followed the work of Norgren and his colleagues. In the rat, the parabrachial nucleus (PB) surrounds the superior cerebellar peduncle (scp) in the dorsolateral pons. Traditionally, the PB has been divided into medial and lateral subdivisions; these are, respectively, medial and lateral to the scp (Saper and Loewy, '80). Rostrally, neurons in the PB first appear dorsal and lateral to the scp and caudal to the main body of the pedunculopontine nucleus. Rostral PB is bordered dorsally by the cuneiform nucleus, laterally by the lateral lemniscus, and ventrally by the pontine reticular formation. The medial border of rostral PB includes the central gray, the

dorsolateral tegmental nucleus, and the mesencephalic tract and nucleus of the trigeminal nerve (Mes5).

The caudal half of PB begins as the inferior colliculus separates from the dorsal pons. Caudal PB is bordered dorsally and laterally by the ventral spinocerebellar tract, ventrally by the supratrigeminal nucleus and pontine reticular formation, and medially by Mes5 and the trochlear nerve. Caudal PB is also in close proximity to the fourth ventricle, the locus coeruleus and the motor nucleus of the trigeminal nerve. PB is replaced caudally by the vestibular nuclei.

The Kolliker-Fuse nucleus (KF), situated ventral and lateral to the main body of the PB, is also considered to be a part of the parabrachial nucleus (Saper and Loewy, '80; Fulwiler and Saper, '84). KF is bordered medially by the supratrigeminal nucleus, ventrally by the principal sensory nucleus of the trigeminal nerve, and laterally by the middle cerebellar peduncle.

Cytoarchitecture. In a study of PB cytoarchitecture in the rat, Fulwiler and Saper ('84) demonstrated that the PB is composed of ten cytologically distinct subnuclei. These subnuclei reside within the boundaries of the lateral, medial and Kolliker-Fuse subdivisions (Fig. 1). Lateral PB contains several homogenous groups of cells which may be distinguished by their morphology, spatial clustering, or a combination of both. Rostrally, the superior lateral subnucleus (sl) appears as a prominent, triangular cluster of darkly-staining, multipolar cells. The extreme lateral subnucleus (exl), a relatively small cell group, indents the medial border of the lateral lemniscus. Cells in exl have similar staining characteristics to those in sl. The

internal lateral subnucleus (il), located at mid-PB levels, is a distinctive round cluster of large, round cells. The external lateral subnucleus (el), contains medium-sized, densely packed cells, and is unique among PB subnuclei for its metachromatic staining. The central lateral subnucleus (cl) occupies most of the area dorsal to the scp in the rostral two-thirds of PB. Cells in cl are ovoid to fusiform in shape and stain less darkly than cells in other subnuclei. Along the ventral and dorsal aspects of cl, two clusters of neurons can be identified which are similar in appearance to cl cells but have a greater packing density. These clusters are: the ventral lateral subnucleus (vl), which lies dorsal to the narrow portion of the scp, and the dorsal lateral subnucleus (dl), which is located ventral to the spinocerebellar tract.

Medial PB contains two subnuclei. The medial subnucleus (med) is composed of a heterogenous population of neurons. Three cell types, based on cell size and morphology, have been identified in the medial subnucleus. These include: large, fusiform or multipolar neurons in the caudal two-thirds of med, medium-sized, polygonal cells in rostral med, and small, round neurons in caudalmost med. The extreme medial subnucleus (exm) is distinguished by its homogenous cluster of large, multipolar neurons which lie ventral to the lateral part of the scp. The Kolliker-Fuse subnucleus (KF), located ventral and lateral to the superior cerebellar peduncle (scp), consists of medium- to large-sized, pyramidal shaped neurons with distinct nucleoli.

Two additional areas within the PB are defined: the 'waist' area, which includes the caudal portions of the vl and med subnuclei, and the

'cap' area, which encircles the lateral border of the scp and consists of med, el and possibly, KF (Fulwiler and Saper, '84). These areas are not cytologically distinct but are useful when describing patterns of labeling seen after injections into, for example, the central nucleus of the amygdala or the substantia innominata.

Efferent Conections. The efferent connections of the parabrachial nucleus have been well characterized (for review, Saper and Loewy, '80; Fulwiler and Saper, '84). The PB projects extensively to visceral-related nuclei in the cortex, amygdala, hypothalamus, thalamus and brainstem (Table 1). Each PB efferent projection arises from a characteristic subnuclear population composed of one or more subnuclei (Fulwiler and Saper, '84). Briefly, the PB projection to the cortex (i.e., insular and infralimbic) arises predominantly from the medial and external medial subnuclei. Projections to the amygdala are restricted to the external lateral subnucleus and waist area. The hypothalamus receives input from the superior lateral, central lateral, extreme lateral and dorsal lateral subnuclei. PB projections to the brainstem originate largely from the Kolliker Fuse nucleus. And the PB thalamic projection arises primarily from the internal lateral, medial, external medial and central lateral subnuclei.

Afferent Connections. The parabrachial nucleus also receives dense input from many of the same autonomic nuclei to which it sends a projection (Table 2). Parabrachial afferents may display a subnuclear topography in their terminations but this has been incompletely studied. In an early study, Norgren ('78) noted some degree of topography in the NTS projection to the PB; he found that the rostral

NTS innervates primarily the medial part of the PB and that the caudal NTS projects mainly to the lateral PB. The cortical projection to the PB also appears to be topographically organized (Saper, '82). Injections into the dorsal part of the insular cortex produce anterograde labeling in the ventral and medial parts of the PB whereas injections into the ventral insular cortex produce more widespread labeling, including the area of the PB dorsally adjacent to the superior cerebellar peduncle. In addition, the hypothalamic and amygdalar afferents may also terminate in discrete areas of the PB (Moga et al., '86).

Immunocytochemistry. Like other visceral-autonomic nuclei, the parabrachial nucleus contains many different types of neuropeptide-like immunoreactive cells and fibers, each of which exhibits its own characteristic distribution within the PB (Block and Hoffman, '87). A number of pathways associated with these peptidergic cells and fibers have been identified (Table 3). For example, neurons that project from the NTS to the PB stain for neurotensin-, somatostatin-, substance P-, cholecystokinin-, galanin-, corticotropin releasing factor-, angiotensin II-, and neuropeptide Y- immunoreactivity (Mantyh and Hunt, '84; Milner and Pickel, '86a,b; Herbert et al., '87). The PB neurons that project to the amygdala contain neurotensin-, enkephalin-, substance P-, and calcitonin gene related peptide-immunoreactivity (Block et al., '83; Shimada et al., '85; Zardetto-Smith and Gray, '86).

The peptide content of descending pathways (i.e., from cortex, hypothalamus and amygdala) to the PB is largely unknown. Thus far, a small number of substance P-immunoreactive (SP-ir) neurons in the

central nucleus of the amygdala have been found to project to the PB (Milner and Pickel, '86a). The PB also receives SP-ir and neurotensin-immunoreactive input from the hypothalamus, particularly from the perifornical area of the lateral hypothalamus (Milner and Pickel, '86a,b). Neurophysin II (i.e., oxytocin) containing fibers in the PB probably arise from the paraventriuclar hypothalamus (Swanson, '77).

Role in Respiration. Early physiological studies of the parabrachial nucleus focused on its role in respiration. Based on his lesions of the brainstem at different levels, Lumsden ('23) postulated that the upper part of the pons contained a 'pneumotaxic centre', a center which could inhibit the activity of the lower apneustic centers, and thus, was important in the generation of normal respiratory rhythm. The first direct evidence for the existence of this pneumotaxic center was given by Cohen and Wang ('59) who recorded unit discharges phase-locked to respiration in the general region of the PB. Three sets of respiratory neurons were consequently noted in the PB and the neighboring Kolliker-Fuse nucleus: expiratory, located medially; inspiratory, recorded laterally; and phase spanning inspiratory-expiratory, found between them (Bertrand and Hugelin, '71).

Anesthetized animals that have bilateral lesions of the PB exhibit a slow, deep pattern of breathing (Bertrand and Hugelin, '71; von Euler et al., '76). With bilateral vagotomy, the pattern of breathing becomes apneustic (inspiratory gasping). Chronic vagotomized preparations with PB lesions which breathe apneustically when anesthetized, eventually return to a slow, deep pattern of breathing when awake (St. John et al., '72). Thus, the PB does not appear to be

a primary source of respiratory rhythm generation. However, electrical stimulation of the PB region can cause a premature termination of the current respiratory phase (Feldman and Gautier, '76; von Euler and Trippenbach, '76; Cohen, '71). Thus, the role of the PB in respiration may be to 'finely tune the pattern generator' (Mitchell and Berger, '81).

Cardiovascular Regulation. In several early surveys of the brainstem, a marked rise in blood pressure and/or an increase in heart rate was noted following electrical stimulation of the dorsolateral pons (Wang and Ranson, '39; Chai and Wang, '62; Coote et al., '73). Nuclei implicated in this pressor response included the PB, locus coeruleus, fastigial nucleus of the cerebellum (via its fibers in the brachium conjunctivum) and reticular formation (e.g., Miura and Reis, '69; Ward and Gunn, '76). Subsequent anatomical studies noted that the PB was extensively connected with nuclei involved in cardiovascular regulation (for review, Saper, '78; Loewy and McKellar, '79). Recent physiological studies have provided strong evidence that the PB is important in cardiovascular regulation (Mraovitch et al., '82; Galeno and Brody, '83; Cechetto and Calaresu, '83).

Electrical stimulation restricted to the PB in the rat and cat elicits a profound pressor response consisting of tachycardia, elevated mean arterial pressure, renal and mesenteric vasoconstriction, and vasodilation in skeletal muscle (Mraovitch et al., '82; Galeno and Brody, '83). This pressor response persists after acute midbrain hemisections or bilateral NTS lesions, indicating that it is intrinsic to PB neurons (Mraovitch et al., '82). Furthermore, many neurons in the

PB respond to either carotid sinus and/or aortic depressor nerve stimulation, demonstrating that the PB receives baroreceptor and chemoreceptor input (Cechetto and Calaresu, '83). This input may be the source of the cardiac cycle related discharge of PB neurons (Sieck and Harper, '80a).

In the rat, the PB is one of a few nuclei projecting to the cardiomotor neurons in the nucleus ambiguus (Stuesse and Fish, '84). As the nucleus ambiguus forms the vagal efferent limb of the baroreceptor reflex, the PB may be an important modulator of this reflex. Following concurrent stimulation of the carotid sinus nerve (CSN) and the PB, the decrease in arterial pressure and bradycardia characteristic of the baroreceptor reflex is abolished, indicating an inhibitory interaction between the PB and baroreceptor mechanisms of the CSN (Mraovitch et al., '82). Recently, Hubbard et al. ('87) found that rats with bilateral lesions of the PB show an increased baroreflex sensitivity following injections of phenylephrine.

Sleep. Cardiovascular- and respiratory-related neurons in the PB show changes in firing rate and pattern during the sleep-wake cycle (Sieck and Harper, '80a,b). The firing of medial PB neurons in phase with the cardiac cycle is most apparent during the awake and desynchronized sleep states, and is greatly reduced or absent during synchronized sleep. Changes in the firing of respiratory-related PB neurons parallels the variations in respiratory patterns associated with the different sleep-wake states. For example, high neuronal discharge rates with marked variability are found in the medial PB during desynchronized sleep, a sleep state which can be characterized

by its fast, irregular breathing pattern. In contrast, during synchronized sleep, PB neurons show a slow rate of discharge consistent with the slower rate of breathing found during this state. Sieck and Harper ('80b) suggest that the correlations between PB neuronal discharge and sleep-wake state may be a result of, or contribute to, the different control of autonomic functions during the sleep-wake cycle.

Nociception. Bilateral lesions of the caudal, medial PB do not alter nociceptive thresholds as assessed by the tail flick and hot plate assays (Hammond and Proudfit, '80). However, these lesions do attentuate the analgesia induced by morphine, suggesting that the PB may be involved in the expression of morphine analgesia. The PB contains a high density of opiate receptors (Atweh and Kuhar, '77), and a high concentration of opioid-immunoreactive cells and terminals (Williams and Dockray, '83). Furthermore, the PB is reciprocally connected with the dorsal raphe nucleus and the periaqueductal gray matter (Sakai et al., '77; Beitz, '82a; unpublished observations). Numerous studies have demonstrated the involvement of these nuclei in the mediation of morphine analgesia (for review, Mayer and Price, '76; Fields and Basbaum, '78). Thus, the PB may also be an integral part of the brainstem mechanisms mediating opiate analgesia.

Electrical stimulation of the PB inhibits the responses of upper thoracic spinothalamic neurons to somatic input (Girardot et al., '87) and to cardiopulmonary sympathetic afferent input, particularly the C-fiber component (Brennan et al., '87). As the spinothalamic tract is involved in the transmission of nociceptive information, these studies

suggest that the PB may be an important modulator of nociception at the spinal level.

Recently, the PB was found to receive input from the large, flattened neurons in lamina I of the spinal cord (Cechetto et al., '85). Many of these neurons projecting to the PB stain for the opioids, met-enkephalin and dynorphin (Standaert et al., '86). These lamina I neurons receive nociceptive input (Light et al., '79). Possibly, this spinal projection to the PB may modulate the autonomic responses of the PB to painful stimuli.

Feeding. Electrical stimulation of the PB, particularly its caudal waist area, elicits feeding behavior in the rat (Micco, '74). As an anatomical substrate for this response, the PB sends a heavy projection to the medullary reticular formation which, in turn, projects to motor nuclei involved in oral-facial functions, such as mastication and swallowing (Saper and Loewy, '80; Takeuchi et al., '80; Travers and Norgren, '83). In addition, the PB projects directly to the lateral part of the facial nucleus; this area controls the facial muscles surrounding the mouth (Takeuchi et al., '80; Saper and Loewy, '80). Schwartzbaum ('83) has theorized that the PB integrates orolingual (i.e., feeding) responses to taste and other sensory input. As evidence, many 'gustatory' neurons in the caudal, medial PB receive mechanoreceptive or visceral (i.e., vagal) input (Ogawa et al., '82; Hermann and Rogers, '85). In the awake rabbit, most of this mechanoreceptive input is related to feedback from orolingual movement rather than from the properties of the ingestant (Schwartzbaum, '83).

Several lines of evidence suggest that the PB may play a role in the regulation of food ingestion. The PB projects heavily to the ventromedial hypothalamus (VMH), which has long been implicated in the feeding process (for review, Woods et al., '86). A majority of the neurons in the superior lateral subnucleus of the PB that project to the VMH stain for the neuropeptide, cholescystokinin (CCK) (Fulwiler and Saper, '85). In the rat, the VMH contains receptors for CCK (Zarbin et al., '83), and an injection of this neuropeptide into the VMH suppresses feeding behaviors (Stern et al., '76; McCaleb and Myers, '80). The hyperphagia and obesity produced by VMH lesions can largely be abolished by subdiaphragmatic vagotomy, suggesting that the visceral afferent input to the VMH is involved in producing the effects seen after VMH ablation (Powley, '77). The PB is the major relay of this visceral afferent information to the VMH (Ricardo and Koh, '78; Saper and Loewy, '80). Thus, the CCK-containing pathway from the PB to the VMH may be important in the regulation of feeding in the hypothalamus.

Fluid Regulation. Anatomical studies suggest that the PB may play a role in fluid and electrolyte balance. The PB is connected with several midline structures, such as the area postrema, subfornical organ, and median preoptic nucleus (Shapiro and Miselis, '85; Saper et al., '85), which have been implicated in fluid regulation (Simpson, '81; Eng and Miselis, '81; Edwards and Ritter, '82). Many cells and fibers in the PB stain for the neuropeptides, angiotensin II and atriopeptin (Lind et al., '85; Standaert et al., '86b). Both central and intravenous administration of angiotensin II result in a strong dipsogenic response (Epstein et al., '70; Robinson and Evered, '87),

while central administration of atriopeptin attentuates the dipsogenic actions of angiotensin II (Lappe et al., '86).

Direct, physiological evidence that the PB participates in this function can be found in the study by Ohman and Johnson ('86). Following bilateral ablation of the ventrolateral PB, they noted an exaggerated drinking response after systemic administration of angiotensin II and isoproterenol, suggesting an alteration in the central thirst mechanisms.

Micturition. Barrington ('25) first described a 'micturition reflex centre' in the dorsolateral pontine tegmentum just ventral to the medial edge of the scp. Lesions of this area resulted in an inability to empty the urinary bladder. Later experiments, employing electical stimulation, lesion and/or HRP techniques, further localized this reflex center (i.e., Barringon's nucleus) to the central gray, medial to the PB and Mes5, and just rostral to locus coeruleus (Lalley et al., '72; deGroat, '75; Satoh et al., '78). Recently however, Lumb and Morrison ('87) found that either chemical or electrical stimulation of the lateral PB also evokes urinary bladder contractions. As the lateral PB does not project to the spinal cord, it is unknown by what pathways the PB may influence this reflex.

Endocrine Function. A few studies have implicated the PB in the release of hormones from both the anterior and posterior hypophysis. Electrical stimulation of dorsal and lateral parts of the PB produces a small increase in plasma levels of arginine vasopressin (AVP); this effect is markedly increased following ganglionic blockade (Sved, '86). The pathway from the PB to the PVH may subserve this response (Fulwiler

and Saper, '84; Ciriello et al., '84). And, in an early study, Ward et al. ('76) noted decreased plasma concentrations of adrenal corticotropin hormone (ACTH) following electrical stimulation of an area in the rostral pons of the cat which included the parabrachial region and locus subcoeruleus. Future studies are needed to more precisely locate the source of this response.

Table 1. Efferent Connections of the Parabrachial Nucleus

(Saper and Loewy, '80; Fulwiler and Saper, '84)

Cortex - Infralimbic
- Insular

Septo-olfactory area

Bed Nucleus of the Stria Terminalis

Amygdala - Central N.
- Anterior
- Medial N.
- Basomedial N.
- Posterior Basolateral N.

Substantia Innominata

Pons - contralateral PB
- Facial Nucleus

Medulla - N. Solitary Tract
- Nucleus Ambiguus
- Ventrolateral Medulla
- Reticular Formation
- Hypoglossal N.

Spinal Cord

Hypothalamus - Preoptic
- Paraventricular N.
- Lateral
- Ventromedial N.
- Dorsomedial N.
- Arcuate N.

Thalamus - Intralaminar N.
- Midline N.
- Ventromedial Basal N.

Midbrain - Substantia Nigra
- Central Gray
- Edinger-Westphal N.
- Raphe N.

Table 2. Afferent Connections of the Parabrachial Nucleus

Bed Nucleus of the Stria Terminalis	(Swanson and Cowan, '79; Holstege et al., '85)
Central Nucleus of the Amygdala	(Hopkins and Holstege, '78; Krettek and Price, '78; Price and Amaral, '81; Takeuchi et al., '82; Veening et al., '84)
Lateral Hypothalamus	(Saper et al., '79; Hosoya and Matsushita, '81; Berk and Finkelstein, '82; Takeuchi and Hopkins, '84)
Paraventricular N., Hypothalamus	(Swanson, '77; Takeuchi and Hopkins, '84; Luiten et al., '85)
Preoptic Area of the Hypothalamus	(Conrad and Pfaff, '76; Saper and Levisohn, '83; Chiba and Murata, '85)
Ventromedial/Dorsomedial Hypothalamus	(Takeuchi and Hopkins, '84)
Insular/Infralimbic Cortex	(Saper, '82; Shipley and Sanders, '82; van der Kooy et al., '84; Yasui et al., '85)

Table 2. continued

Nucleus of the Solitary Tract----------(Norgren and Leonard, '73;
Norgren, '76, '78;
Ricardo and Koh, '78)

Area Postrema----------(Shapiro and Miselis, '85)

Ventrolateral Medulla----------(Loewy et al., '81)

Spinal Cord/Spinal Trigeminal Nucleus------(Cechetto et al., '85)

Table 3. Peptidergic Pathways of the Parabrachial Nucleus

Source	Termination	Neuropeptide	Reference
Spinal Cord	PB	ENK, DYN	Standaert et al., '86a
NTS	PB	CCK, ENK, SS	Mantyh and Hunt, '84
		NT, SP	Milner and Pickel, '86a,b
		GAL, NPY, CRF, AII	Herbert et al., '87
CeA	PB	SP	Milner and Pickel, '86b
LH	PB	SP, NT	Milner and Pickel, '86a,b
PVH	PB	OXY	Swanson, '77
PB	Thalamus	CCK, ENK, NT,	Mantyh and Hunt, '84
		SS, SP	
		CGRP	Shimada et al., '85
PB	Raphe Magnus	ENK	Beitz, '82b
PB	VMH	CCK	Fulwiler and Saper, '85;
			Zaborszky, '84
		CGRP	Shimada et al., '85
PB	LH	CGRP	Shimada et al., '85
PB	MnPO	ENK, CRF	Lind and Swanson, '84;
		SP	Block et al., '84
PB	CeA	NT, SP	Block et al, '83
		CGRP	Shimada et al., '85
		ENK	Zardetto-Smith and
			Gray,'86
PB	BST	CGRP	Shimada et al., '85

Figure 1. Drawings of the parabrachial nucleus through four levels (rostral to caudal, upper left to bottom right) illustrating the approximate locations of the subnuclei. Shaded areas indicate fiber tracts.

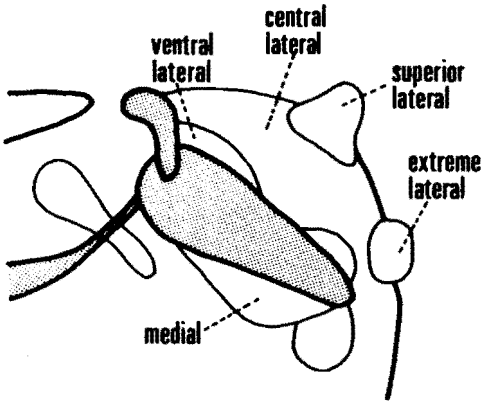
ventral lateral
central lateral
superior lateral
extreme lateral
medial

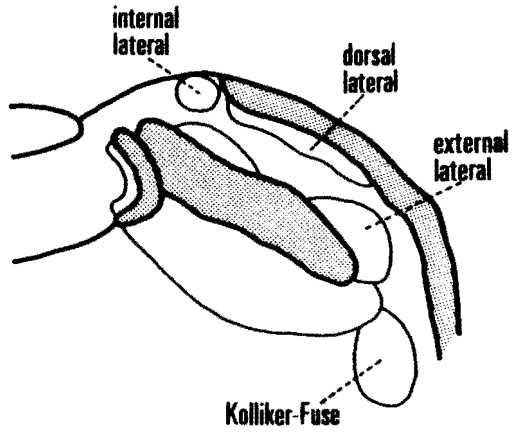
internal lateral
dorsal lateral
external lateral
Kolliker-Fuse

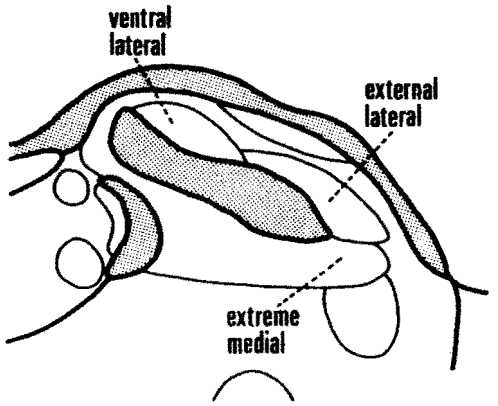
ventral lateral
external lateral
extreme medial

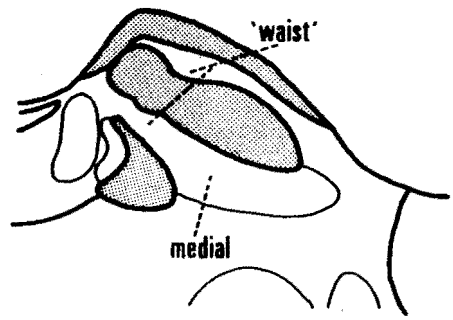
'waist'
medial

CHAPTER III

PEPTIDERGIC PATHWAYS FROM THE CENTRAL NUCLEUS OF THE AMYGDALA TO THE PARABRACHIAL NUCLEUS

INTRODUCTION

The central nucleus of the amygdala (CeA) sends a dense axonal projection to the parabrachial nucleus (PB) in the pons (Krettek and Price, '78; Price and Amaral, '81; Takeuchi et al., '82). This pathway is present in primates (Price and Amaral, '81), cats (Krettek and Price, '78) and rats (Krettek and Price, '78; Veening et al., '84), and is reciprocal (Takeuchi et al., '82; Fulwiler and Saper, '84; Veening et al., '84). Recent physiological studies have focused on the role of the CeA and PB in cardiovascular and respiratory functions. For example, electrical stimulation of the central nucleus alters the firing rate of neurons in the parabrachial nucleus, some of which are also activated by stimulation of the carotid sinus (Cechetto and Calaresu, '83). Also, stimulation of either the CeA and/or the PB produces respiratory activation and a large pressor response (Mraovitch et al., '82; Galeno and Brody, '83; Harper et al.,'84). These findings probably reflect the role of the CeA and PB in the integration of autonomic responses associated with a variety of adaptive behaviors (Kaada, '72; Loewy and McKellar, '80; Smith and DeVito, '84).

The CeA contains many different types of peptide immunoreactive neurons, each of which exhibits its own characteristic distribution within the CeA (Wray and Hoffman, '83, Veening et al., '84; Cassell et al., '86). Neurotensin (NT-ir)-, corticotropin releasing factor (CRF-ir)-, somatostatin (SS-ir), and enkephalin (ENK-ir)-immunoreactive neurons are especially numerous (Roberts et al., '80a; Wray and Hoffman, '83; Veening et al., '84; Cassell et al., '86) within the CeA. Roberts et al. ('80a) has described the CeA as a focus for diverging/converging peptide pathways. However, only a few of the destinations of these pathways have been reported. For example, peptidergic efferents from the CeA to the bed nucleus of the stria terminalis (Uhl et al.,'78) and the dorsal vagal complex (Kawai et al., '82; Higgins and Schwaber, '83; Veening et al., '84) have been identified. As yet, no peptide has been identified in the CeA projection to the PB, although a recent attempt was made (Veening et al., '84). Data on the organization of peptide pathways between the CeA and PB is an important prerequisite for understanding how these regions function in the integration of behaviors which have strong autonomic components. In this study, we use a modification of the combined retrograde tracing and immunocytochemical method (Sawchenko and Swanson, '81; Skirboll et al., '84) to test for the presence of NT-ir, CRF-ir, SS-ir and ENK-ir in CeA neurons which project to the PB. Preliminary findings of this investigation were previously reported (Moga and Gray, '84).

METHODS

The subjects of this study were 150-300 gm male Long-Evans rats (n=23). Under sodium pentobarbital anesthesia (50 mg/kg), unilateral (n=21) and bilateral (n=2) 50 nl injections of 2.0% Fast Blue dye (D.R. Illing) in distilled water were made into the parabrachial nuclei with a 1.0 ul Hamilton syringe fitted with a glass micropipette with an outside diameter of 25-50 um. The stereotaxic coordinates (AP=-9.5, ML=2.0, DV=-7.1) for the PB were derived from the Paxinos and Watson (1982) rat brain atlas. Injections were made over a 15 min. period, and the pipette was left in place for a minimum of 10 additional minutes. Thirty-six to forty-eight hours prior to sacrifice, each animal was re-anesthetized, and 5-7 ul of colchicine (dissolved in saline, 10 ug/ul) were injected into each lateral ventricle at approximately -0.8 posterior to the bregma level illustrated in Paxinos and Watson (1982). Post-Fast Blue injection survival times ranged from 7 to 10 days. Animals were sacrificed with a lethal dose of sodium pentobarbital. They were perfused through the ascending aorta with 0.01M phosphate buffered saline (pH 7.6, 38^{o}C) followed by 0.167M phosphate buffered 4.0% paraformaldehyde (pH 7.6, 4^{o}C). After perfusion, the skull was placed in a stereotaxic frame (Kopf) and the brain was sliced into coronal blocks. The blocks of brain tissue were post-fixed in 4.0% paraformaldehyde for 30 minutes to 2 hours and then cut serially using a vibratome (Lancer). Sections from the injection site (40 um) were mounted onto chrom-alum-coated slides. Adjacent coronal sections (20 um) of the amygdala and hypothalamus were

collected in 3 or 4 vials of cold (4.0°C) phosphate buffered saline (PBS). Each series of adjacent sections was rinsed in PBS containing 0.1% Triton-X (Mallinckrodt) for 20 minutes followed by a 30 minute incubation in normal goat serum (diluted to 10.0% in PBS), and then another rinse in PBS (10 minutes). Anti-neurotensin, anti-met-enkephalin, anti-peptide E, and anti-somatostatin were used at a dilution of 1:500; anti-CRF was diluted 1:300. All primary antibodies were obtained from Immunonuclear Corporation, except for anti-peptide E which was generously supplied by Dr. S.J. Watson. Immunoabsorption of the above antisera with homologous antigen served as controls for specificity. Each set of sections was gently agitated in one of the above primary antiserum at room temperature for 60 minutes, and then in a cold room (4°C) for 14-24 hours. Next, the sections were rinsed in PBS and incubated in rhodamine-conjugated goat antirabbit IgG (Cooper Biomedical, diluted 1:10 in PBS-Triton-X) at 45°C for 10 min. and then at room temperature for 60 minutes. Sections were transferred to cold PBS and mounted onto chrom-alum-coated slides, and cover-slipped using DePeX (BDH Chemicals) mounting media. The material was examined with an Olympus microscope equiped with a 100W mercury light source. Fast Blue was visualized with an excitation wavelength centered at 330-360 nm (Olympus ultraviolet filter system). Rhodamine immunofluorescence was viewed with the Olympus green (546 nm) filter system. Cells that contained both Fast Blue and rhodamine immunofluorescence were detected by switching between filter systems. Sections were photographed with Polaroid coaterless land pack film 667, ASA 3000/36 DIN. In three cases with comparable and extensive CeA retrograde labeling, the

retrogradely labeled, neuropeptide- immunoreactive and double-labeled neurons in the CeA were counted (from every one out of four sections through the CeA) using a 40x UV fluorite objective.

RESULTS

Distribution of Retrogradely Labeled Neurons

The distribution of retrogradely labeled cells varied depending on the site of the injection in the PB. A maximal number of retrogradely labeled neurons within the CeA was obtained in animals with injections located at mid-rostrocaudal levels in the PB. With injections centered in the ventrolateral PB (Fig. 1C, E-G), heavy labeling occurred throughout the rostrocaudal extent of the CeA in all subdivisions (e.g. Fig 5A). With injections centered in the lateral PB (e.g., Fig. 1B), labeled cells were found throughout the rostrocaudal extent of the ipsilateral CeA but were located predominantly in its caudal half within the lateral and lateral capsular subdivisions. Light labeling, located primarily within the medial CeA, was seen with injections centered within the medial PB (e.g Fig. 1D) and the dorsomedial PB (e.g. Fig. 1H). Labeling was not observed in the CeA in animals with injections located in the cuneiform nucleus or adjacent regions of the cerebellum.

After injections into the PB, retrogradely labeled neurons were also observed in the anterior amygdaloid area, ventral pallidum, intercalated cell group of the amygdala, substantia innominata, organum

vasculosum of the lamina terminalis, median preoptic nucleus, lateral and medial preoptic areas, infralimbic cortex, insular cortex, lateral prefrontal cortex, bed nucleus of the stria terminalis, retrochiasmatic area, zona incerta, lateral hypothalamus, paraventricular hypothalamus, dorsomedial hypothalamus, and arcuate nucleus. Retrograde labeling in all of the above areas was predominantly ipsilateral to the injection site; however, a few contralaterally labeled cells were always present.

Distribution of Immunoreactive Neurons

The distribution of CRF-ir, NT-ir, SS-ir and ENK-ir cells within the CeA was the same as that described in previous immunocytochemical studies of the CeA (Wray and Hoffman, '83; Veening et al, '84; Cassell et al, '86); therefore, the present findings are only briefly summarized. CRF-ir and NT-ir immunoreactive neurons were mainly confined to the lateral subdivision of the CeA with only an occasional CRF-ir or NT-ir neuron seen in the medial and lateral capsular subdivisions. Most of the SS-ir neurons were observed within the lateral subdivision of the CeA, although SS-ir neurons were also commonly seen in the medial CeA. The immunoreactivity observed using antibodies to met-enkephalin and peptide E appeared indistinguishable and hereafter will be referred to as enkephalin-immunoreactivity (ENK-ir). ENK-ir neurons were distributed within the lateral and lateral capsular subdivisions of the CeA.

Double-Labeled Neurons

Neurons labeled for both neuropeptide and retrograde tracer were consistently found in the lateral subdivision of the CeA. Few double-labeled neurons were found in the medial and lateral capsular subdivisions. In three cases, the injections (Fig. 1 - E, F, G) were centered in the ventrolateral PB, and comparable retrograde labeling was found throughout the CeA. Immunoreactive and double-labeled neurons in the CeA after these injections were counted (Table 1) to assess the relative contribution of each neuropeptide to the CeA-PB pathway. These cell counts include labeled cells from every CeA subdivision. Figures 2-5 are photomicrographs of retrogradely labeled, immunoreactive and double-labeled cells in the CeA at its mid-rostrocaudal extent (approximately the bregma -2.8 mm level illustrated in the Paxinos and Watson ('82) atlas). Figure 6 shows the characteristic distributions of double-labeled cells within the CeA for each neuropeptide examined.

Neurotensin (NT-ir). Cells double-labeled for NT-ir and fast blue were numerous and were concentrated in the caudal half of the CeA within its lateral subdivision. A few double-labeled cells were observed in the lateral capsular subdivison. Many (40-53%) NT-ir neurons in the CeA were retrogradely labeled. Figure 2 shows an example of three retrogradely-labeled NT-ir cells and their location in the CeA. NT-ir double-labeled cells were also seen in the intercalated cell group of the amygdala, lateral division of the bed nucleus of the stria terminalis (BST), perifornical area of the lateral hypothalamus

and parvocellular subdivision of the paraventricular nucleus of the hypothalamus.

Corticotropin Releasing Factor (CRF-ir). Many CRF-ir cells were labeled with fast blue, and they were found predominantly at caudal levels in the lateral subdivision of the CeA, although a few double-labeled neurons were seen in the medial subdivison. Of the four types of peptidergic neurons studied in the CeA, CRF-ir neurons exhibited the highest percentage (54-66%) of cells retrogradely labeled with Fast Blue. An example of CRF-ir neurons labeled with Fast Blue is presented in Figure 3. Additional double-labeled CRF-ir neurons were located in the intercalated cell group of the amygdala, the lateral division of the BST, lateral hypothalamus-perifornical area and the parvocellular paraventricular nucleus of the hypothalamus.

Somatostatin (SS-ir). Cells double-labeled for Fast Blue and SS-ir were observed in the CeA following injections of tracer into the PB. The percentage of SS-ir neurons labeled with Fast Blue was lower than that for CRF-ir and NT-ir, and ranged from 31-50%. Double-labeled SS-ir neurons were for the most part limited to the lateral subdivision although a few cells were located in the medial subdivison. Their distribution extended more rostrally than doubled-labeled NT-ir or CRF-ir neurons. Figure 3 shows an example of two somatostatin-immunoreactive cells in the lateral CeA which were also retrogradely labeled with Fast Blue. Cells labeled for both SS-ir and Fast Blue were also seen in the lateral division of the BST and the lateral hypothalamus.

Enkephalin (ENK-ir). Cells double-labeled for ENK-ir and Fast Blue were never observed in the CeA after injections of the tracer into the PB. However, ENK-ir cells were often observed adjacent to Fast Blue labeled cells (Figure 5). A few double-labeled ENK-ir cells were observed in the medial preoptic area and the parvocellular paraventricular nucleus of the hypothalamus.

DISCUSSION

In the present study, the combined retrograde tracing-immunofluorescence method was used to identify the presence of CRF-ir, NT-ir and SS-ir in CeA neuronal efferents to the PB. The percentage of CRF-ir, NT-ir and SS-ir double-labeled cells per subject showed little variation, i.e., 54-66%, 40-53% and 31-50%, respectively (see Table 1). However, the total number of CRF-ir, NT-ir and SS-ir immunoreactive neurons per subject tended to vary considerably, from 85-183, 60-194 and 100-129, respectively. These data illustrate two important points concerning interpretation of the results of this double-labeling technique. First, this technique provides a conservative estimate of the number of immunoreactive neurons contributing to a particular pathway. Second, in judging the relative contribution of a peptidergic population to a neural pathway, the percentage of neurons participating rather than the absolute number should be considered as a more reliable index. This confirms the observations of two recent studies reviewing the limitations and applicability of the combined retrograde tracing-

immunocytochemical method (Sawchenko and Swanson, '81; Skirboll et al., '84).

CeA Projection to the PB

Many investigators have noted that the majority of peptide-containing neurons in the CeA are located within its lateral subdivision (e.g., Wray and Hoffman, '83; Veening et al., '84) and yet, most of its major efferent projections have been reported to arise from cells located in the medial subdivision (Hopkins and Holstege, '78; Schwaber et al., '82; Veening et al., '84; Cassell et al., '86). Our results show that a large part of the CeA-PB pathway originates from the lateral CeA. Results from several tracing studies (Hopkins and Holstege, '78; Krettek and Price, '78; Price and Amaral, '81) have indicated that the CeA projection to the PB terminates throughout both medial and lateral PB without any apparent topography. Recently, Saper (unpublished data, discussed in Fulwiler and Saper, '84) reported that the CeA projects to distinct areas within the PB, most probably to the central, ventral and external lateral subnuclei, the 'waist area' and the medial PB. In the present study, optimal retrograde labeling in the lateral CeA was obtained with injections centered in the central, ventral and external lateral subnuclei described by Fulwiler and Saper, '84. Injections centered within the medial or dorsomedial PB resulted in labeling confined mainly to the medial CeA. The lateral and medial CeA may project to different, yet overlapping, areas within the PB. Possibly, Veening et al. ('84) were unable to find a CeA peptidergic

projection to the PB because their tracer injections missed the subzones of the PB that receive projections from the lateral CeA. This explanation seems likely since they reported that their retrograde labeling was located predominantly in the medial CeA where very few peptidergic neurons are located. Further studies are needed to clarify possible hodological differences between the medial and lateral CeA.

CeA and PB Peptidergic Afferents and Efferents

Three CeA peptidergic projection zones have been identified. The PB and the BST, the major target zones, receive input from a significant percentage of corticotropin releasing factor-, neurotensin- and somatostatin-immunoreactive neurons in the CeA (Uhl et al., '78; Gray, unpublished observations). A small number of CRF-ir, NT-ir and SS-ir neurons contribute to the CeA pathway to the DVC (Kawai et al., '82; Higgins and Schwaber, '83; Veening et al., '84). Enkephalin-immunoreactive neurons within the CeA send efferents to the BST (Uhl et al., '78), but probably do not innervate the PB or the DVC (Veening et al., '84). All of these peptidergic pathways arise primarily from the lateral CeA, except for the SS-ir projection to the DVC which originates from both medial and lateral CeA (Higgins and Schwaber, '83; Veening et al., ' 84).

Only a few C7a peptidergic afferents have been described. Cholecystokinin-immunoreactive (CCK-ir) terminals in the CeA arise from the ventral tegmental-substantia nigra region (Hokfelt et al., '80). Vasoactive intestinal polypeptide-immunoreactive fibers travel to the

CeA via the medial forebrain bundle and probably originate from cells located in the central grey matter (Marley et al., '81). NT-ir fibers in the CeA arise from the caudal brainstem, possibly from either the PB and/or the DVC (Kawakami et al., '84).

Thus, significant gaps still remain in our knowledge of the peptidergic pathways of the CeA. In particular, the peptide content of CeA pathways to the hypothalamus, central grey and A5 catecholamine cell group is unknown.

A number of peptidergic efferents and afferents of the PB have now been identified. As already noted, the CeA is a major source of CRF-ir, SS-ir and NT-ir terminals to the PB. In smaller numbers, the bed nucleus of the stria terminalis, lateral hypothalamus and paraventricular nucleus of the hypothalamus also contribute CRF-ir, NT-ir and SS-ir fibers to the PB. Notably, enkephalin-ir neurons in the CeA do not project to the PB, however, ENK-ir neurons in the medial NTS do project to the PB (Mantyh and Hunt, '84). Also from the caudal brainstem, the PB receives neurotensin-, somatostatin-, substance P (SP-ir)-, cholecystokinin-, and avian pancreatic polypeptide (probably neuropeptide Y, Lundberg et al., '84)-immunoreactive fibers from the medial NTS (Milner et al, '84; Mantyh and Hunt, '84). Regarding the efferents of the parabrachial nucleus, Mantyh and Hunt ('84) have found CCK-ir, ENK-ir, NT-ir, SS-ir and SP-ir in the PB projection to the ventral part of the thalamus. Other efferent peptidergic populations reported in the PB include a CCK-ir projection to the ventromedial hypothalamus (Zaborszky, '84; Fulwiler and Saper, '85), and CRF-ir and ENK-ir projections to the median preoptic area (Lind and Swanson, '84).

From this accumulating mass of peptidergic data on the PB, there emerge certain areas of terminal overlap. Most conspicuous is the convergence of both forebrain and caudal brainstem NT-ir fibers to the ventrolateral PB. In their combined use of immunocytochemistry and autoradiography, Milner et al. ('84) found an overlapping distribution of NT-ir fibers and anterogradely labeled terminals from the caudal and medial NTS in the ventrolateral PB. They postulated that NT-ir may be contained within the efferents of the medial NTS to the PB, an observation later confirmed by Mantyh and Hunt ('84). In this study, we observed many retrogradely labeled NT-ir cells in the CeA following injections into this ventrolateral quadrant. Thus, the ventrolateral PB may be an important region for the interaction of NT-ir neurons located in both CeA and medial NTS.

Functional Considerations

Physiological and anatomical studies indicate that the central nucleus mediates the autonomic components of behavioral responses to stress-inducing environmental stimuli (e.g., attack and defense behaviors, responses to aversive stimuli). Among the amygdalar nuclei, only the CeA has strong reciprocal connections with brainstem autonomic regions (for review, see Price and Amaral, '81). Reflecting these autonomic connections, CeA stimulation in the rat and cat elicits cardiovascular, respiratory and gastric responses which are typically seen during stress-related behaviors (e.g. Henke, '82; Galeno and Brody, '83; Frysinger et al., '84). The cardiovascular (i.e. pressor)

response obtained from the awake rat consists of tachycardia, elevated mean arterial pressure, renal and mesenteric vasoconstriction, and vasodilation in skeletal muscle (Galeno and Brody, '83). This response is strikingly similar to the pressor response observed following stimulation of the parabrachial nucleus in the cat (Mraovitch, '82). Correspondingly, respiratory responses elicited from CeA stimulation are nearly identical to those obtained from the PB (Harper et al., '84). Thus, the CeA cardiovascular and respiratory responses may be mediated through direct projections to the PB. In contrast, gastric changes observed following stimulation of the CeA are more likely mediated via direct projections to the dorsal vagal complex (Henke, '82).

The CeA has also been implicated in responses to noxious input. For example, lesions in the amygdala have been shown to reduce an animal's reaction to painful stimulation (Schreiner and Kling, '53). More recently, direct injections of neurotensin into the CeA of the rat produced a significant increase in the nociceptive threshold of the rat (Kalivas et al., '82). Substantial evidence now exists linking pain and cardiovascular pathways (for review, see Randich and Maixner, '84). Since the central nucleus is involved in both cardiovascular responses and affective reactions to noxious inputs, the linkage of pain and cardiovascular function may occur partially in the CeA. This possible linkage of nociception, pressor response and respiratory activation within the CeA may provide an anatomical basis for the proposal of Randich and Maixner ('84) that elevations in blood pressure, with a subsequent inhibition of pain and/or associated behavioral changes, may

reduce the stress experienced by an animal during aversive environmental stimulation.

Other recent studies have emphasized the importance of the CeA in the development of pathological responses to stress. For example, chronic stimulation of the CeA produces gastric ulcers; and bilateral ablation of the CeA reduces the incidence and severity of stress-induced gastric ulcers in the rat (Henke, '82). Bilateral ablation of the CeA or its output pathways also attenuates the translation of noise stress into increased sympathetic nerve activity in both normotensive and spontaneously hypertensive (SHR) rats (Galeno et al., '84). Galeno et al. ('84) speculate that the enhanced pressor response of the SHR rat to noise stress may be the result of an abnormal amplification of sensory information through the amygdala. Such a hypothesis is consistent with the multiplicity of sensory inputs to the CeA (Turner, '81; Ottersen, '81).

Neuropeptides found in the CeA and its output pathway to the PB are also involved in stress responses. For example, intracisternal administration of neurotensin and somatostatin reduces the incidence of stress-induced gastric ulcers in rats (Hernandez et al., '83). Intracerebroventricular application of corticotropin releasing factor stimulates sympathetic outflow (i.e., tachycardia, increased blood pressure, vasoconstriction); and these effects probably occur through actions in the brain rather than through the neuroendocrine system (Brown et al., '82; Sutton et al., '82). We speculate that CRF, NT and SS may be important putative neurotransmitters in the CeA-PB pathway,

and that this peptidergic pathway may be an important mediator of stress-related responses.

Figure 1. Drawings of the relative positions of representative Fast Blue injections in the parabrachial nucleus. Black shading indicates the center of each injection site where necrosis occurred. Hatched areas represent the apparent spread of the fluorescent dye.

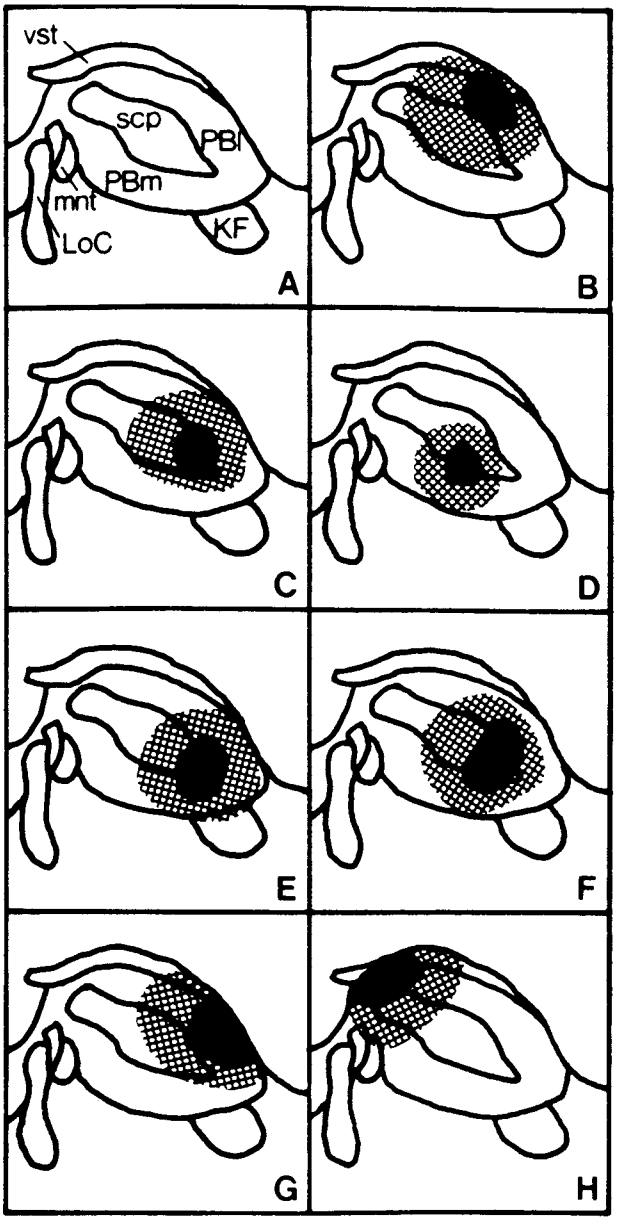
vst
scp
PBl
PBm
mnt
LoC
KF
A
B
C
D
E
F
G
H

Figure 2. Fluorescent photomicrographs of a coronal section through the caudal CeA illustrating the distribution of (A) cells projecting to the PB and (B) cells immunoreactive to neurotensin. Figures C (Fast Blue-labeled cells) and D (NT-ir cells) are high power photomicrographs of three double-labeled cells (indicated by white arrows) found within the lateral subdivision of the CeA in A and B. (L, lateral subdivision; LC, lateral capsular subdivision; M, medial subdivision; st, stria terminalis). Bar = 100 um.

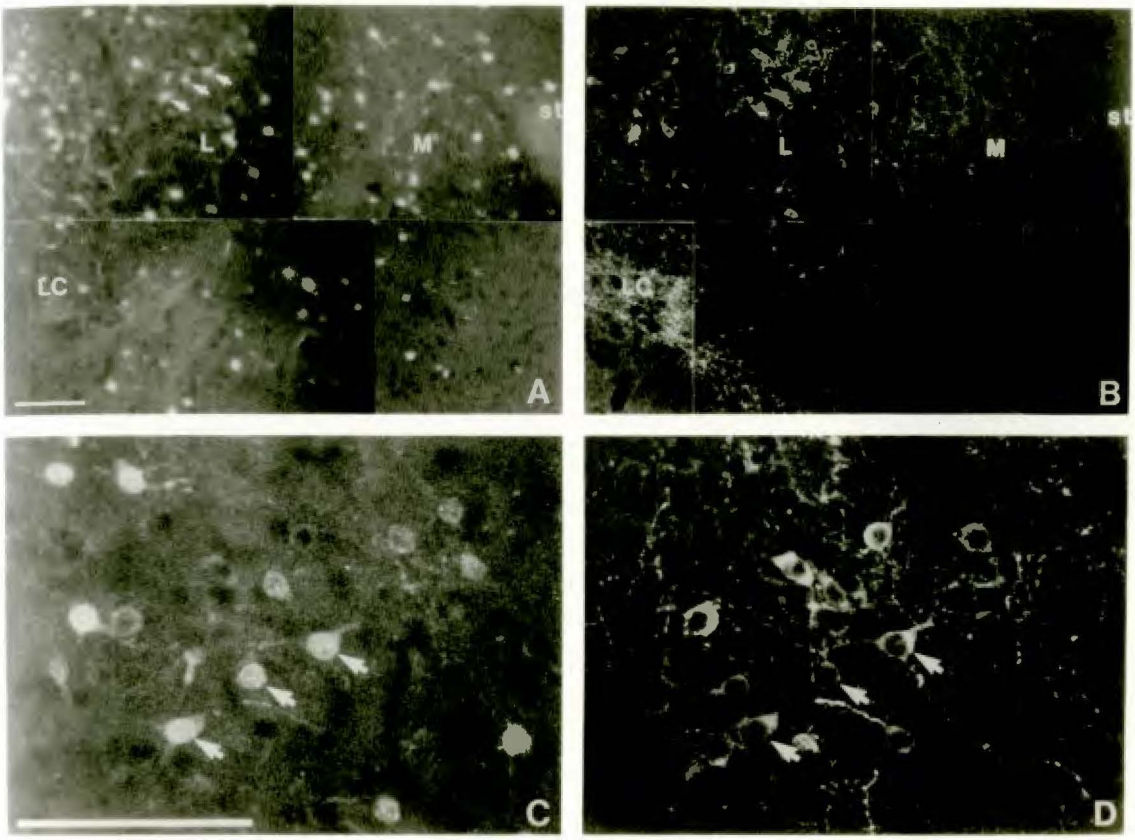
L
M
st
LC
A
L
M
st
LC
B
C
D

Figure 3. Fluorescent photomicrographs of a coronal section through the caudal CeA illustrating the distribution of (A) cells projecting to the PB and (B) cells immunoreactive to corticotropin releasing factor. Figures C (Fast Blue-labeled cells) and D (CRF-ir cells) are high power photomicrographs of 2 double-labeled cells (indicated by white arrows) found within the lateral subdivision of the CeA in A and B. (L, lateral subdivision; LC, lateral capsular subdivision; M, medial subdivision; st, stria terminalis). Bar = 100 um.

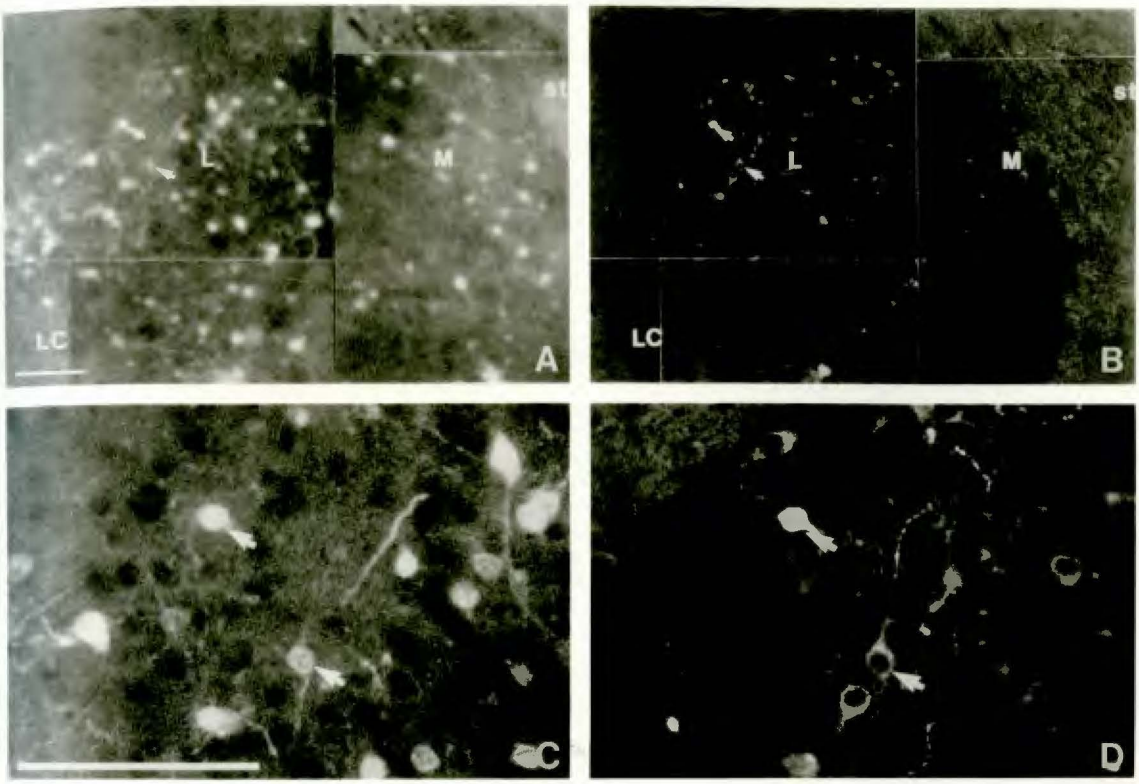
L
M
st
LC
A
L
M
st
LC
B
C
D

Figure 4. Fluorescent photomicrographs of a coronal section through the caudal CeA illustrating the distribution of (A) cells projecting to the PB and (B) cells immunoreactive to somatostatin. Figures C (Fast Blue-labeled cells) and D (SS-ir cells) are high power photomicrographs of 2 double-labeled cells (indicated by white arrows) found within the lateral subdivision of the CeA in A and B. (L, lateral subdivision; LC, lateral capsular subdivision; M, medial subdivision; st, stria terminalis). Bar = 100 um.

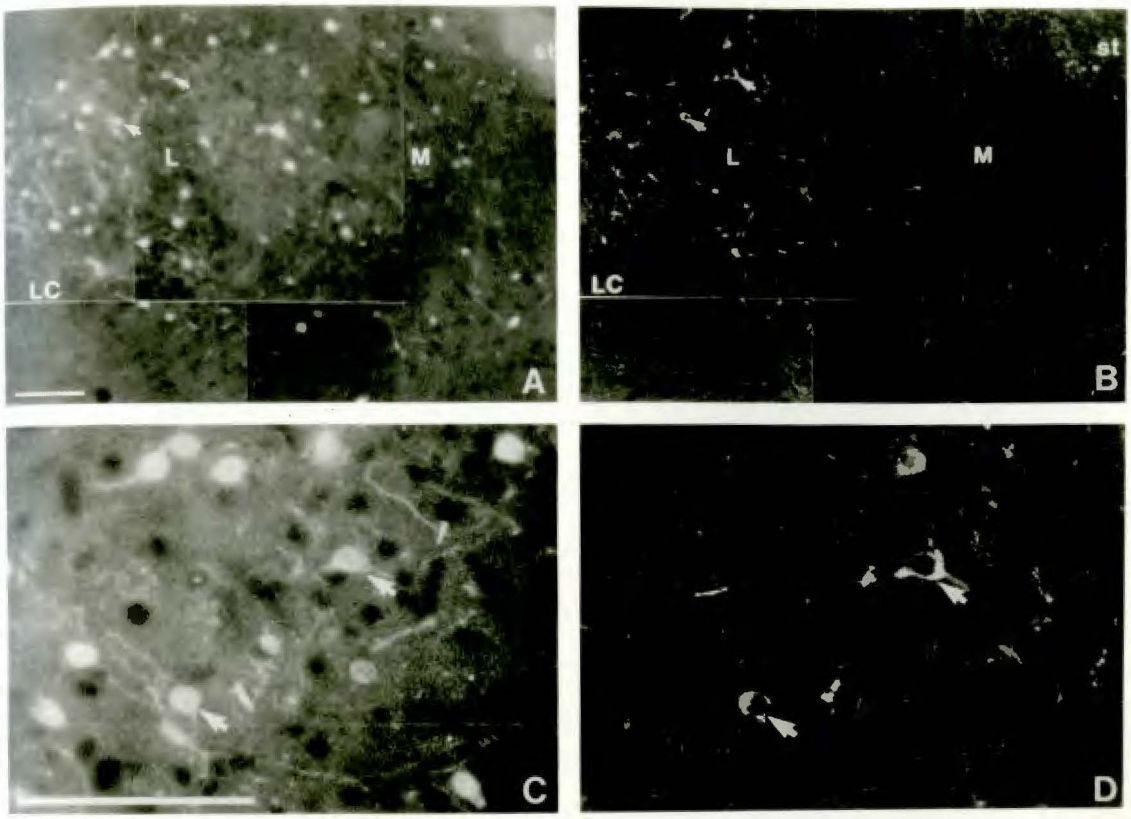
L
M
LC
A
st
L
M
LC
B
C
D

Figure 5. Fluorescent photomicrographs of a coronal section through the caudal CeA illustrating the distribution of (A) cells projecting to the PB and (B) cells immunoreactive to enkephalin. Figures C (Fast Blue-labeled cells) and D (ENK-ir cells) are high power photomicrographs of cells found in A and B. Note the absence of double-labeled cells. (L, lateral subdivision; LC, lateral capsular subdivision; M, medial subdivision). Bar = 100 um.

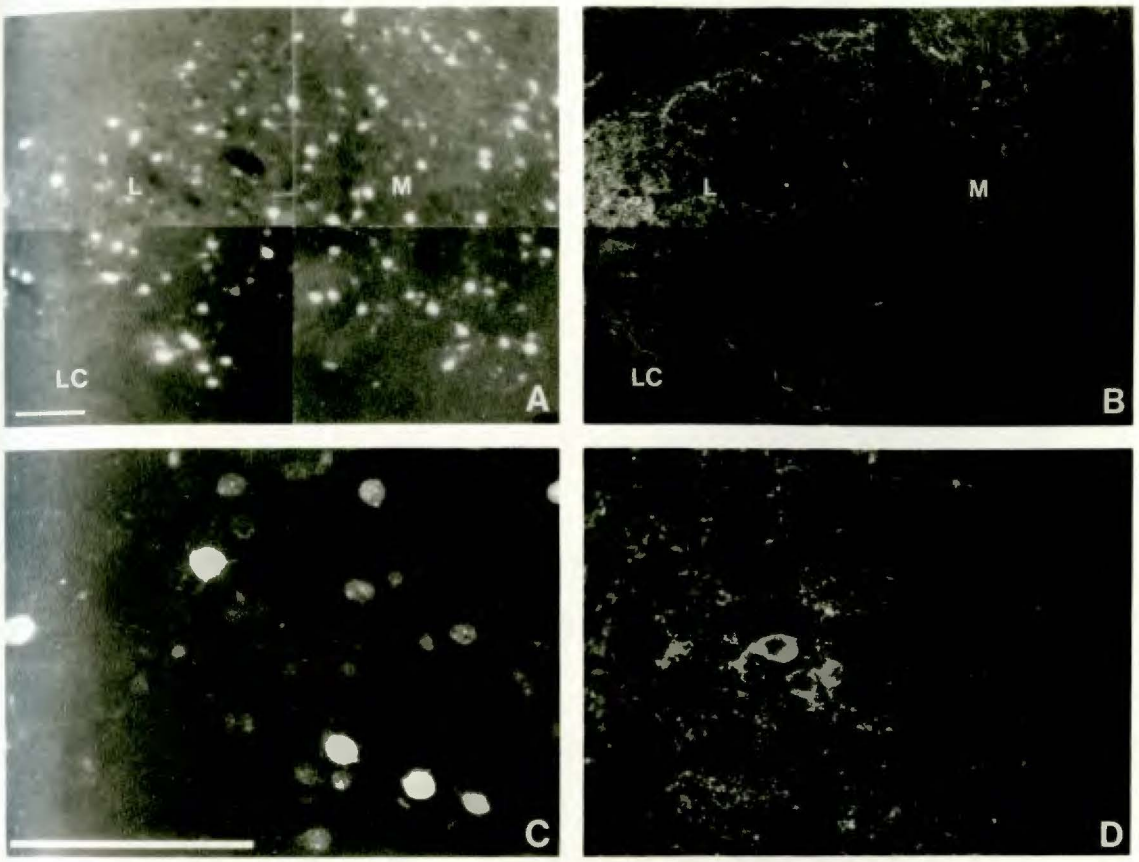
L
M
LC
A
L
M
LC
B
C
D

Figure 6. Summary diagram illustrating the characteristic distributions of Fast Blue (○), peptide-immunoreactive (●), and double-labeled (✱) cells within the CeA. Part A is a line drawing of the CeA, its subdivisions and neighboring nuclei; it is derived from the Paxinos and Watson (1982) atlas. The medial subdivision of the CeA depicted here includes both ventral and medial subdivisions described by Cassell et al. (1985). Parts B-E show the distributions, respectively, of neurotensin-, corticotropin releasing factor-, somatostatin- and enkephalin-immunoreactive cells within the CeA and their relation to both double-labeled and Fast Blue labeled cells.

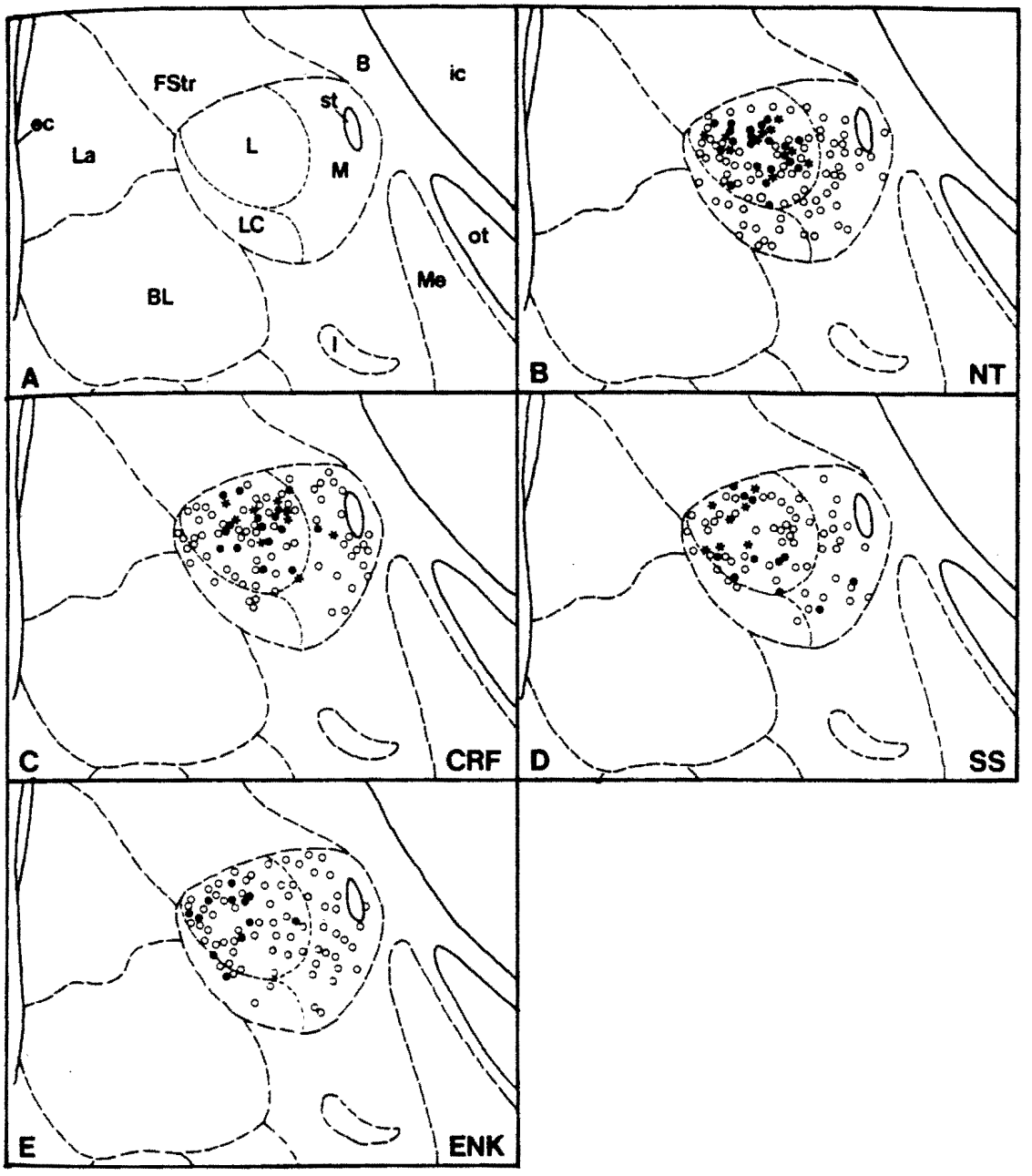
FStr
B
ic
st
ec
La
L
M
LC
ot
Me
BL
I
A
B
NT
C
CRF
D
SS
E
ENK

Table 1. Number and percent of immunoreactive cells in the CeA that contain Fast Blue

antigen	subject	Number of sections sampled	Number of immunoreactive cells	Number of double-labeled cells	Percent of double-labeled cells
CRF	E	14	85	56	66
	F	14	133	73	55
	G	14	183	98	54
NT	E	13	60	31	52
	F	12	75	30	40
	G	10	194	102	53
SS	E	16	129	55	43
	F	16	113	56	50
	G	17	100	31	31
ENK	E	13	81	0	-
	F	11	67	0	-
	G	10	48	0	-

1. The injection sites for subjects E, F and G are presented in Figure 1.

2. The total number of sections that contained immunoreactive cells in each subject.

3. The total number of cells that contained both Fast Blue and immunofluorescence.

CHAPTER IV

PEPTIDERGIC PATHWAYS FROM THE BED NUCLEUS OF THE STRIA TERMINALIS TO THE PARABRACHIAL NUCLEUS

INTRODUCTION

The bed nucleus of the stria terminalis (BST) is a rostral forebrain structure closely related to the amygdala, its major source of afferent input (Weller and Smith, '82; DeOlmos et al., '85;). The BST has traditionally been divided into medial and lateral subdivisions (Krettek and Price, '78; DeOlmos et al., '85). The medial subdivision is extensively connected with nuclei, such as the medial preoptic nucleus, ventromedial hypothalamus and medial nucleus of the amygdala, that are involved in neuroendocrine regulation and reproductive behaviors (Swanson, '76; Saper et al., '76; Krettek and Price, '78). In contrast, the lateral subdivision (BSTL) is distinguished by its reciprocal connections with nuclei involved in central autonomic regulation (Loewy and McKellar, '80). In particular, the BSTL sends a dense projection to the parabrachial nucleus in the pons (Holstege et al., '85). Physiological studies have implicated the PB in a variety of autonomic functions, including fluid regulation (Ohman and Johnson, '86), and cardiovascular (Mraovitch et al., '82) and respiratory (Cohen, '71) responses. In contrast, few studies have examined the role of the BSTL in autonomic function (Swanson and Sharpe, '73; Hilton

and Spyer, '71). However, based on the size of the BSTL-PB pathway, the BSTL may be an important modulator of PB function.

The BST contains many different types of neuropeptide-immunoreactive neurons, each of which exhibits its own characteristic distribution within the BST (Woodhams et al., '83). Neurotensin (NT-ir)-, corticotropin releasing factor (CRF-ir)-, somatostatin (SS-ir)-, and enkephalin (ENK-ir)-immunoreactive neurons are especially numerous within the lateral subdivision of the BST (Woodhams et al., '83; Swanson et al., '83). Possibly, some of these peptidergic neurons may contribute to the BSTL-PB pathway.

Recently, neurons in the central nucleus of the amygdala (CeA) that project to the PB were found to stain for CRF-ir, NT-ir and SS-ir but not for ENK-ir (Moga and Gray, '85b). Other studies have demonstrated that Golgi-stained neurons in the BSTL and CeA are similar in appearance (McDonald, '83) and that both nuclei project to similar areas in the brainstem (Schwaber et al., '82). A study of the peptidergic projection from the BSTL to the PB would provide further data for anatomical comparisons between BSTL and CeA. In this study, using the combined retrograde tracing- immunohistochemical method, I examine whether CRF-, NT-, SS- or ENK- immunoreactivity is present in BSTL neurons that project to the PB.

To accurately map the retrogradely labeled, immunoreactive and double-labeled neurons observed within the BSTL in this experiment, I first examined the cytoarchitecture of the BST in Nissl-stained sections, and in so doing, observed a number of distinct cell groups within the BST. Recently, investigators have noted additional

subdivisions within the BST (e.g., DeOlmos et al., '85; McDonald, '83) but there has been no complete description of the BST subnuclei. Thus, a description of the subnuclear organization of the BST, based on my observations of Nissl-stained sections, is also included in this study. preliminary findings of this study were previously reported (Moga and Gray, '85a; Moga et al., '87).

METHODS

Twenty-one male Long-Evans rats (250-350g) were used in this study. Each animal was anesthetized with 7% chloral hydrate. Injections (50-100 nl) of 2% Fast Blue (D. R. Iling) were made into the parabrachial nucleus with a 1.0 ul Hamilton syringe fitted with a glass micropipette. Injections were made over a 15-minute period, and the pipette was left in place for an additional 10 minutes. After 11-13 days survival, the animals were treated with 150-200 ug colchicine (Sigma) in 10 ul saline injected into the lateral ventricle. Thirty-six to 48 hours later, the animals were reanesthetized with chloral hydrate and then perfused through the heart with 0.01M phosphate-buffered saline (pH 7.6, 37^{o}C) followed by 0.1M phosphate-buffered 4% paraformaldehyde (pH 7.6, 4^{o}C). After perfusion, the skull was placed in a stereotaxic frame (Kopf), and the brain was sliced into coronal blocks. The blocks of brain tissue were post-fixed in 4% paraformaldehyde for 30 minutes to 2 hours and then cut serially on a vibratome (Lancer). Sections from the injection site (40 um) were mounted onto chrom-alum-coated slides. Adjacent coronal sections

(20 um) of the forebrain were collected in four vials of cold phosphate- buffered saline (PBS). Each series of adjacent sections was rinsed in PBS for 20 minutes and then placed in a primary antiserum with gentle agitation for 14-24 hours in a cold room (4°C). After the overnight incubation in primary antibody, the sections were then rinsed in PBS for 20 minutes, incubated in biotinylated goat anti-rabbit IgG (Bethesda Research Laboratory) for 30 minutes at room temperature, rinsed again in PBS for 15 minutes, and incubated in streptavidin-Texas Red (Bethesda Research Laboratory) for 30 minutes. All sections were then transferred to cold PBS, mounted onto chrom-alum-coated slides, and coverslipped with DePeX (BDH Chemicals).

The following primary antisera were used in this study: anti-corticotropin releasing factor (lot #465), provided by Dr. T.L. O'Donohue (Olschowka et al., '82); anti-neurotensin (lot #8351022) and anti-somatostatin (lot #8535027), obtained from the Immunonuclear Corporation (Emson et al., '82; Kohler and Chan-Palay, '82), and anti-met-enkephalin, provided by Dr. R. Elde (Haber and Elde, '82). The antisera were diluted 1:500 (SS, ENK, NT) and 1:2000 (CRF) in a solution containing PBS, 0.1% Triton-X-100 (Mallinckrodt) and 1% normal goat serum. As a control for antisera specificity, 1 ml of each diluted antisera was preincubated with 25-50ug of its respective synthetic neuropeptide for one hour, and the sections processed as usual to determine whether any residual staining remained. Although immunohistochemical staining was eliminated in these controls, it is possible that these antisera may recognize unidentified neuropeptides containing similar amino acid sequences. Thus, the neuropeptide

immunoreactivity detected in this study is more accurately described as neuropeptide-like immunoreactivity (-ir), reflecting our uncertainty as to the precise targets of the antisera.

All material was examined with an Olympus microscope equipped with a 100W mercury light source. Fast Blue was visualized with an excitation wavelength centered at 330-360 nm (Olympus ultraviolet filter system). Texas Red immunofluorescence was viewed with the Olympus green (546 nm) filter system. Cells that contained both retrograde fluorescence and immunofluorescence were detected by switching between filter systems. Sections were photographed with Polaroid coaterless Land pack film 667, ASA 3000. The distributions of labeled cells were plotted with a Leitz Ortholux microscope (filter systems A and NZ) equipped with digital stage position readout heads (Minnesota Datametrics, MD-1). The x- and y-coordinates of the labeled neurons were recorded by a Rockwell AIM 65 microcomputer and then plotted onto an x-y plotter. After plotting, the slides were soaked in xylene to remove the coverslips, and then counterstained with thionin to determine the subnuclear location of the labeled cells.

For the cytoarchitectural study, 15 micron sections were cut from paraffin embedded rat brains in both the coronal and sagittal planes, and then stained with thionin. These sections were examined and photographed to determine the subnuclear boundaries within the BST. Neurons in the BST were characterized according to their size and shape, the distinctiveness of their nucleolus, and the pattern and intensity of their cytoplasmic staining. Clusters of neurons with identical characteristics were defined as a subnucleus.

RESULTS

BST Subnuclei

My observations of the BST subnuclei agree, in general, with the brief description of DeOlmos et al., '85, and so, I have retained their terminology while preparing the following description. Based on its cytoarchitecture and connections, the BST may be divided into medial, lateral and ventral subdivisions (Moga et al., '87). The medial BST begins at the dorsomedial border of the nucleus accumbens and extends to the rostral border of the thalamus; thus, it spans the entire rostro-caudal length of the BST. This subdivision may be divided into anterior medial, posterior medial, posterior intermediate, subventricular, intermediate and ventral medial subnuclei. The anterior medial (AM) subnucleus forms the most rostral extent of the medial BST (Fig. 1A). AM consists of a heterogeneous cell population which includes small, ovoid, dark staining cells with little cytoplasm and large, medium staining cells with coarse granular cytoplasm. Caudally, cells in AM merge imperceptibly with those in the posterior medial subnucleus; however, these two nuclei are separated by the body of the post-commissural stria terminalis. The intermediate (IM) subnucleus forms a wedge of cells rostrally between AM and the anterior lateral (AL) subnucleus, and is just dorsal to the anterior commissure (Fig. 1B). In succeeding sections, IM can be distinguished by its medium-sized, pale-staining cells which are located between AL and the receding anterior commissure (Fig. 1C). Ventral medial (VM) BST

consists of loosely-packed, medium-staining, fusiform-shaped cells located beneath the anterior commissure and oriented parallel to it (Fig. 1B). VM extends caudally, ventral and lateral to the receding anterior commissure, to form a closely packed, ovoid group surrounded by the IM, posterior lateral and ventral lateral BST subnuclei, and the parastrial nucleus (Fig. 1D). The posterior medial (PM) subnucleus consists of medium staining, tightly packed neurons partially encapsulated by a cell-poor area (Fig. 1E-G). Rostrally, PM is a distinctive round cluster located above the receding anterior commissure (Fig. 1E); caudally, as the fibers from the fornix and stria medullaris descend, PM shifts to form a tight band of cells oriented diagonally (Fig. 1F,G). Posterior intermediate (PI) BST lies between the band-shaped PM, medially, and posterior lateral and preoptic BST, laterally (Fig. 1G). PI consists of medium staining neurons which are similar to, but more loosely packed, than those in PM. Subventricular BST (SV), a small oval-shaped subnucleus located beneath the surface of the lateral ventricle, consists of small, ovoid, closely packed neurons with indistinct nucleoli (Fig. 1D).

The lateral BST can be divided into dorsal, ventral, posterior, supracapsular and juxtacapsular subnuclei. The dorsal lateral (DL) subnucleus is an oval-shaped, homogeneous cluster of round, lightly-staining neurons with a prominent nucleolus and little cytoplasm (Fig. 1B,C). This distinctive cell cluster is found throughout the rostral half of the BST, dorsal to the anterior commissure and adjacent to the caudate-putamen and internal capsule. With the crossing of the anterior commissure, DL moves dorsally to become continuous with cells

in the supracapsular (SC) subnucleus. SC consists of cells encapsulated within the fibers of the stria terminalis; these cells resemble a number of BST cell types, predominantly those in DL, and are found throughout the course of the stria (Fig. 1E). DL is surrounded medially and ventrally by the anterior lateral (AL) subnucleus (Fig. 1B,C). AL neurons are medium-staining and teardrop-shaped with an indistinct nuclear border and little cytoplasm; they are oriented parallel to the strial fibers which surround DL. The posterior lateral (PL) subnucleus first appears at mid-BST levels (i.e., the crossing of the anterior commissure) as scattered cells beneath AL and DL (Fig. 1C). More caudally, PL is found adjacent to the juxtacapsular subnucleus and the internal capsule in a position formerly occupied by AL and DL (Fig. 1D-F). Cells within PL are medium-sized, multipolar and medium-staining with one to two nucleoli. The juxtacapsular (JXC) subnucleus is a loosely packed, lens-shaped cluster of small, round, lightly-staining cells lying between the internal capsule, laterally, and DL, AL and PL, medially (Fig. 1D).

Ventral BST includes the ventral lateral and preoptic BST subnuclei, and the parastrial nucleus. When viewed in the sagittal plane, ventral lateral (VL) BST appears as two clusters of cells. Rostral VL is a heterogeneous cell cluster distinguished by its medium-dark staining, closely packed, fusiform cells oriented in a horizontal (i.e., medial to lateral) direction (Fig. 1B). Caudal VL contains large, darkly staining, closely packed, multipolar cells with prominent nucleoli; these cells resemble the preoptic neurons which are scattered beneath VL (Fig. 1D). The parastrial (PS) nucleus is a

lens-shaped nucleus located beneath the anterior commissure between the BST and the cell-poor strial part of the preoptic area (Raisman and Field, '73; Simerly et al., '84). PS contains small, darkly staining, ovoid to fusiform cells which are tightly packed and are oriented diagonally from the anterior commissure to VL (Fig. 1B-E). The PS has been considered separate from the BST due to its lack of amygdala input (Raisman and Field, '73; Simerly et al., '84). However, cytoarchitecturally, the PS appears continuous with VL at rostral BST levels. Both VL and PS contain similar neuropeptide-immunoreactive cells and fibers. And, the ventral BST cell groups (i.e., VL, PS and the preoptic BST) are extensively connected with the hypothalamus (Moga et al., '87). These findings suggest that PS is related to the other ventral BST subnuclei and have led us to include the PS in this description.

The preoptic (PO) subnucleus consists of large, multipolar, dark-staining neurons and is located caudally, ventral to PI and PM. PO may be divided into medial and lateral portions. Lateral PO is adjacent to the internal capsule and dorsal to the medial forebrain bundle; its neurons are oriented perpendicular to the descending strial fibers (Fig. 1G; McDonald, '83). Medial PO forms an ovoid cluster, and has been previously described as the preoptic continuation of the BST (Fig. 1F; Swanson, '76).

Distribution of Retrogradely Labeled Neurons

After Fast Blue injections into the parabrachial nucleus, retrogradely labeled neurons were found throughout the forebrain in

nuclei previously shown to project to the PB (e.g., central nucleus of the amygdala, lateral hypothalamus, paraventricular hypothalamus). These afferent cell populations are described in detail in another study (Moga et al., in preparation). Within the BST, retrogradely labeled neurons were numerous in the lateral subdivision throughout its rostrocaudal extent. However, the distribution of the labeled neurons within BSTL varied with the site of injection in the PB. After injections centered in the external lateral PB subnucleus (Fig. 2A; for PB subnuclei, see Fulwiler and Saper, '84), many intensely labeled neurons were found in the dorsal lateral, anterior lateral and supracapsular BST subnuclei with only a small number of lightly labeled neurons in the ventral lateral and posterior lateral subnuclei. In contrast, after injections centered in either the ventral lateral or medial PB subnuclei (Fig. 2B), a large number of intensely labeled neurons was found in the posterior lateral subnucleus with few labeled neurons in DL, AL PO, VL, and VM. When injections included the rostral, lateral portion of the medial PB subnucleus (Fig. 2C), neurons in the ventral lateral BST subnucleus showed intense labeling. Injections into the caudal waist area of PB (Fig. 2D) showed a mixed pattern of labeling; many labeled cells were found throughout the lateral BST subnuclei.

After a lateral PB injection which also included the caudal part of the pedunculopontine nucleus, the retrograde labeling in the BST was identical to that seen after injections restricted to the PB. However, in this case, numerous retrogradely labeled neurons were observed in the medial preoptic area; very few of these cells were double-labeled

with the peptides examined here, in agreement with the recent report of Swanson et al. ('87).

Distribution of Immunoreactive Neurons

Although CRF-, NT- and SS-immunoreactive neurons were previously reported in the BST (Swanson et al., '83; Woodhams et al., '83; Gray and Magnuson, '87), their subnuclear organization was not emphasized. Neurotensin-immunoreactive (NT-ir) cells were numerous in the dorsal lateral subnucleus where they formed a discrete oval group coextensive with DL. Through successively more caudal sections, this NT-ir group moved dorsally to become continuous with NT-ir cells in the supracapsular subnucleus. Caudally, NT-ir cells formed a small cluster in the medial part of the preoptic BST subnucleus. A few NT-ir cells were also found in PL, AM, PS, VM, PI, PM and lateral PO.

At rostral levels, somatostatin-immunoreactive (SS-ir) cells were less numerous than NT-ir cells. They showed a slight concentration in DL but were generally scattered throughout PL, AM, PS and along the dorsal and ventral surfaces of the anterior commissure. SS-ir neurons were especially numerous in the caudal BST subnuclei, particularly in the posterior lateral, posterior intermediate and lateral preoptic subnuclei. In PL, they formed a distinct cluster located between the internal capsule and the postcommissural stria terminalis. A few SS-ir cells were also found amidst the fibers of the receding anterior commissure in the intermediate subnucleus.

Enkephalin-immunoreactive (ENK-ir) neurons were numerous throughout DL with lesser numbers found in VL, PL, SC, AM, and VM. A small cluster of ENK-ir cells was located rostrally between the parastrial nucleus and the ventral lateral subnucleus. Only a few ENK-ir cells were found caudal to the crossing of the anterior commissure, and those were primarily in PM and PI.

Corticotropin releasing factor-immunoreactive (CRF-ir) neurons were the most numerous of the four types of peptidergic neurons examined in the BST. At rostral levels, CRF-ir cells were concentrated in two groups: one, in the dorsal lateral subnucleus, and the other, bridging both PS and VL. After the PS-VL split at more caudal levels, CRF-ir cells were found in both PS and VL, and in lesser numbers, in AM and PL. Most caudally, CRF-ir cells were located in PM and PL, and, most abundantly, in lateral PO.

Double-labeled neurons

Retrogradely labeled neurons that also contained either SS-ir, CRF-ir or NT-ir (i.e., double-labeled neurons) were most numerous in the dorsal lateral BST subnucleus (Figs. 3,4,6-8), particularly after injections centered in the external lateral PB subnucleus (Fig. 2A). Double-labeled cells in the posterior lateral and ventral lateral BST subnuclei were few, and these were often found after injections into, respectively, the medial portion of the medial PB (Fig. 2B) and the lateral portion of medial PB (Fig. 2C). Two injections which included most of the PB subnuclei produced comparable and extensive retrograde

labeling in the BST. In these two cases, the retrogradely labeled, immunoreactive, and double-labeled neurons in the BST were counted to assess the relative contribution of each neuropeptide to the BST-PB pathway (Table 1). Cell counts of labeled neurons within the dorsal lateral subnucleus were also included in Table 1 since 51, 77 and 84% of the cells double-labeled for, respectively, SS-ir, CRF-ir and NT-ir were located in the DL subnucleus. The distributions of double-labeled cells within the BST subnuclei are depicted in Figures 6-9. These BST levels were chosen because they contain the majority of neuropeptide-containing cells which project to the PB.

Corticotropin releasing factor. Cells labeled with both CRF-ir and Fast Blue were numerous throughout the dorsal lateral subnucleus (Figs. 3,6). A few double labeled cells were also found in VL, AL, PL and SC (Fig. 6). Fourteen percent of the retrogradely labeled neurons in the BST were CRF-immunoreactive (Table 1). Sixteen percent of the CRF-ir neurons in the BST, and 33% of the CRF-ir neurons in the dorsal lateral subnucleus, were retrogradely labeled (Table 1). Elsewhere in the forebrain, retrogradely labeled CRF-ir neurons were located in the central nucleus of the amygdala, intercalated nuclei of the amygdala, lateral hypothalamus, medial parvocellular paraventricular hypothalamus and lateral preoptic area (Moga and Gray, '85b,c,d; Chapters III,V).

Neurotensin. Many neurons in the dorsal lateral BST subnucleus were labeled for both NT-ir and Fast Blue (Figs. 4,7). An occasional NT-ir double-labeled cell was also found in the adjacent AL and SC (Figs. 4,5,7). Similarly to CRF-ir, 14% of the retrogradely labeled neurons in the BST contained NT-ir (Table 1). Twenty percent of the

NT-ir cells in the BST, and 34% of the NT-ir cells in the dorsal lateral subnucleus, were retrogradely labeled (Table 1). NT-ir retrogradely labeled cells were also seen in the central nucleus of the amygdala, intercalated nuclei of the amygdala, sublenticular substantia innominata, preoptic area, medial parvocellular paraventricular hypothalamus, lateral hypothalamus, retrochiasmatic area, zona incerta and periaqueductal gray (Moga and Gray, '85b,c,d; Chapters III,V).

Somatostatin. Cells double-labeled for SS-ir and Fast Blue were found in DL, AL, PL and SC with a slight concentration in DL (Fig. 8). In contrast to CRF-ir and NT-ir, only 4% of the retrogradely labeled cells in the BST were SS-ir (Table 1). Fourteen percent of the SS-ir neurons in the BST, and 50% of the SS-ir neurons in the dorsal lateral subnucleus, were retrogradely labeled (Table 1). Somatostatin-immunoreactive double-labeled cells were also seen in the central nucleus of the amygdala, lateral hypothalamus and medial parvocellular paraventricular hypothalamus (Moga and Gray, '85b,d; Chapters III,V).

Enkephalin. Enkephalin-immunoreactive neurons in the BST were never double-labeled with Fast Blue after PB injections even though both ENK-ir and retrogradely labeled cells were concentrated in DL (Fig. 9). However, double-labeled ENK-ir cells were observed in the medial parvocellular paraventricular hypothalamus, and less commonly, in the medial preoptic area (Moga and Gray, '85d).

DISCUSSION

The principal finding to emerge from this study is that CRF-ir, NT-ir and SS-ir neurons in the lateral BST provide a substantial peptidergic input to the parabrachial nucleus, and that ENK-ir neurons in the BST do not contribute to this pathway. Similarly, in a previous study, we found that neurons in the CeA that project to the PB contain CRF-ir, NT-ir and SS-ir but not ENK-ir (Moga and Gray, '85b). Recently we have demonstrated that many CRF-ir and NT-ir neurons in the perifornical lateral hypothalamus (LH) and retrochiasmatic hypothalamus (RCh) project to the PB (Moga and Gray, 85d). The PB also receives peptidergic input from NT-ir, CRF-ir and SS-ir neurons in the nucleus of the solitary tract (NTS, Mantyh and Hunt, '84; Milner and Pickel, '86a; Herbert et al., '87).

The results from the present study suggest that the BSTL projection to the PB is topographically organized. Retrogradely labeled neurons in the dorsal lateral BST subnucleus were particularly numerous after fast blue injections which included the external lateral and central lateral PB subnuclei, whereas, labeled neurons in posterior lateral BST neurons were numerous after injections which included the medial PB subnucleus. In addition, injections into the waist area of the PB produced a comparable amount of retrograde cell labeling in both DL and PL. The ventral lateral BST may project to a discrete area within the PB; cell labeling in this small BST subnucleus was only noted after injections which included the lateral portion of the rostral, medial PB subnucleus. As further evidence that the BSTL

descending pathways are topographically organized, Gray and Magnuson ('87) found that the BSTL projection to the dorsal vagal complex originates largely from the posterior lateral BST. Similarly, the BSTL projection to the ventral lateral medulla also arises from a limited population of neurons within the BSTL, namely the posterior lateral subnucleus (unpublished observations).

Similarities between CeA and BSTL

Recently, a number of investigators have presented evidence in support of the view that the BSTL and CeA constitute one anatomical entity (e.g., DeOlmos et al., '85; Holstege et al., '85). For example, a continuum of cells stretching from the BSTL through the sublenticular substantia innominata to the CeA is labeled after retrograde tracer injections into the dorsal vagal complex (Schwaber et al., '82), raphe nuclei (Holstege et al., '85) and parabrachial nucleus (Moga and Gray, '85b). Golgi-stained neurons in the lateral BST resemble those found in the central nucleus of the amygdala (McDonald, '83); and similar neuropeptides are abundant in both the BSTL and CeA (Woodhams et al., '83; DeOlmos et al., '85).

As additional evidence of the close relation between the BSTL and CeA, we have found that the BSTL projection to the PB is similar to the CeA-PB pathway in a number of respects. Both lateral BST and CeA project heavily to the PB, and both pathways terminate in similar PB subnuclei (Moga et al., '86). The peptidergic projections from the CeA and BSTL to the PB arise from largely circumscribed areas within these

nuclei, namely the DL and CeL; these projections have been found to stain for identical neuropeptides; and, they terminate primarily within the external lateral PB subnucleus (Moga and Gray, '85b; present study). The pathways from the BSTL and CeA to the dorsal vagal complex also originate from specific subnuclei (i.e., posterior lateral BST and CeM), and also contain similar neuropeptides (Gray and Magnuson, '87). These findings would suggest that subdivisions in the CeA (Wray and Hoffman, '83; Cassell et al., '86) may have counterparts in the lateral BST. In particular, the dorsal lateral BST subnucleus may correspond to the lateral subdivision of the CeA, and the posterior lateral BST, to CeM (Gray and Magnuson, '87).

However, differences may exist between the lateral BST and CeA. For example, BSTL contains two subnuclei (i.e., the ventral lateral and anterior lateral subnuclei) that do not appear to have counterparts in the CeA. In particular, the anterior lateral subnucleus resembles both DL and PL in its connections and neuropeptides; and yet, its distinct Nissl-staining sets its apart from both of these subnuclei and from the CeA. Like the other ventral BST subnuclei, the ventral lateral subnucleus is extensively connected with the hypothalamus; in addition, it receives heavy input from the CeA, input that is not reciprocated. These differences suggest that the BSTL and CeA are not entirely homologous.

Peptide Pathways of BST

Few studies have examined the BST efferent cell populations for their peptide content. Recently, Gray and Magnuson ('87) demonstrated

that CRF-, NT-, SS- and substance P-immunoreactive neurons in the BST project to the dorsal vagal complex. In this study we have found a heavy peptidergic projection to the parabrachial nucleus which also originates from the CRF-ir, NT-ir and SS-ir neurons. Besides its efferents to the amygdala and brainstem, the BST also projects to the hypothalamus (Swanson and Cowan, '79) but the peptides in this projection are unknown.

In contrast, the neuropeptide content of the BST afferent cell populations, particularly those in the amygdala, has been studied extensively. Using a combination of stria terminalis transections, lesions of the amygdala and immunohistochemistry, the amygdala projection to the BST has been found to stain for: neurotensin (Uhl et al., '78), enkephalin (Uhl et al., '78; Rao et al., '87), substance P (Sakanaka et al., '81), vasoactive intestinal polypeptide (VIP, Roberts et al., '80b; Eiden et al., '85), somatostatin (McDonald, '87) and neuropeptide Y (Allen et al., '84). The BST also receives VIP input from the mesencephalon, most probably from the raphe nuclei (Eiden et al., '85), and calcitonin gene-related peptide input from the PB (Shimada et al., '85).

Functional Considerations

The bed nucleus of the stria terminalis is extensively interconnected with nuclei, such as the PB, CeA, nucleus of the solitary tract and paraventricular hypothalamus, that are involved in central cardiovascular regulation (Loewy and McKellar, '80). However, there has been little physiological evidence for a cardiovascular role for

the BST. Vasodepressor responses have been noted after electrical stimulation of the dorsal preoptic hypothalamus; this area may include the ventral BST subnuclei (Kabat et al., '35; Hilton and Spyer, '71; Faiers et al., '76). In contrast, numerous physiological studies of the CeA have been completed. Electrical stimulation of the CeA elicits respiratory activation and a pressor response (Galeno and Brody, '83; Harper et al., '84). These responses are strikingly similar to those obtained from stimulation of the PB (Mraovitch et al., '82; Frysinger et al., '84). Thus, the cardiovascular and respiratory responses of the CeA may be mediated through its projections to the PB. In light of its similarities to the CeA, the BSTL and its projection to the PB may also be important in both cardiovascular and respiratory control.

A few studies have implicated the lateral BST in neuroendocrine regulation. For example, in both ovarectomized, estrogen-primed and proestrus female rats, electrical stimulation of the lateral BST prevents luteinizing hormone discharge and blocks ovulation (Beltramino and Taleisnik, '80). In anesthetized rats, electrical stimulation of the postcommissural lateral BST results in decreased plasma corticosterone levels (Dunn, '87). These findings are similar to those obtained from electrical stimulation of the CeA (Beltramino and Taleisnik, '78; Dunn and Whitener, '86), and suggest that the CeA and BSTL play similar roles in neuroendocrine regulation.

Several lines of evidence suggest that the BSTL may be involved in fluid and electrolyte balance. Fibers immunoreactive to angiotensin II, a potent dipsogen, are numerous within the dorsal part of the BSTL (Lind et al., '85). Microinjections (48.6 picomoles) of angiotensin II

into this area of the BSTL elicit a drinking response (Swanson and Sharpe, '73). Furthermore, the lateral BST is connected with several nuclei, including the PB, that have been implicated in fluid regulation. For example, rats with bilateral ablations of the external lateral PB subnucleus exhibit an exagerrated drinking response after systemic administration of angiotensin II (Ohman and Johnson, '86). As the dorsal lateral BST sends a dense projection to the external lateral PB (unpublished observations), this pathway may possibly relay information concerning angiotensin-induced thirst.

The significance of NT-ir, CRF-ir and SS-ir in BSTL neurons that project to the PB is unclear. Microinjections of neuropeptides into central autonomic nuclei elicit a variety of visceral responses (e.g., Kalivas et al., '82; Denavit-Saubie et al., '82). However, there has been no study examining the effects of CRF, NT or SS microinjections into the PB; such a study may help elucidate the function of these neuropeptides in the BSTL-PB pathway.

Figure 1. Photomicrographs of 30 micron thick, thionin-stained coronal sections through seven levels (rostral to caudal, A-G) of the BST illustrating the BST subnuclei. Approximate distance from bregma is indicated at the top of each photomicrograph. (ac, anterior commissure; AL, anterior lateral subnucleus; AM, anterior medial subnucleus; BAC, bed nucleus of the anterior commissure; DL, dorsal lateral subnucleus; fx, fornix; ic, internal capsule; IM, intermediate subnucleus; JXC, juxtacapsular subnucleus; PI, posterior intermediate subnucleus; PL, posterior lateral subnucleus; PM, posterior medial subnucleus; PO, preoptic subnucleus; PS, parastrial nucleus; SC, supracapsular subnucleus; sm, stria medullaris; st, stria terminalis; SV, subventricular subnucleus; VL, ventral lateral subnucleus; VM, ventral medial subnucleus).

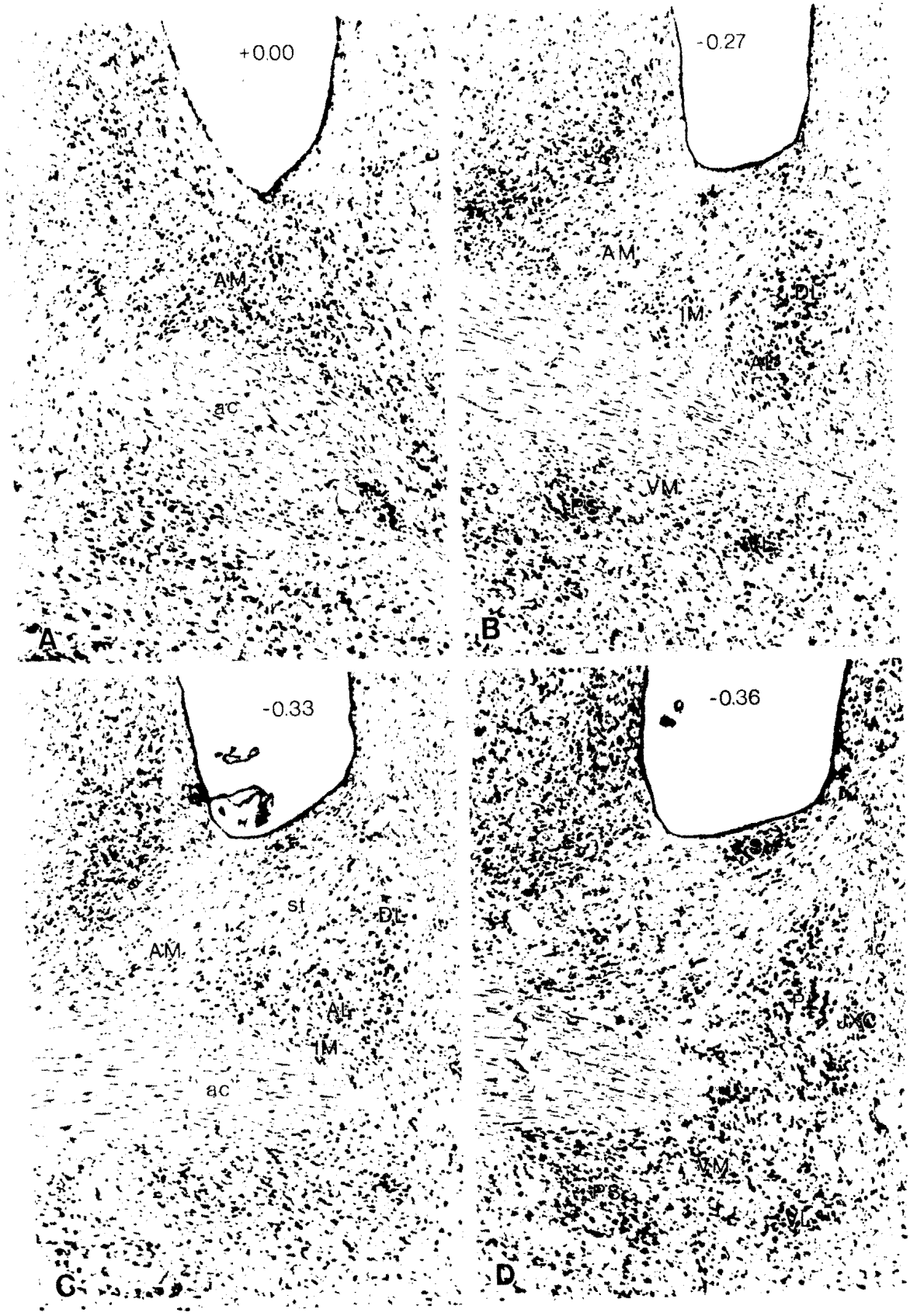
+0.00
AM
ac
A
-0.27
AM
IM
DL
VM
PS
B
-0.33
st
DL
AM
AL
IM
ac
C
-0.36
VM
PS
D

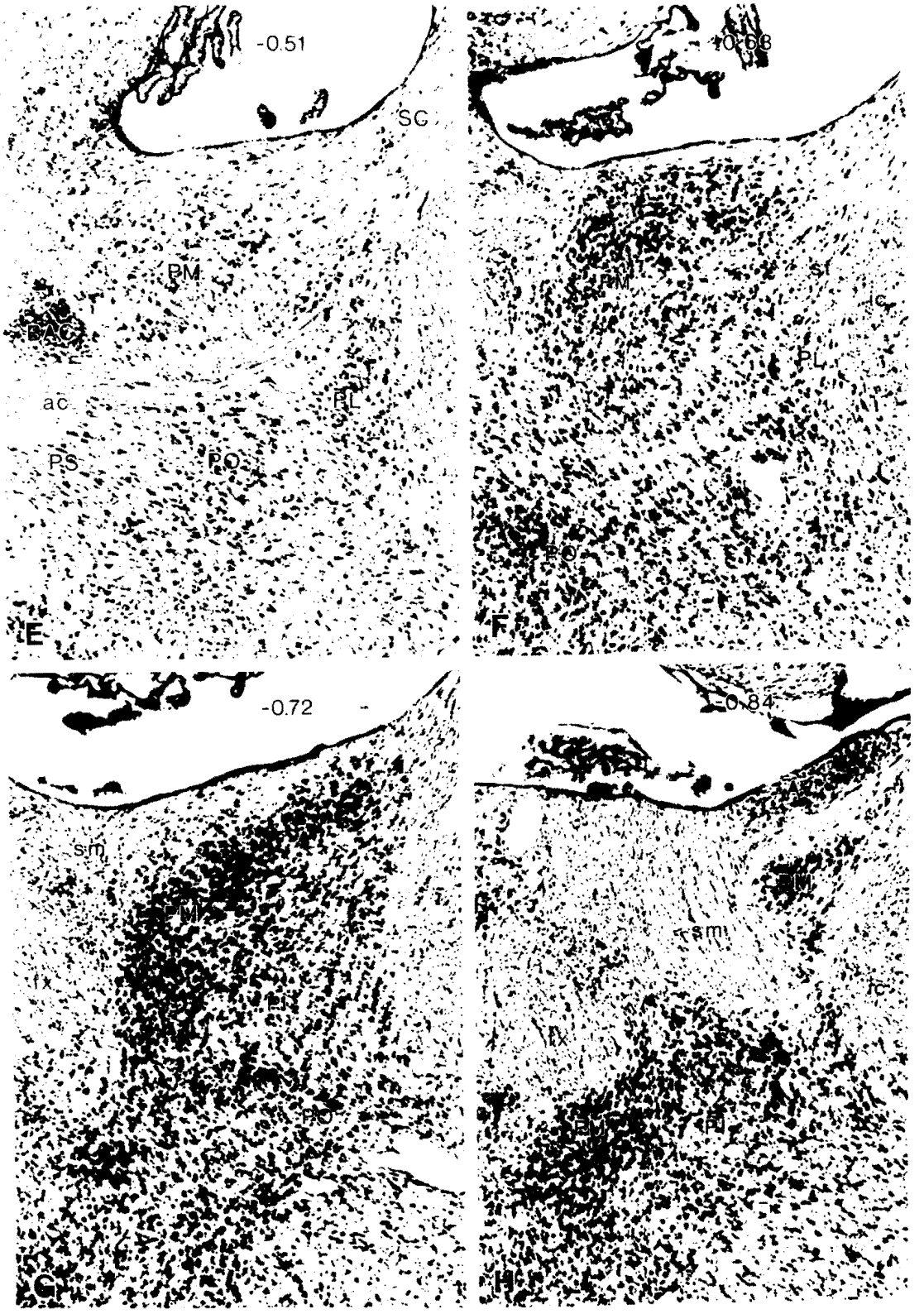
-0.51
SC
PM
BAC
ac
PS
PO
PL
E
-0.68
PM
st
ic
PL
PO
F
-0.72
sm
PM
fx
PL
PO
G
-0.84
PM
sm
ic
fx
PL
PM
H

Figure 2. Drawings of representative fast blue injection sites in the parabrachial nucleus. Shading indicates the center of each injection site and the spread of the fluorescent dye.

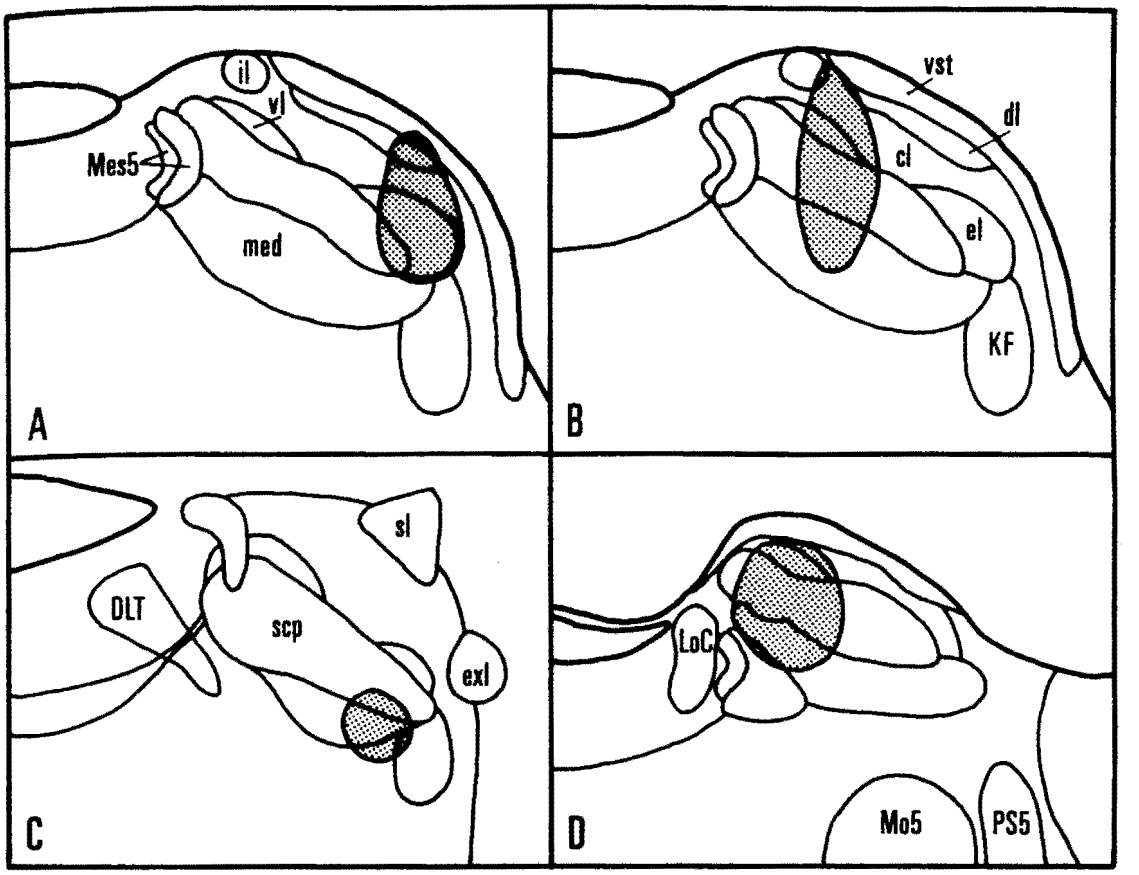
il
vl
Mes5
med
A
vst
dl
cl
el
KF
B
sl
DLT
scp
exl
C
LoC
Mo5
PS5
D

Figure 3. Composite fluorescent photomicrographs of a coronal section through mid-level BST illustrating the distribution of (A) cells projecting to the PB, and (B) cells immunoreactive to corticotropin releasing factor (CRF). Double-labeled cells (indicated by white arrows) were numerous, particularly in the dorsal lateral subnucleus. Bar = 100 um. (DL, dorsal lateral subnucleus; AL, anterior lateral subnucleus; LV, lateral ventricle; ic, internal capsule).

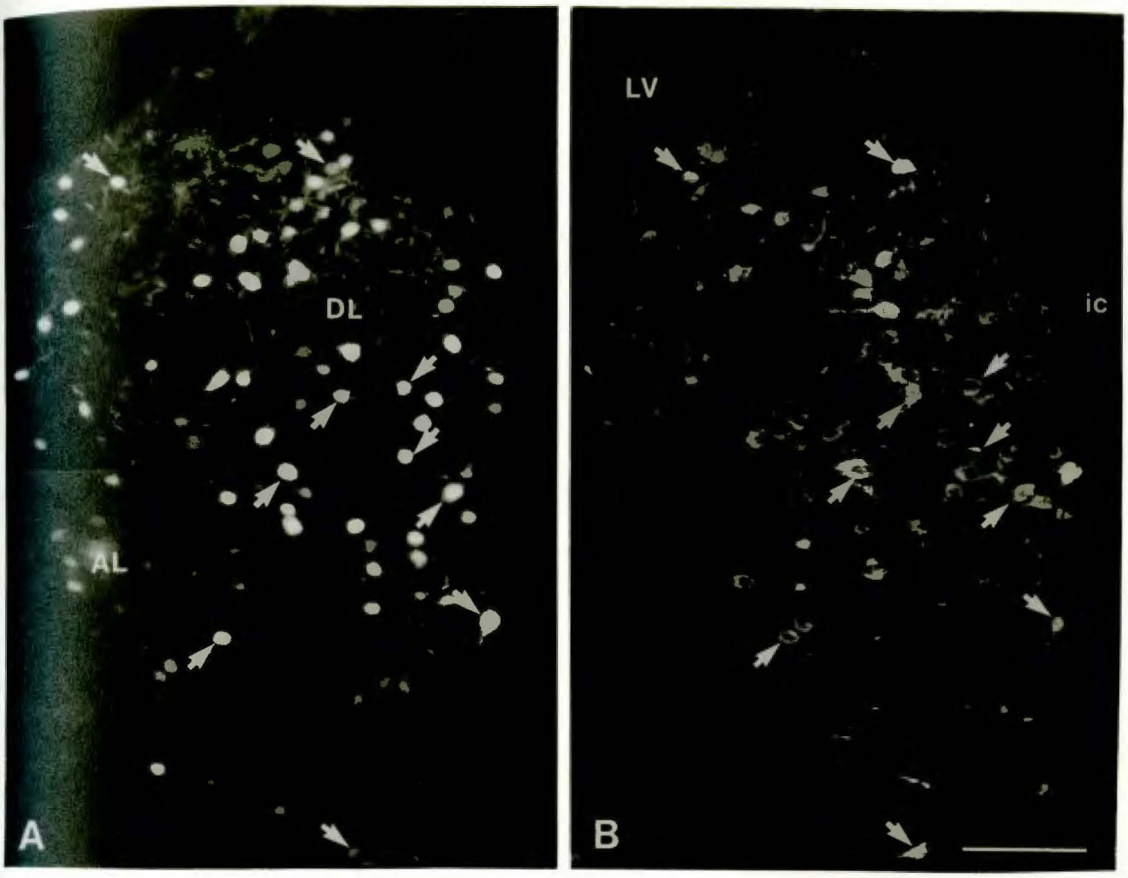
DL
AL
A
LV
ic
B

Figure 4. Fluorescent photomicrographs of a coronal section through the dorsal lateral BST subnucleus illustrating (A) cells retrogradely labeled after fast blue injections in the PB, and (B) cells immunoreactive to neurotensin. Double-labeled cells (indicated by white arrows) were often observed in this subnucleus. Bar = 100 um.

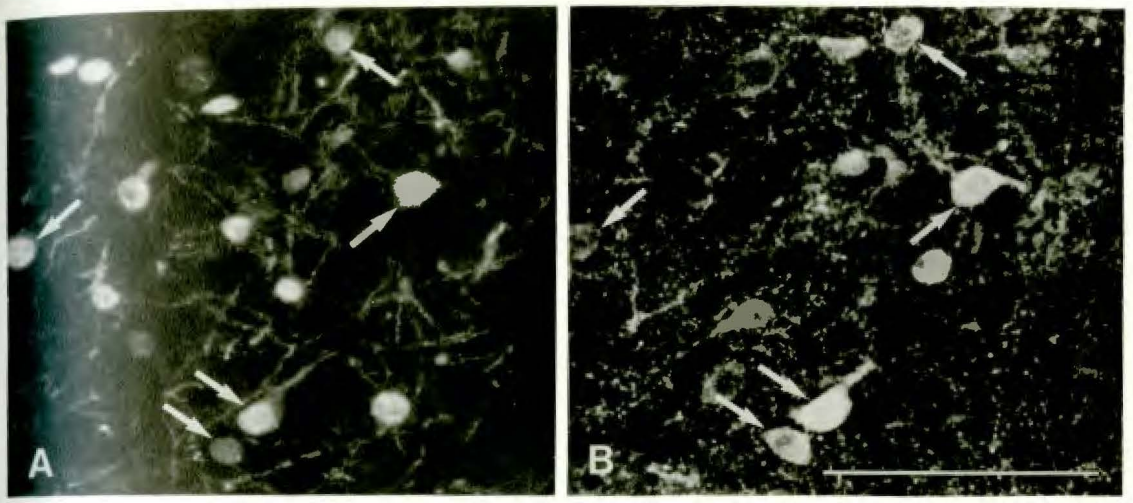
A
B

Figure 5. Fluorescent photomicrographs of a coronal section through the the supracapsular BST subnucleus illustrating (A) cells projecting to the PB, and (B) cells immunoreactive to NT. Double-labeled cells (indicated by white arrows) were occasionally observed in this subnucleus. Cells in SC were characteristically found embedded within the ascending fibers of the stria terminalis (st). Bar = 100 um. (ic, internal capsule; LV, lateral ventricle).

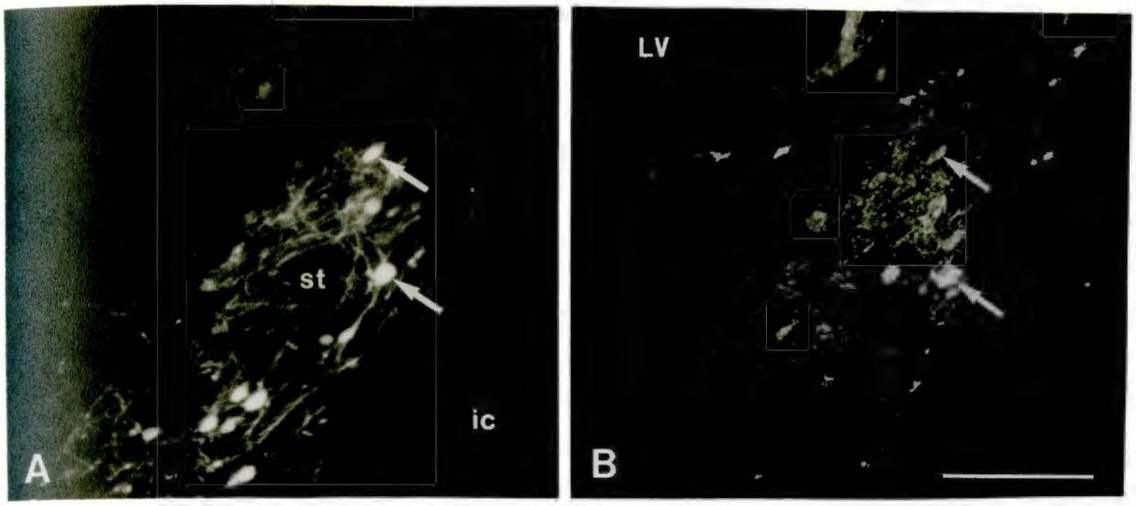
st
ic
A
LV
B

Figure 6. Line drawings of four coronal sections through the BST (A-D, rostral to caudal) illustrating the distributions of Fast Blue (▲), CRF-immunoreactive (△) and double-labeled (*) cells found with the BST and adjacent preoptic nuclei after Fast Blue injections into the PB.

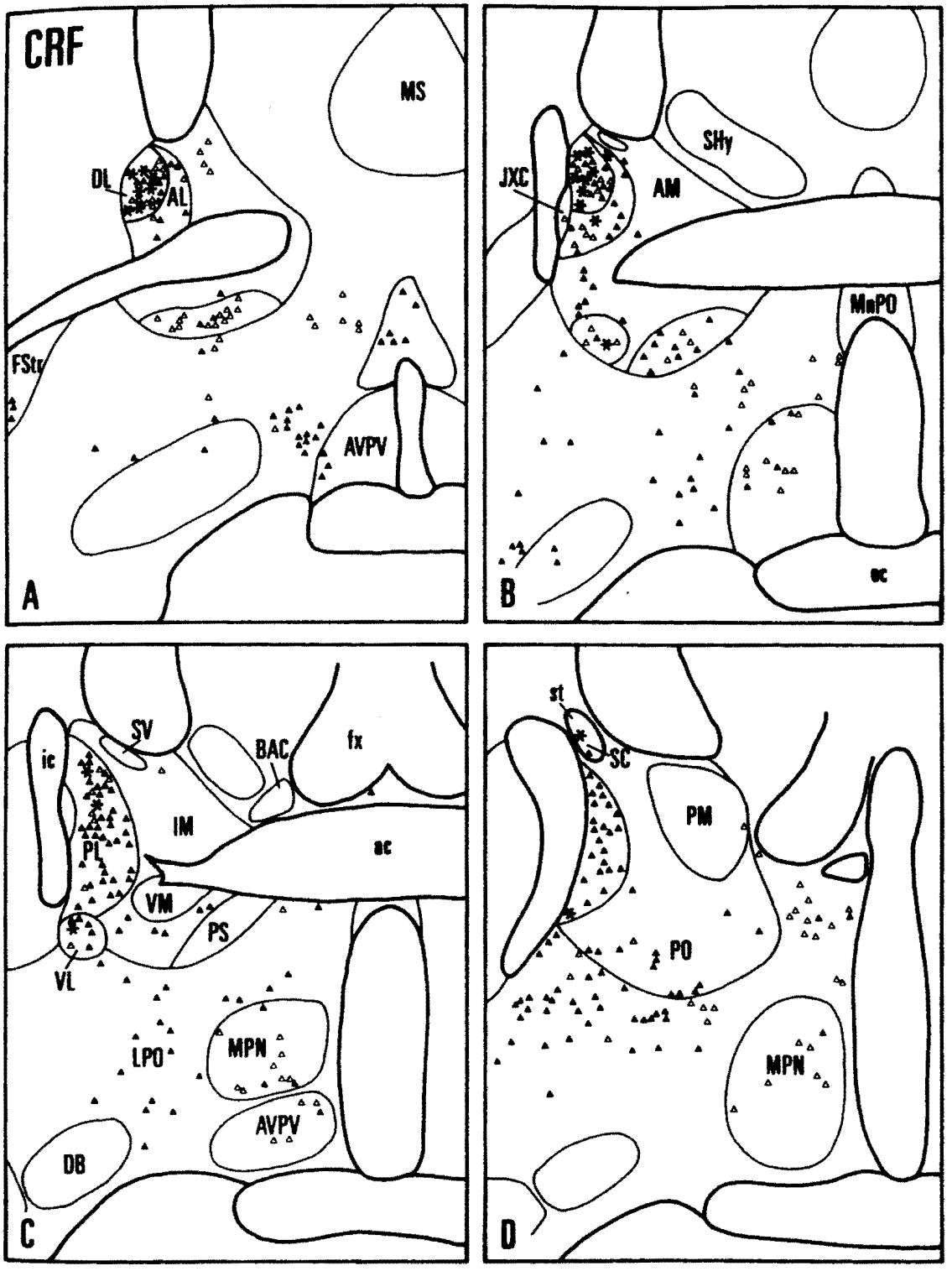
CRF
MS
DL
AL
FStr
AVPV
A
SHy
JXC
AM
MnPO
oc
B
SV
BAC
fx
ic
IM
ac
PL
VM
PS
VL
LPO
MPN
AVPV
DB
C
st
SC
PM
PO
MPN
D

Figure 7. Line drawings of four coronal sections through the BST (A-D, rostral to caudal) illustrating the distributions of Fast Blue (▲), NT-immunoreactive (△) and double-labeled (*) cells found with the BST and adjacent preoptic nuclei after Fast Blue injections into the PB.

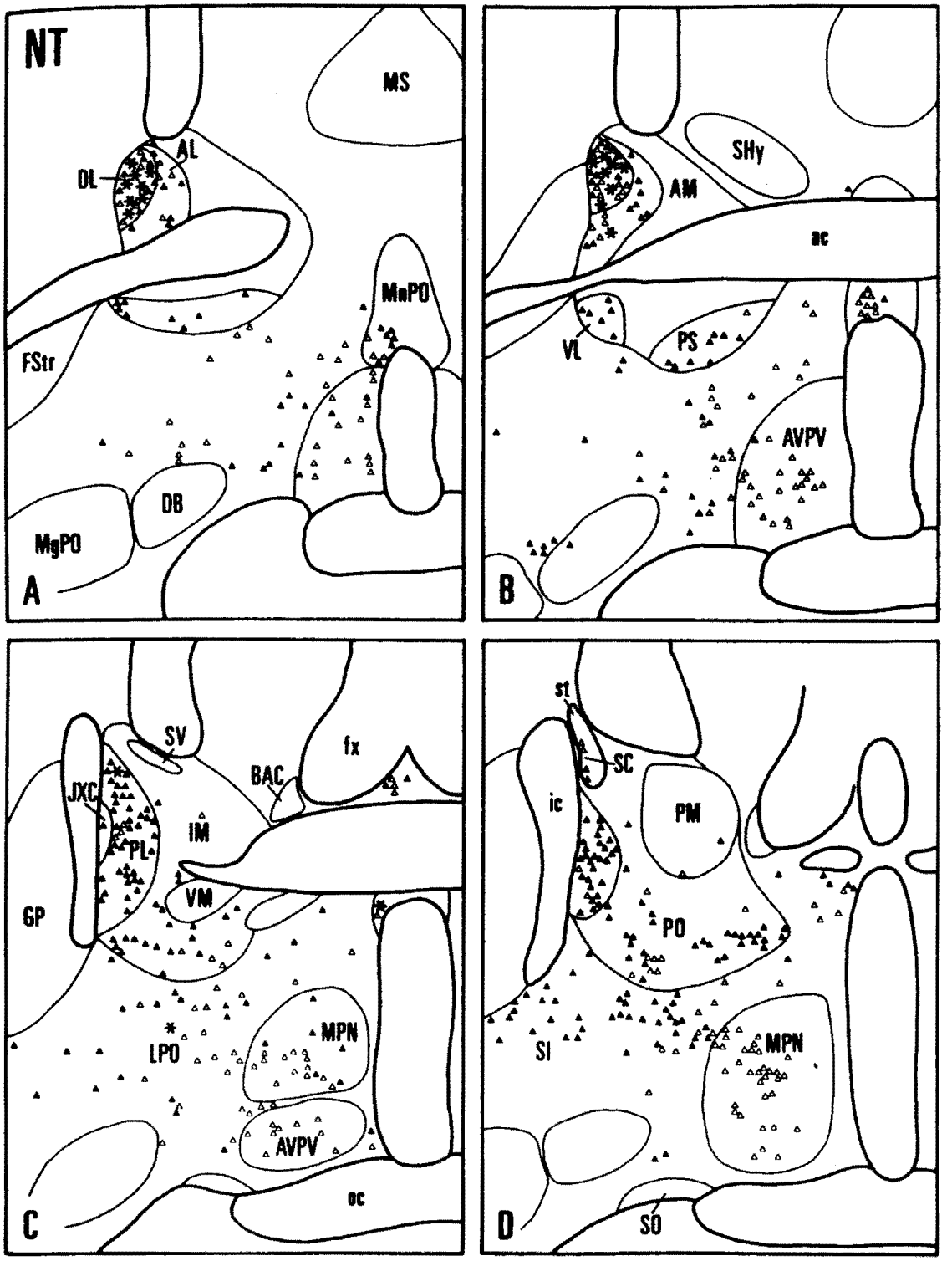
NT
MS
AL
DL
MnPO
FStr
DB
MgPO
A
SHy
AM
ac
VL
PS
AVPV
B
SV
fx
BAC
JXC
IM
PL
VM
GP
LPO
MPN
AVPV
oc
C
st
SC
ic
PM
PO
SI
MPN
SO
D

Figure 8. Line drawings of four coronal sections through the BST (A-D, rostral to caudal) illustrating the distributions of Fast Blue (▲), SS-immunoreactive (△) and double-labeled (*) cells found with the BST and adjacent preoptic nuclei after Fast Blue injections into the PB.

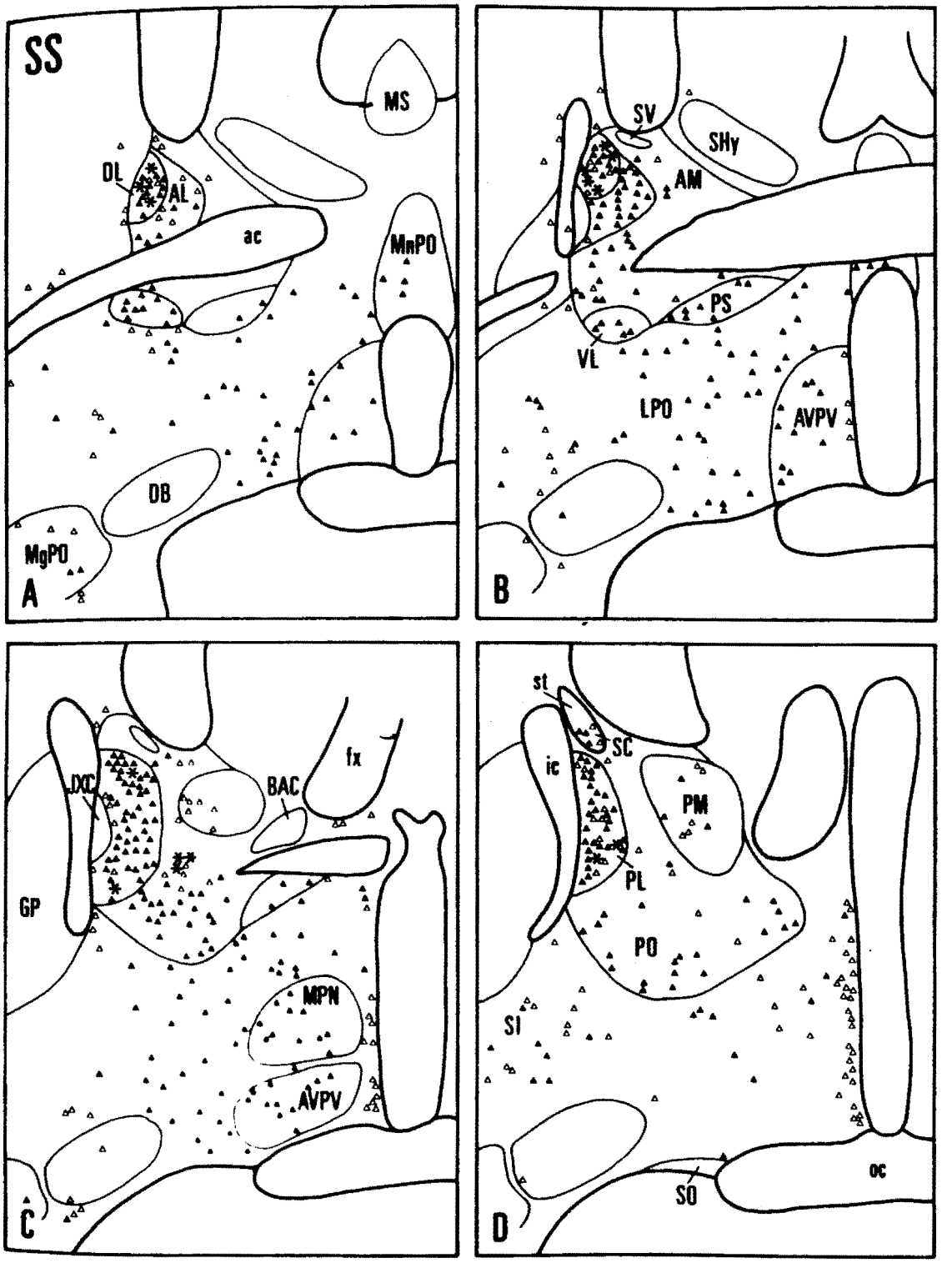
SS
MS
DL
AL
ac
MnPO
DB
MgPO
A
SV
SHy
AM
PS
VL
LPO
AVPV
B
LXC
BAC
fx
GP
MPN
AVPV
C
st
SC
ic
PM
PL
PO
SI
oc
SO
D

Figure 10. Line drawings of four coronal sections through the BST (A-D, rostral to caudal) illustrating the distributions of Fast Blue (▲) and ENK-immunoreactive (△) cells found within the BST and adjacent preoptic nuclei after Fast Blue injections into the PB. Note the lack of double-labeled cells in the BST.

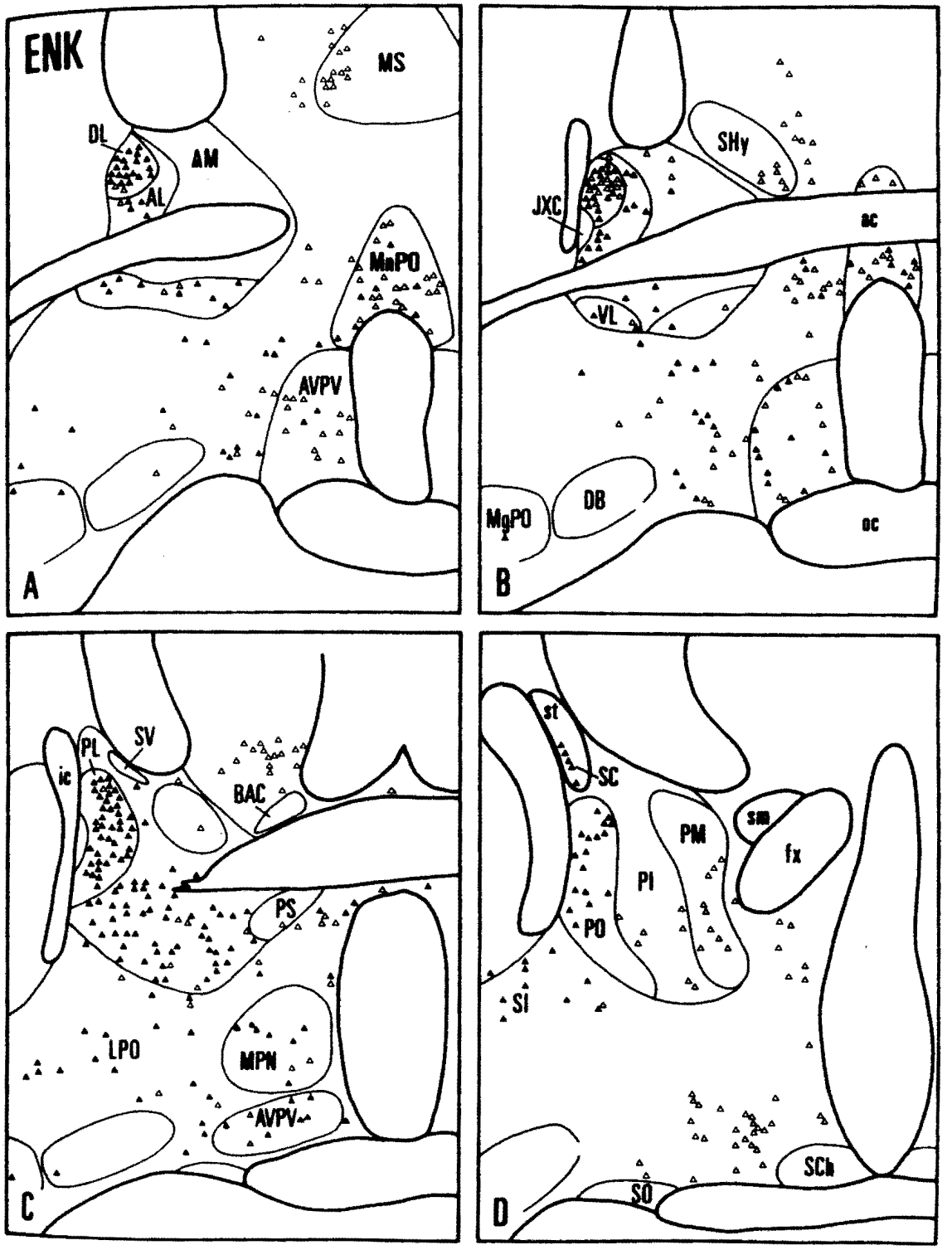
ENK
MS
DL
AM
AL
MnPO
AVPV
A
SHy
JXC
ac
VL
MnPO
DB
oc
B
ic
PL
SV
BAC
PS
LPO
MPN
AVPV
C
st
SC
sm
PM
fx
PI
PO
SI
SCh
SO
D

Table 1. Number and Percent of Immunoreactive, Retrogradely Labeled and Double-labeled Cells in the Bed Nucleus of the Stria Terminalis

Peptide	Number of Immunoreactive Cells		Number of Retrogradely Cells		Number of Double-labeled Cells		Percent of Immunoreactive Cells in DL Projecting to PB	Percent of Total Pathway W/peptide[2]
	Total	DL[1]	Total	DL[1]	Total	DL[1]		
CRF	1277	467	1440	558	201	155	33	14
NT	1085	558	1651	667	223	188	34	14
SS	606	84	1845	687	83	42	50	4

1. Number of cells in the dorsal lateral BST subnucleus.

2. Percent of total retrogradely labeled cells staining for a neuropeptide.

CHAPTER V

PEPTIDERGIC PATHWAYS FROM THE HYPOTHALAMUS TO THE PARABRACHIAL NUCLEUS

INTRODUCTION

Physiological studies have shown that the hypothalamus is able to influence autonomic reflexes through its projections to autonomic nuclei in the brain stem and spinal cord (Zerihun and Harris, '83; Rogers and Nelson, '84; Lawrence and Pittman, '85). The hypothalamic projection to the parabrachial nucleus (PB) in the pons is particularly dense and extensive. Through this pathway, the hypothalamus may modulate a number of visceral functions associated with the PB, including: fluid regulation (Ohman and Johnson, '86), micturition (Lumb and Morrison, '87), and cardiovascular (Mraovitch et al., '82) and respiratory (Cohen, '71) responses.

The hypothalamic projection to the parabrachial nucleus arises from a number of nuclei including the paraventricular, lateral, dorsomedial, arcuate and preoptic nuclei (Conrad and Pfaff, '76; Swanson, '77; Saper et al., '79; Hosoya and Matsushita, '81; Berk and Finkelstein, '82; Saper and Levisohn, '83; Takeuchi and Hopkins, '84; Chiba and Murata, '85; Luiten et al., '85; Milner and Pickel, '86a). Regarding its neuropeptide content, neurotensin- and substance P-immunoreactive neurons in the paraventricular and lateral hypothalamus

have been found to project to the PB (Milner and Pickel, '86a,b). Atriopeptin-immunoreactive neurons in the anteroventral periventricular nucleus of the hypothalamus also innervate the PB (Saper et al., '85). However, the hypothalamus contains neurons which are immunoreactive to a number of other neuropeptides, some of which are also present in fibers within the PB, these include: angiotensin II (Lind et al., '85), dynorphin (Khachaturian et al., '82), alpha-melanocyte stimulating hormone (O'Donohue et al., '79), corticotropin releasing factor (Swanson et al., '83), somatostatin (Finley et al., '81), enkephalin (Simantov et al., '77), galanin (Rokaeus et al., '84) and vasopressin (Sofroniew, '80). Because some of these neuropeptides may be present in the hypothalamic projection to the PB, this experiment examines the PB afferent cell populations in the hypothalamus for their neuropeptide content using the combined retrograde fluorescence-immunohistochemical method. Preliminary findings of this study were previously reported (Moga and Gray, '85d).

METHODS

Thirty male Long-Evans rats (250-350g) were used in this study. Each animal was anesthetized with 7% chloral hydrate. Injections (50-100 nl) of 2% fast blue (D. R. Iling) were made into the parabrachial nucleus with a 1.0 ul Hamilton syringe fitted with a glass micropipette. Injections were made over a 15-minute period, and the pipette was left in place for an additional 10 minutes. After 11-13 days survival, the animals were treated with 150-160 ug colchicine

(Sigma) in 10 ul saline injected into the lateral ventricle. Thirty-six to 48 hours later, the animals were reanesthetized with chloral hydrate and then perfused through the heart with 0.01M phosphate-buffered saline (pH 7.6, 37°C) followed by 0.1M phosphate-buffered 4% paraformaldehyde (pH 7.6, 4°C). After perfusion, the skull was placed in a stereotaxic frame (Kopf), and the brain was sliced into coronal blocks. The blocks of brain tissue were post-fixed in 4% paraformaldehyde for 30 minutes to 2 hours and then cut serially on a vibratome (Lancer). Sections from the injection site (40 um) were mounted onto chrom-alum-coated slides. Adjacent coronal sections (20 um) of the forebrain were collected in four vials of cold phosphate- buffered saline (PBS). Each series of adjacent sections was rinsed in PBS for 20 minutes and then placed in a primary antiserum with gentle agitation for 14-24 hours in a cold room (4°C). Next, the sections were rinsed in PBS for 20 minutes and then incubated in the secondary antibody, biotinylated goat anti-rabbit IgG (Bethesda Research Laboratory), for 30 minutes at room temperature, rinsed again in PBS for 15 minutes, and then incubated in streptavidin-Texas Red conjugate (Bethesda Research Laboratory) for 30 minutes. In a few, early experiments, the secondary antibody used was a rhodamine-conjugated goat antirabbit IgG (Cooper Biomedical, diluted 1:10 in PBS-Triton-X). With this antibody, sections were reacted at 45°C for 10 minutes and then at room temperature for 60 minutes. The biotin-avidin-Texas Red complex proved to be more consistent in staining and more resistant to fading than the rhodamine, and so was used in later experiments. Following incubation in secondary antibody, sections were

transferred to cold PBS, mounted onto chrom-alum-coated slides, and coverslipped with DePeX (BDH Chemicals).

The following primary antisera were used (name, lot and bleed number, source, and reference in which the antisera was previously characterized): anti-corticotropin releasing factor (#465) provided by Dr. T.L. O'Donohue (Olschowka et al., '82); anti-angiotensin II (CD3) provided by Dr. C.F. Deschepper (Deschepper et al., '86); anti-dynorphin (#54 bleed 6), anti-MSH, anti-adrenocorticotropin (#23 bleed 1), anti-arg-vasopressin (#48 bleed 10) and anti-oxytocin (#48 bleed 10), provided by Dr. S.J. Watson (Watson and Akil, '80; Watson et al., '78, '82); anti-somatostatin (#8535027) and anti-neurotensin (#8351022), obtained from the Immunonuclear Corporation (Kohler and Chan-Palay, '82; Beitz, '82); anti-met-enkephalin, provided by Dr. R. Elde (Haber and Elde, '82); and anti-galanin, obtained from Peninsula Labs (Skofitsch and Jacobowitz, '85). Antibody specificity was tested by incubating colchicine-treated sections of the hypothalamus in 1 ml of diluted antibody preincubated for one hour with 25-50 ug of its respective peptide. No immunohistochemical staining was observed in these controls. The antisera were diluted 1:500 (SS, ENK, DYN, NT, AII, ACTH, MSH), 1:1000 (GAL), 1:2000 (CRF), and 1:5000 (OXY, AVP) in a solution containing PBS, 0.1% Triton-X-100 (Mallinckrodt) and 1% normal goat serum.

The material was examined with an Olympus microscope equipped with a 100W mercury light source. Fast blue was visualized with an excitation wavelength centered at 330-360 nm (Olympus ultraviolet filter system). Texas Red immunofluorescence was viewed with the

Olympus green (546 nm) filter system. Cells that contained both retrograde fluorescence and immunofluorescence were detected by switching between filter systems. Sections were photographed with polaroid coaterless land pack film 667, ASA 3000. Sections were plotted with a Leitz Orthoplan microscope (filter systems A and NZ) equipped with digital stage position readout heads (Minnesota Datametrics, MD-1). The x- and y-coordinates of the labeled neurons were recorded by a Rockwell AIM 65 microcomputer and then plotted onto an x-y plotter. After plotting, the slides were soaked in xylene to remove the coverslips and then counterstained with thionin to determine the subnuclear location of the labeled cells.

RESULTS

Distribution of Retrogradely Labeled Neurons

After Fast Blue injections into the parabrachial nucleus, retrogradely labeled neurons were observed throughout the forebrain in nuclei previously shown to project to the PB (e.g., central nucleus of the amygdala, bed nucleus of the stria terminalis). These afferent cell populations are described in detail in other studies (Moga and Gray, '85b,c; Moga et al., in preparation). Within the hypothalamus, retrogradely labeled neurons were particularly numerous after injections into the rostral half of lateral PB (Fig. 1A,B). After a typical PB injection (Fig. 1B), many retrogradely labeled cells were observed rostrally in the median preoptic nucleus. The anteroventral

periventricular nucleus (AVPV), as defined by Simerly et al., '84, contained a few labeled cells. A few neurons were located in the medial preoptic nucleus, primarily along its lateral border. In contrast, labeled neurons were frequently found in the lateral preoptic area. Many retrogradely labeled cells were located in the retrochiasmatic area (RCh, e.g., Fig. 7). Labeled cells in RCh appeared continuous with those in the arcuate nucleus and ventrolateral parts of the ventromedial hypothalamus. In the paraventricular hypothalamus (PVH), cells were found predominantly in the medial and lateral parvocellular subdivisions with a few scattered cells in the anterior and dorsal parvocellular, and posterior magnocellular subdivisions (e.g., Fig. 14). Caudal to the PVH, labeled neurons arched over the fornix to form a particularly dense cluster in the lateral hypothalamus (LH) between the fornix and the internal capsule (Fig. 8). This cluster separated at more caudal levels into a perifornical group and a capsular group of cells. Labeled cells in the capsular LH group extended to the most caudal levels of the hypothalamus where they surrounded the internal capsule and adjacent subthalamus (Fig. 8). The perifornical LH group, with successively caudal sections, moved medially to become continuous with cell labeling in the dorsal hypothalamic area (DH) dorsal to the dorsomedial nucleus (Fig. 8). Only a few retrogradely labeled neurons were found ventrally in the LH. Medially, labeled cells were seen in the diffuse portion of the dorsomedial hypothalamus (DMH, Fig. 13).

A slightly different pattern of hypothalamic labeling was noted after fast blue injections into the caudal 'waist' area of the PB

(Fig. 1c). In these cases (e.g., Fig. 17), retrograde labeling in the hypothalamus appeared more discrete and less numerous than after rostral PB injections. In particular, labeled cells in perifornical LH were less numerous and did not form a dense cluster. In contrast, retrogradely labeled cells in capsular LH were more numerous and formed a dense 'cap' surrounding the subthalamus. In all cases, retrogradely labeled neurons were found bilaterally but with a heavy ipsilateral dominance.

Distribution of Immunoreactive Neurons

The distributions of neuropeptide-immunoreactive neurons in the hypothalamus were similar to those described in a number of immunocytochemical studies (Uhl et al., '79; Uhl and Snyder, '81; Sofroniew, '80; Swanson et al., '83; Lind et al., '85; Finley et al., '81; Khachaturian et al., '82; Watson et al., '78; Watson and Akil, '80; Skofitsch and Jacobowitz, '85); therefore, I will only briefly describe my findings.

Oxytocin-immunoreactive (OXY-ir) and vasopressin-immunoreactive (AVP-ir) cells were confined to the PVH, supraoptic and accessory magnocellular nuclei. In the PVH, OXY-ir cells were found in all three magnocellular subdivisions whereas AVP-ir cells were concentrated in the core of the posterior magnocellular subdivision (Figs. 14,15). Many OXY-ir and AVP-ir cells were also found in the parvocellular subdivisions of the PVH.

Corticotropin releasing factor-immunoreactive (CRF-ir) neurons were prominent in the dorsal part of the medial parvocellular PVH subdivision (Fig. 11). Caudal to the PVH, CRF-ir neurons were numerous in the LH, particularly dorsal and lateral to the fornix. A few CRF-ir neurons were also present in the retrochiasmatic area and dorsal hypothalamic area. Neurotensin-immunoreactive (NT-ir) neurons were found in the dorsal and medial parvocellular, and periventricular subdivisions of the PVH (Fig. 10). NT-ir neurons were numerous in the retrochiasmatic area where they extended laterally over the optic tract. In the LH, NT-ir neurons were concentrated dorsal and lateral to the fornix with a few also present ventral and lateral to the fornix. Most caudally, NT-ir cells were found in the dorsomedial part of VMH and in the arcuate nucleus.

In the PVH, galanin-immunoreactive (GAL-ir) neurons were most numerous in the posterior magnocellular and medial parvocellular subdivisions (Fig. 12). Many GAL-ir neurons were found in LH, particularly dorsal and lateral to the fornix, and ventrally along the brain surface. The DMH contained the heaviest concentration of GAL-ir cells. GAL-ir neurons were also found in RCh, ARC and DHA. A moderate number of angiotensin II-immunoreactive (AII-ir) neurons were present in both magnocellular and parvocellular PVH as well as in RCh (Fig. 9). AII-ir cells in the LH were concentrated dorsal and medial to the fornix; these cells appeared continuous with AII-ir cells in the DH and diffuse portion of the DMH. The arcuate nucleus also contained a few AII-ir cells.

Dynorphin-immunoreactive (DYN-ir) neurons were concentrated in magnocellular PVH with lesser numbers in parvocellular PVH and SO (Fig. 8). DYN-ir neurons were numerous in the lateral hypothalamus, particularly dorsal and medial to the fornix. Concentrations of DYN-ir neurons were also found along the ventral lateral surface of the hypothalamus, and at rostral LH levels, dorsal to the supraoptic nucleus. Met-enkephalin-immunoreactive (ENK-ir) neurons were numerous in the paraventricular nucleus, primarily in its parvocellular subdivisions (Fig. 7). Caudal to the PVH, ENK-ir neurons were especially common medially and ventrally in the hypothalamus, particularly in the arcuate and ventromedial nuclei, and along the ventral surface of the hypothalamus. ENK-ir cells were notably absent in the dorsal and lateral portions of the lateral hypothalamus.

Somatostatin-immunoreactive (SS-ir) neurons in the PVH were concentrated rostrally in the periventricular subdivision (Fig. 13). Caudal to PVH, SS-ir neurons were numerous medially and ventrally in the hypothalamus; these neurons encircled the VMH. A few SS-ir cells were found in DMH, ARC and LH.

Adrenocorticotropin-immunoreactive (ACTH-ir) neurons were restricted to the arcuate nucleus and retrochiasmatic area (Fig. 17). In contrast, melanocyte stimulating hormone-immunoreactive (MSH-ir) neurons were more widespread in the hypothalamus, occurring in the arcuate nucleus, RCh and lateral hypothalamus (Fig. 16).

Double-labeled Neurons

Double-labeled neurons were most numerous after injections into the rostral lateral PB. In one case per neuropeptide, the retrogradely labeled, immunoreactive, and double-labeled neurons in the hypothalamus were counted to assess the relative contribution of each neuropeptide to the hypothalamic-PB pathway. In these cases, the injection site included most of the parabrachial nucleus. Cell counts were restricted to the PVH, perifornical LH, RCh and the arcuate nucleus as these nuclei were previously shown to contain the majority of double-labeled cells (Moga and Gray, '85d). Perifornical LH was defined as that area around the fornix which contained a concentration of neuropeptide- like immunoreactive cells. The retrochiasmatic area was defined as that area in the ventrobasal hypothalamus which is caudal to the optic chiasm and rostral to the caudal boundaries of PVH. The distributions of double-labeled cells within the hypothalamus are depicted in Figures 7-17. The hypothalamic levels chosen for these figures best represent the double-labeling seen for each peptide.

Paraventricular Hypothalamus. A few double-labeled cells were found in the PVH for most of the peptides examined. ENK-ir cells were the most numerous among those double-labeled in the PVH, accounting for approximately 2% of PVH neurons projecting to PB (Fig. 7). These ENK-ir double-labeled neurons were concentrated in the medial parvocellular subdivision of PVH. DYN-ir double-labeled neurons showed a similar distribution to those of ENK-ir but were fewer in number; approximately 1% of the retrogradely labeled cells in the PVH contained

DYN-ir (Fig. 8). Fewer than 1% of the Fast Blue labeled cells in the PVH contained either AII-ir, NT-ir, CRF-ir, GAL-ir or SS-ir (Figs. 9,10,11,12,13). Somatostatin-immunoreactive neurons, when double labeled, were found adjacent to the caudal periventricular concentration of SS-ir neurons in PVH (Fig. 13). Oxytocin-ir double-labeled cells were typically found in the lateral parvocellular subdivision in low numbers (<1%) after lateral PB injections (Fig. 14). AVP-ir double-labeled neurons were occasionally seen (<1%), particularly after 'waist' injections in PB. A few AVP-ir double-labeled cells were large magnocellular neurons which were lightly, though distinctly, labeled with Fast Blue (Fig. 15). Cells labeled for both MSH-ir and Fast Blue were never found in the PVH but were often located just outside the PVH (Fig. 16).

Retrochiasmatic Area. Double-labeled neurons were frequently seen in RCh. DYN-ir cells were the most numerous, accounting for approximately 3% of the RCh neurons with projections to the PB (Fig. 8). About 1% of the retrogradely labeled neurons in RCh stained for NT-ir, and these were located primarily in the lateral part of RCh (Fig. 10). In contrast, AII-ir double-labeled cells, also representing approximately 1% of the RCh-PB projection, were concentrated in the medial part of RCh (Fig. 9). Cells containing both Fast Blue and either GAL-ir or CRF-ir were few (less than 1%; Figs. 11,12). The majority of double-labeled cells in the RCh were round and medium-sized, and resembled proopiomelanocortin-containing cells.

Lateral Hypothalmus. Many double-labeled neurons were located in the perifornical region of LH. Thirty percent of the retrogradely

labeled cells in perifornical LH contained DYN-ir. DYN-ir double-labeled cells were particularly numerous dorsomedial to the fornix with only an occasional cell ventrolateral to the fornix (Fig. 8). AII-ir double-labeled cells showed a similar distribution to DYN-ir (Fig. 9) but were fewer in number - about 20% of the retrogradely labeled cells in LH contained AII-ir. Both CRF-ir and NT-ir double-labeled neurons were common dorsolateral to the fornix with a few cells found below the fornix and adjacent to the internal capsule (Figs. 10,11). Their contributions to the perifornical LH-PB projection were 20%, CRF-ir, and 25%, NT-ir. Cells labeled for both GAL-ir and Fast Blue (5%) were concentrated in the dorsolateral perifornical LH (Fig. 12). Double-labeled GAL-ir neurons were also found scattered below the fornix and near the internal capsule. Double-labeled MSH-ir neurons were unique in their LH distribution for showing a particularly heavy concentration near the internal capsule (Fig. 16). Twenty-two percent of the retrogradely labeled cells in capsular LH stained for MSH-ir. Only a few MSH-ir double-labeled cells were located in perifornical LH. Finally, less than 1% of the retrogradely labeled neurons in LH contained either SS-ir or ENK-ir (Figs. 7,13).

Arcuate Nucleus. Neurons double-labeled for Fast Blue and a proopiomelanocortin-related peptide were frequently seen in the arcuate nucleus (Figs. 16,17). Seventy-one percent of the retrogradely labeled neurons in ARC were ACTH-immunoreactive. Cells labeled with both MSH-ir and Fast Blue were also numerous within the arcuate nucleus, accounting for approximately 49% of the ARC-PB projection. In

addition, an occasional DYN-ir or NT-ir double-labeled cell was also found in ARC (Figs. 8,10).

Other Hypothalamic Nuclei. Double-labeled cells in the preoptic area were rarely seen. The distributions of cells containing CRF-ir, NT-ir and ENK-ir in the preoptic area were depicted in Chapter IV (Fig. 5) of this dissertation. GAL-ir double-labeled cells in the lateral preoptic area were the most consistently seen, followed by NT-ir cells in LPO and the median preoptic nucleus (Fig. 2). Less frequently, a CRF-ir or ENK-ir double-labeled cell was observed in the medial preoptic area. After one injection which included the central gray matter, a few NT-ir neurons in the medial preoptic area were lightly labeled with Fast Blue.

Few retrogradely labeled cells were seen within the ventromedial nucleus of the hypothalamus, and of these, still fewer were double-labeled. In one case, ENK-ir neurons in the ventral lateral VMH were lightly labeled with Fast Blue, probably as a result of tracer spread to the central gray. In the dorsomedial hypothalamus, an occasional small GAL-ir or AII-ir neuron was double-labeled (Figs. 9,12). More often, immunoreactive neurons dorsal to DMH, in the dorsal hypothalamic area (DH), contained Fast Blue. Double-labeled cells in DH included DYN-ir, AII-ir and CRF-ir, and less frequently, ENK-ir and SS-ir (Figs. 7,8,9,11,13).

DISCUSSION

Hypothalamic Peptidergic Pathways to PB

The results from the present study demonstrate that PB afferent cell populations in the hypothalamus contain a wide variety of neuropeptides. Based on the eleven antisera used in this study, most of the neuropeptide-immunoreactive neurons projecting to the PB were concentrated in the perifornical LH, retrochiasmatic area, paraventricular hypothalamus and arcuate nucleus.

In the perifornical lateral hypothalamus, a significant percentage of the neurons projecting to the PB stain for CRF-ir (20%), NT-ir (25%), AII-ir (20%), and DYN-ir (30%). A smaller percentage stain for GAL-ir (5%), SS-ir (<1%) and ENK-ir (<1%). In the caudal lateral hypothalamus (i.e., capsular LH), 22% of the retrogradely labeled neurons contained MSH-ir. Very few other double-labeled cells were noted in this portion of LH. Previous studies have shown that neurons contributing to the LH-PB pathway also stain for substance P (SP-ir)- and atrial natriuretic polypeptide (ANP-ir)-immunoreactivity (Saper et al., '85; Milner and Pickel, '86b).

Neuropeptide-immunoreactive neurons in both perifornical and capsular LH project to a number of other brain nuclei. In a recent study, Cechetto and Saper ('88) examined the peptide content of the LH projection to the spinal cord using a similar set of antisera. After Fast Blue injections into the spinal cord (SC), they found retrogradely labeled neurons in perifornical LH that stained for NT-ir (few), SP-ir

(few), GAL-ir (few), DYN-ir (25%) and ANP-ir (20%). In capsular LH, 95% of the retrogradely labeled neurons stained for MSH-ir. No retrogradely labeled CRF-ir neurons were found in LH in this study. Comparing data from these two studies demonstrates that the types and percentages of neuropeptide-immunoreactive neurons contributing to these two LH pathways may be distinct. These anatomical studies offer evidence that different LH pathways may have different peptide compositions.

Other immunohistochemical findings suggest that each neuropeptide cell population in LH projects to a number of different nuclei. For example, dynorphin-like immunoreactive neurons in perifornical LH project to the spinal cord, dorsal vagal complex, periaqueductal gray, PB, central nucleus of the amygdala and entorhinal area (Kohler et al., '84; Cechetto and Saper, '88; Zardetto-Smith et al., '85; present study). In addition, MSH-ir neurons in LH are retrogradely labeled after injections in the PB, spinal cord, inferior colliculus, CA1, entorhinal area and cortex (Kohler et al., '84; Shiosaka et al., '85; Saper et al., '85; Cechetto and Saper, '88; present study). Neuropeptide-immunoreactive neurons in LH may send collaterals to two or more target nuclei. In a recent study, Veening et al. ('87) found that about 50% of LH neurons projecting to the PB also project to the dorsal vagal complex.

Less that 2% of the retrogradely labeled cells in the PVH stained for either AVP-ir, OXY-ir, NT-ir, CRF-ir, AII-ir, SS-ir, GAL-ir, DYN-ir, or ENK-ir. Neuropeptides have previously been demonstrated in PVH pathways to the dorsal vagal complex (DVC) and spinal cord. A high

percentage of neurons in the PVH that project to the spinal cord stain for either AVP-ir (35%) or OXY-ir (25%) (Cechetto and Saper, '88). In contrast, very few (<1%) OXY-ir and AVP-ir double-labeled cells were seen after PB injections. Similarly, only a few AVP-ir and OXY-ir neurons were retrogradely labeled after DVC injections (Sawchenko and Swanson, '82); however, the numbers in this study may have been higher with colchicine treatment. The PVH projection to the SC also includes GAL-ir (few), SP-ir (few), NT-ir (few), CCK-ir (few) and ENK-ir (10%) neurons but not DYN-ir, CRF-ir or SS-ir neurons, whereas the PVH-PB projection originates from all of these neuropeptide-immunoreactive neurons except for CCK-ir. Of the few neuropeptides examined in the PVH-DVC pathway, only small numbers of SS-ir and ENK-ir neurons were double-labeled. The PVH peptidergic pathways to the brainstem and spinal cord are similar in their neuropeptide compositions and in their small percentages of double-labeled cells.

Neurons in the retrochiasmatic area were recently shown to project to the PB, and a few were found to contain NT-ir (Milner and Pickel, '86a). In the present study, many ACTH-ir, MSH-ir, DYN-ir and AII-ir, and a few GAL-ir and CRF-ir neurons in the RCh were retrogradely labeled after a PB injection. In contrast, the RCh projection to the spinal cord contains MSH-ir but not GAL-ir, NT-ir, CRF-ir or DYN-ir (Cechetto and Saper, '88). In addition, RCh neurons also project to the dorsal vagal complex (Swanson and Kuypers, '80) but the peptide content of this pathway is unknown.

Immunohistochemical studies have previously shown that cells immunoreactive for the proopiomelanocortin (POMC) derived peptides

(e.g., beta-endorphin, alpha-MSH, ACTH) are present in the ARC and NTS of the rat (O'Donohue et al., '79; Joseph et al., '83). There is also a population of neurons in LH and zona incerta which stain for the MSH-like peptide but not for any other POMC peptide; the MSH-like peptide in these cells apparently arises from an unknown biosynthetic mechanism (Watson and Akil, '80). By tracing descending POMC fibers from the arcuate nucleus, investigators surmised that at least some of the POMC fibers in the PB arise from the ARC (Khachaturian et al., '84). The present study demonstrates a projection from the ARC to the PB. Furthermore, 71% of the retrogradely labeled cells in ARC contain ACTH-ir, and 49% contain MSH-ir. As the POMC derived peptides are colocalized in the same arcuate neurons (Watson et al., '78; Sofroniew, '79; Watson and Akil, '80), one would expect these percentages to more closely approximate each other. This discrepancy may be due to different PB injection sites; the injection site for the MSH-ir cell count was located in rostral lateral PB, whereas that for ACTH-ir was centered in the caudal 'waist' of PB. Possibly, the ARC projection to the PB may be topographically organized.

Other Peptidergic Afferents of the PB

In addition to the peptidergic pathways described here, the PB also receives a dense CRF-ir, NT-ir and SS-ir input from both the central nucleus of the amygdala and the bed nucleus of the stria terminalis (Moga and Gray, '85a,b). Many different neuropeptide-immunoreactive neurons in the nucleus of the solitary tract project to

the PB; these include CRF-ir, NT-ir, SS-ir, CCK-ir, GAL-ir, AII-ir, ENK-ir, SP-ir and neuropeptide Y-immunoreactive neurons (Mantyh and Hunt, '84; Milner and Pickel, '86a,b; Herbert et al., '87). Enkephalin- and dynorphin-immunoreactive neurons in both the spinal cord and the spinal trigeminal nucleus project to the PB (Standaert et al., '86a). Recently, we have noted double-labeled NT-ir and SP-ir neurons in the periaqueductal gray matter after PB injections (unpublished observations).

These peptidergic afferents may be topographically distributed within the PB. Recently, we found that afferents to the PB terminate in specific PB subnuclei (Moga et al.,'86; Herbert and Saper, unpublished observations). For example, both the NTS and CeA project heavily to the external lateral and waist PB subnuclei. In contrast, hypothalamic nuclei terminate almost exclusively in the central lateral and dorsal lateral PB subnuclei. The peptidergic inputs from the CeA and NTS would converge in the PB, whereas those from the hypothalamus and CeA would be largely segregated. This biochemical specificity and topographical distribution of input to the PB may provide a substrate for the diversity of visceral responses associated with the PB.

Functional Considerations

A variety of adaptive behaviors can be elicited by electrical and chemical stimulation of the hypothalamus, including feeding, drinking, defense, mating and exploratory behavior (e.g., Folkow and Rubinstein, '65; Mogensen and Stevenson, '67; Hoebel, '69; Pfaff, '80; Grossman et

al., '78; Yardley and Hilton, '86). Some of these behaviors or fractional components of them can also be elicited from the PB (Coote et al., '73; Micco, '74; van der Kooy, '79; Yardley and Hilton, '86). This suggests that the hypothalamic projections to the PB may be an essential part of the anatomical substrate underlying the complex behaviors evoked from the hypothalamus.

For example, the projections from the lateral hypothalamus to the PB may mediate the feeding and drinking responses of the LH. Following injections of [^{14}C]-deoxyglucose into freely moving rats, Roberts ('80) electrically stimulated the lateral hypothalamus at sites which elicited gnawing, eating and drinking. Autoradiographic analysis of these rat brains revealed a heavily labeled descending pathway which traveled through the lateral tegmentum to terminate in the parabrachial nucleus, suggesting that the LH-PB pathway is metabolically active during feeding and drinking. Similarly, the PVH projection to the PB may be important in norepineprine-induced feeding responses. Injections of either norepinephrine (NE) or clonidine (CLON) into the PVH have been shown to elicit a robust feeding response in satiated rats (Leibowitz, '78, '80). To determine the course of PVH fibers mediating this response, Weiss and Leibowitz ('85) made a series of coronal knife cuts in the diencephalon and lower brainstem. Rats that sustained damage in either the periventricular gray area of the caudal thalamus and midbrain or the dorsal lateral part of the caudal pons did not respond to injections of either NE or CLON into the PVH, suggesting that fibers mediating this response travel through the periventicular gray to the PB in the dorsal lateral pons.

Defense behavior consists of both autonomic and behavioral components (Abrahams et al., '60,'64; Hilton and Zbrozyna, '63). This behavior can be elicited from a number of nuclei in the hypothalamus and brainstem (for review, Yardley and Hilton, '86), many of which project to the PB. However, electrical stimulation of the PB evokes only part of the defense autonomic component; specifically, the hind-limb vasodilation characteristic of the defense reaction is absent following PB stimulation (Coote et al., '73; Mraovitch et al., '82). Furthermore, the behavioral response (i.e., flight or fight) that is typical of the defense reaction has not been reported for the PB. Whether the hypothalamic projection to the PB mediates part of the autonomic response of the defense reaction remains to be studied.

The role of neuropeptides in hypothalamic pathways to the PB is unknown. Neuropeptides are concentrated in autonomic structures such as the hypothalamus, CeA, BST, PB, NTS and midbrain central gray (Pickel, '85). Microinjections of neuropeptides into central autonomic nuclei elicit a variety of visceral responses (e.g., Kalivas et al., '82; Denavit-Saubie et al., '82). However, few studies have specifically examined the role of neuropeptides in the PB. In one study, the application of the opioid agonists, FK-33824 and DADLE, to the rostral dorsal surface of the pons caused a significant decrease in respiratory frequency; this effect was attributed to opioid diffusion to the medial PB (Hurle et al., '85). More conclusively, Denavit-Saubie et al. ('78) found that opioid agonists depress the spontaneous firing activity of respiratory-related neurons in the medial PB. Possibly, the projection from ENK-ir neurons in the PVH to

the PB, noted in the present study, may mediate these effects. Clearly more studies are needed before any conclusions can be drawn as the role of neuropeptides in the PB.

Figure 1. Drawings of representative Fast Blue injection sites in the parabrachial nucleus. Shading indicates the center of each injection site and the spread of the fluorescent dye.

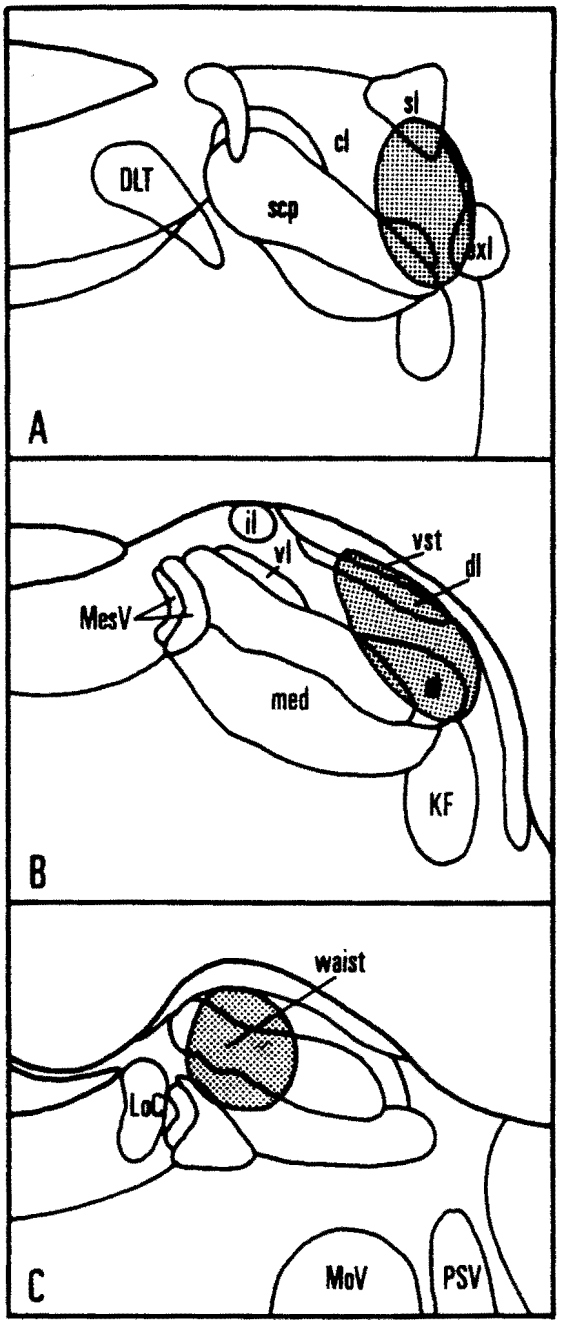
sl
cl
DLT
scp
axl
A
il
vl
vst
dl
MesV
med
KF
B
waist
LoC
MoV
PSV
C

Figure 2. Fluorescent photomicrographs of a coronal section the median preoptic nucleus illustrating the distribution of (A) cells projecting to the PB (FB), and (B) cells immunoreactive to neurotensin (NT). One double-labeled cells is indicated by the white arrow. Bar = 100 um. (3V, third ventricle).

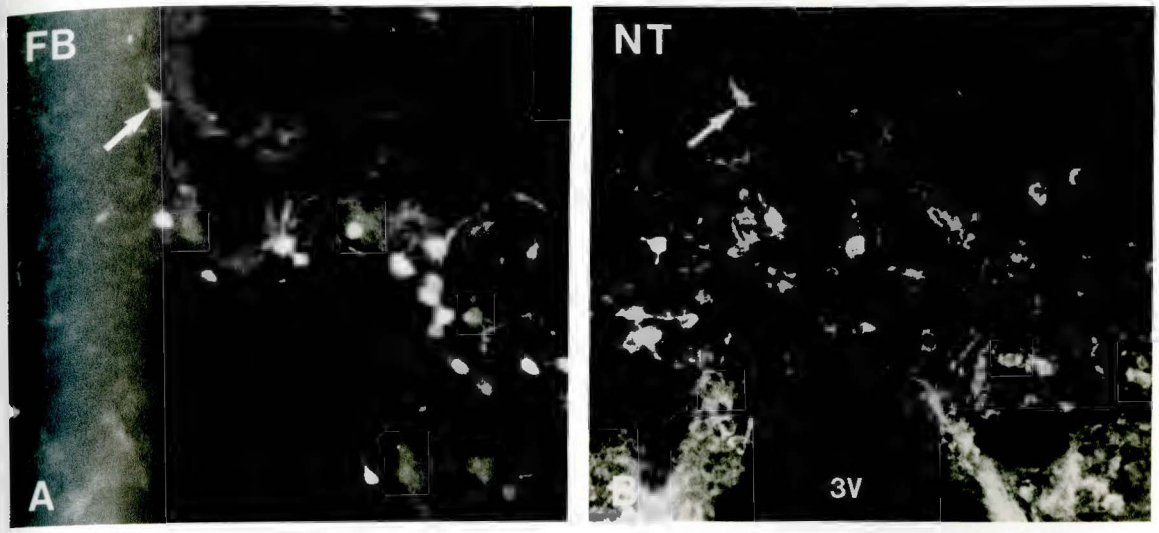
FB
A
NT
3V
B

Figure 3. Fluorescent photomicrographs of a coronal section through the caudal half of the paraventricular hypothalamus illustrating (E) cells retrogradely labeled after fast blue injections in the PB, and (F) cells immunoreactive to oxytocin (OXY). An OXY double-labeled cell (white arrow) is indicated in the lateral parvocellular subdivision. Bar = 100 um.

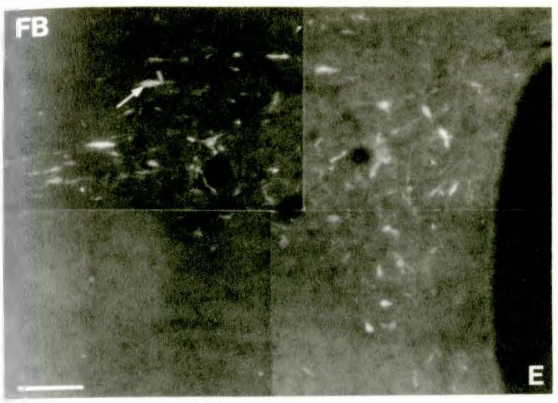
FB
E

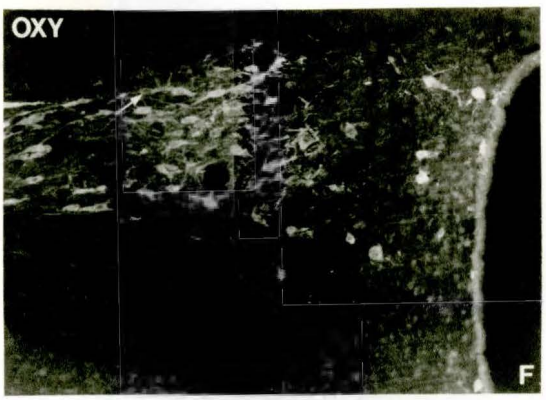
OXY
F

Figure 4. Fluorescent photomicrographs of a coronal section through the paraventricular hypothalamus illustrating (A) cells projecting to the PB, and (B) cells immunoreactive to corticotropin releasing factor (CRF). Parts C (fast blue-labeled cells) and D (CRF-ir cells) are high power photomicrographs of one double-labeled cell (indicated by white arrow) found within the medial parvocellular subdivision. Bar = 100 um.

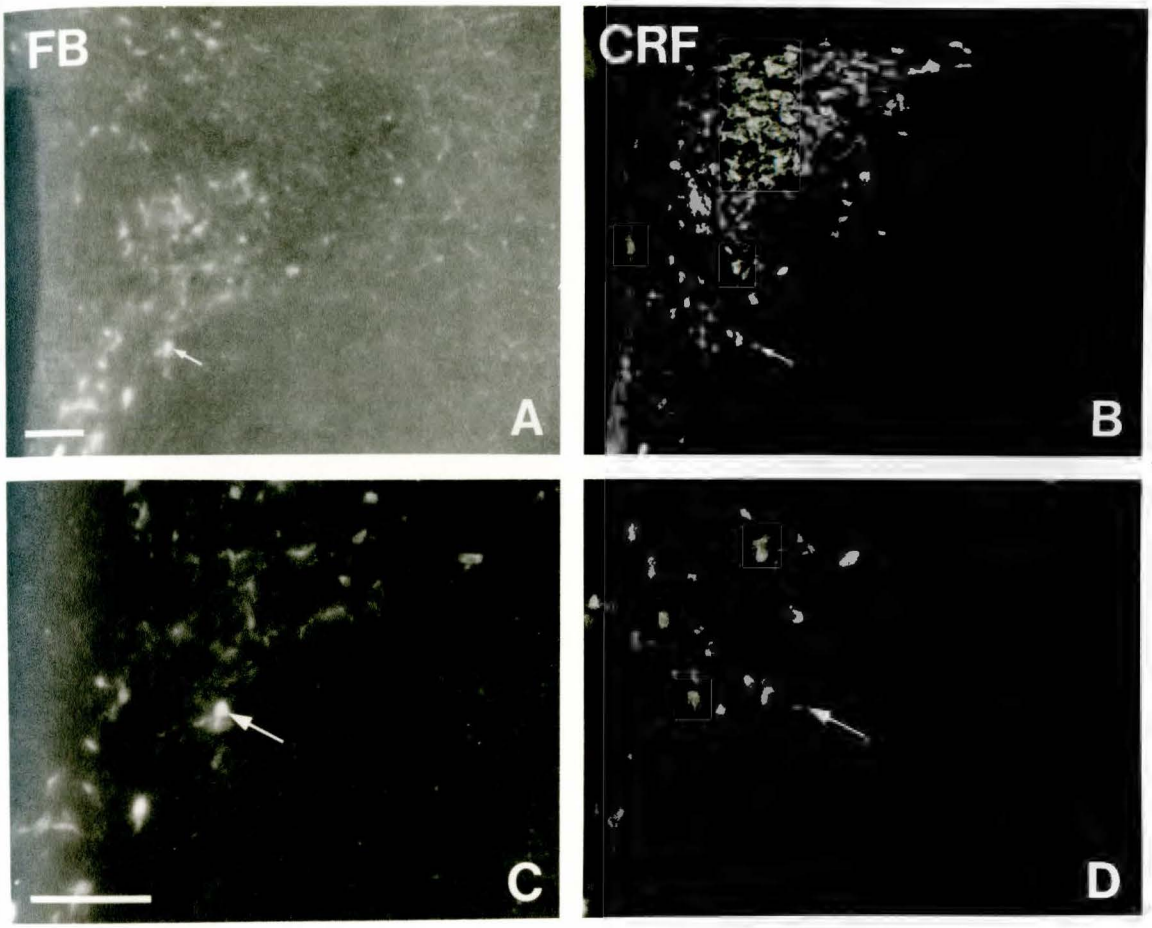
FB
A
CRF
B
C
D

Figure 5. Fluorescent photomicrographs of a coronal section through the lateral hypothalamus illustrating (A) cells projecting to the PB, and (B) cells immunoreactive to neurotensin (NT). Four double-labeled cells are indicated by white arrows ventrolateral to the fornix (fx). Bar = 100 um.

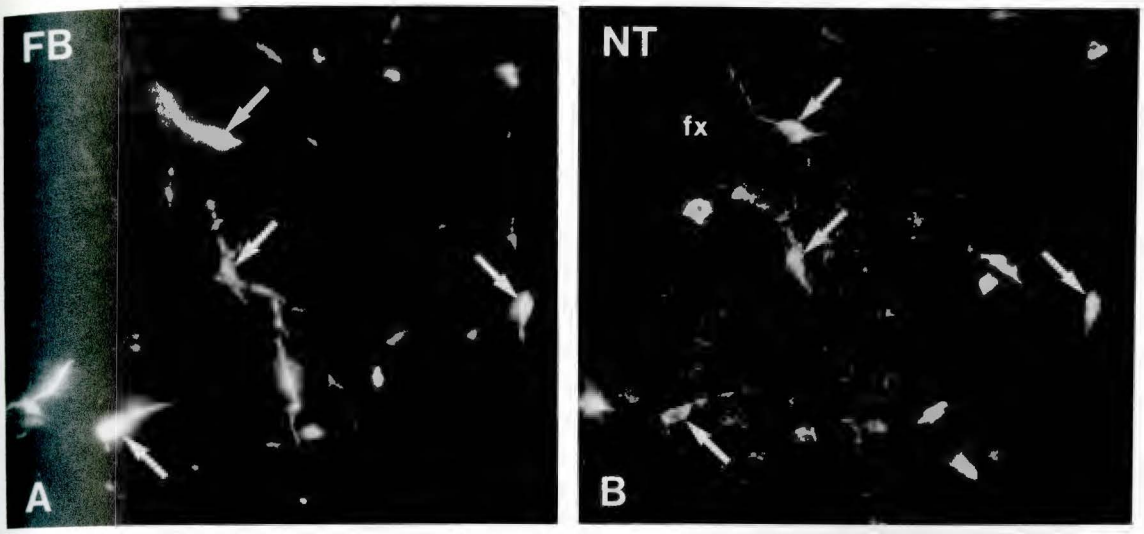
FB
A
NT
fx
B

Figure 6. Fluorescent photomicrographs of a coronal section through the perifornical area of the lateral hypothalamus illustrating (A) cells projecting to the PB, and (B) cells immunoreactive to dynorphin (DYN). Six double-labeled cells (indicated by white arrows) are located dorsolateral to the fornix (f). Bar = 100 um.


FB
A
f


DYN
B
f

Figure 7. Line drawings of coronal sections through four levels of the hypothalamus (A-D, rostral to caudal) illustrating the distributions of Fast Blue (●), ENK-immunoreactive (○) and double-labeled (*) cells after Fast Blue injections into the PB.

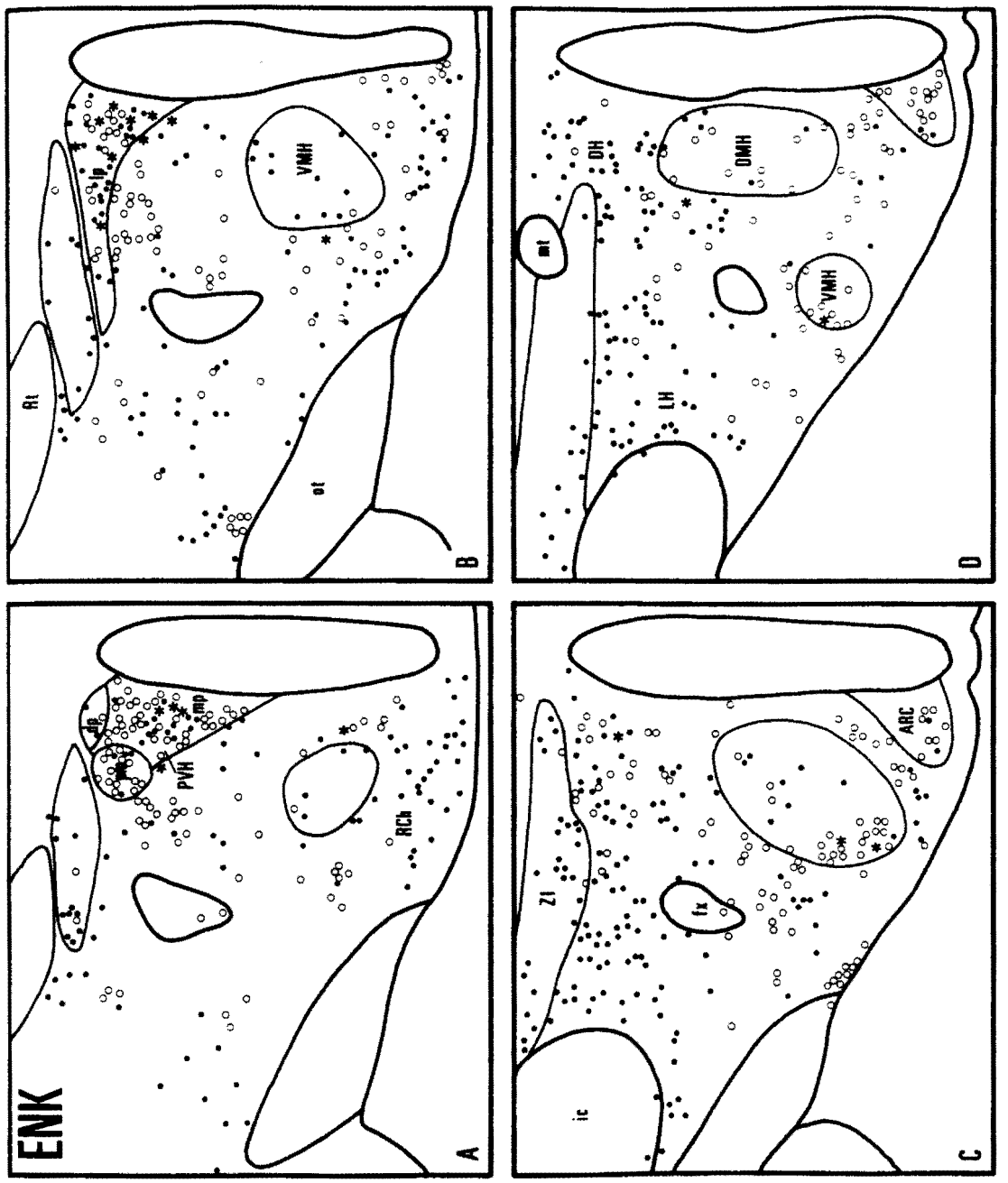
ENK
A
B
C
D
RCh
PVH
mp
VMH
Rt
ot
DH
DMH
LH
mt
ARC
Zi
ix
ic

Figure 8. Line drawings of coronal sections through four levels of the hypothalamus (A-D, rostral to caudal) illustrating the distributions of Fast Blue (●), DYN-immunoreactive (○) and double-labeled (*) cells after Fast Blue injections into the PB.

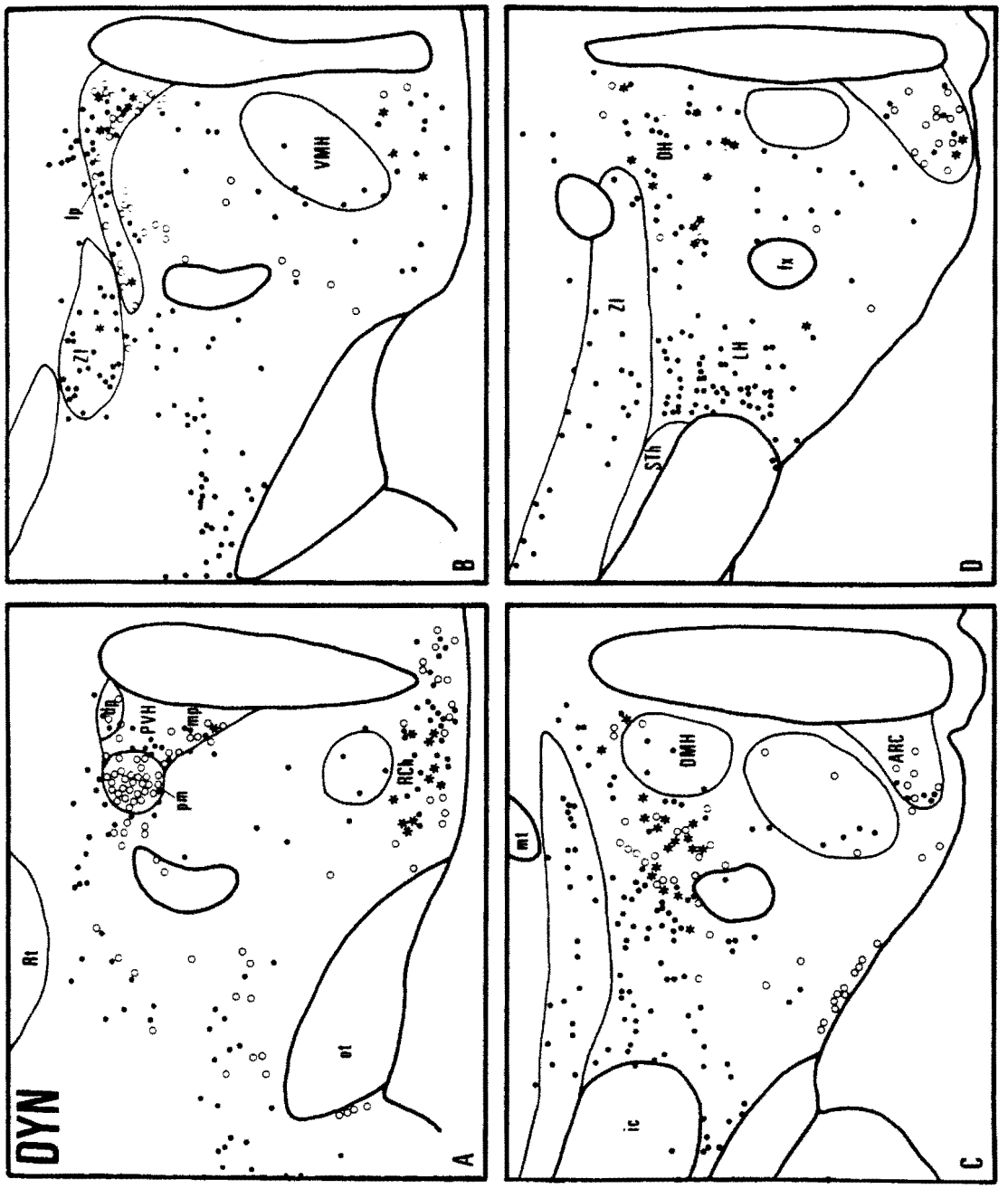
DYN
A
B
C
D
Rt
ot
PVH
mp
pm
RCh
VMH
lp
ZI
DMH
ARC
mt
ic
DH
lx
LH
STh

Figure 9. Line drawings of coronal sections through four levels of the hypothalamus (A-D, rostral to caudal) illustrating the distributions of Fast Blue (●), AII-immunoreactive (○) and double-labeled (*) cells after Fast Blue injections into the PB.


AII
A
B
C
D
dp
PMd
pm
RCh
fx
PVH
lp
ot
mt
DH
ARC
LH
STh
ZI
ic
DMH
VMH

Figure 10. Line drawings of coronal sections through four levels of the hypothalamus (A-D, rostral to caudal) illustrating the distributions of Fast Blue (●), NT-immunoreactive (○) and double-labeled (*) cells after Fast Blue injections into the PB.

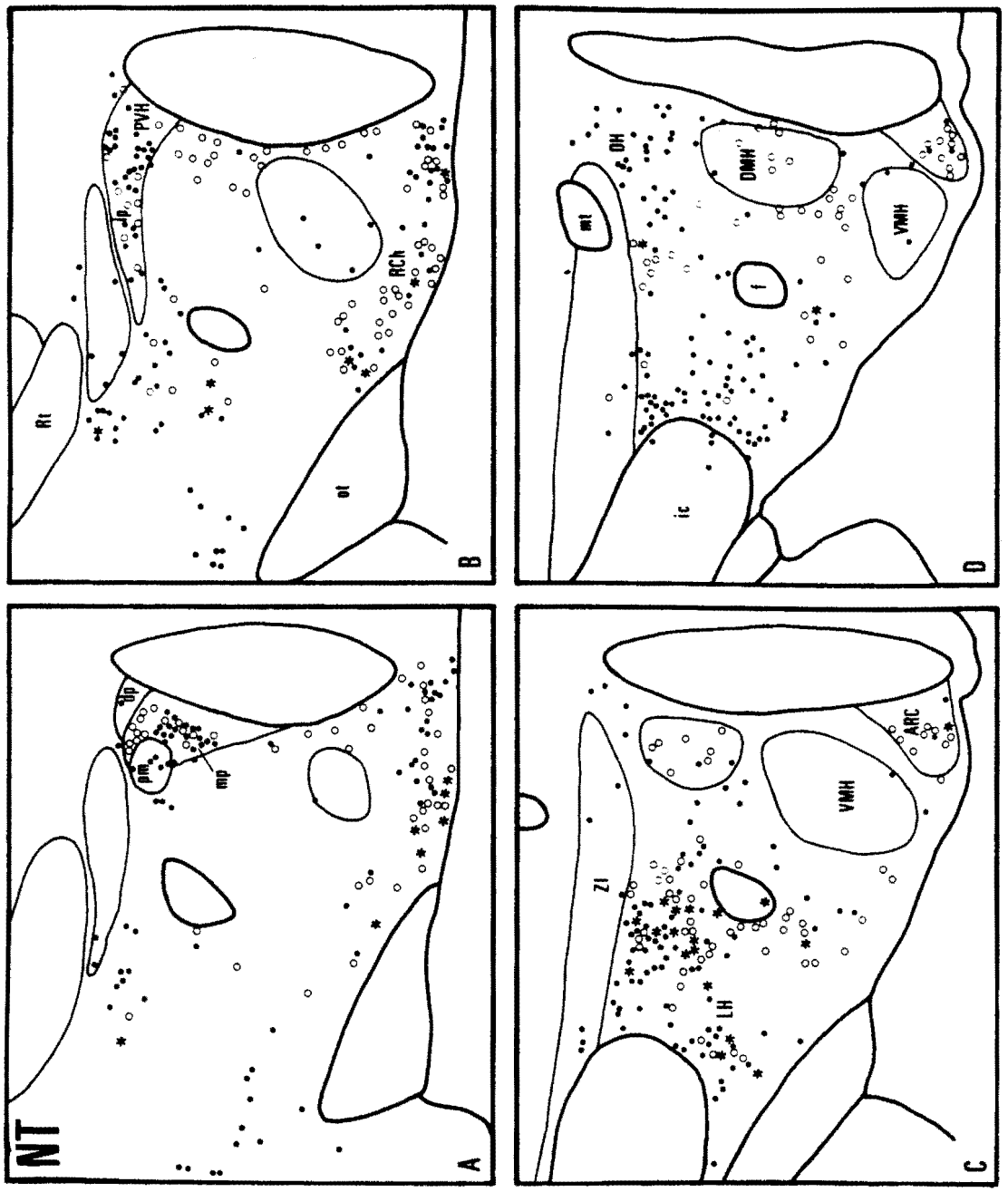
NT
A
dp
pm
mp
B
Rt
PVH
dp
RCh
ot
C
ZI
LH
VMH
ARC
D
ic
mt
DH
DMH
f
VMH

Figure 11. Line drawings of coronal sections through four levels of the hypothalamus (A-D, rostral to caudal) illustrating the distributions of Fast Blue (●), CRF-immunoreactive (o) and double-labeled (*) cells after Fast Blue injections into the PB.

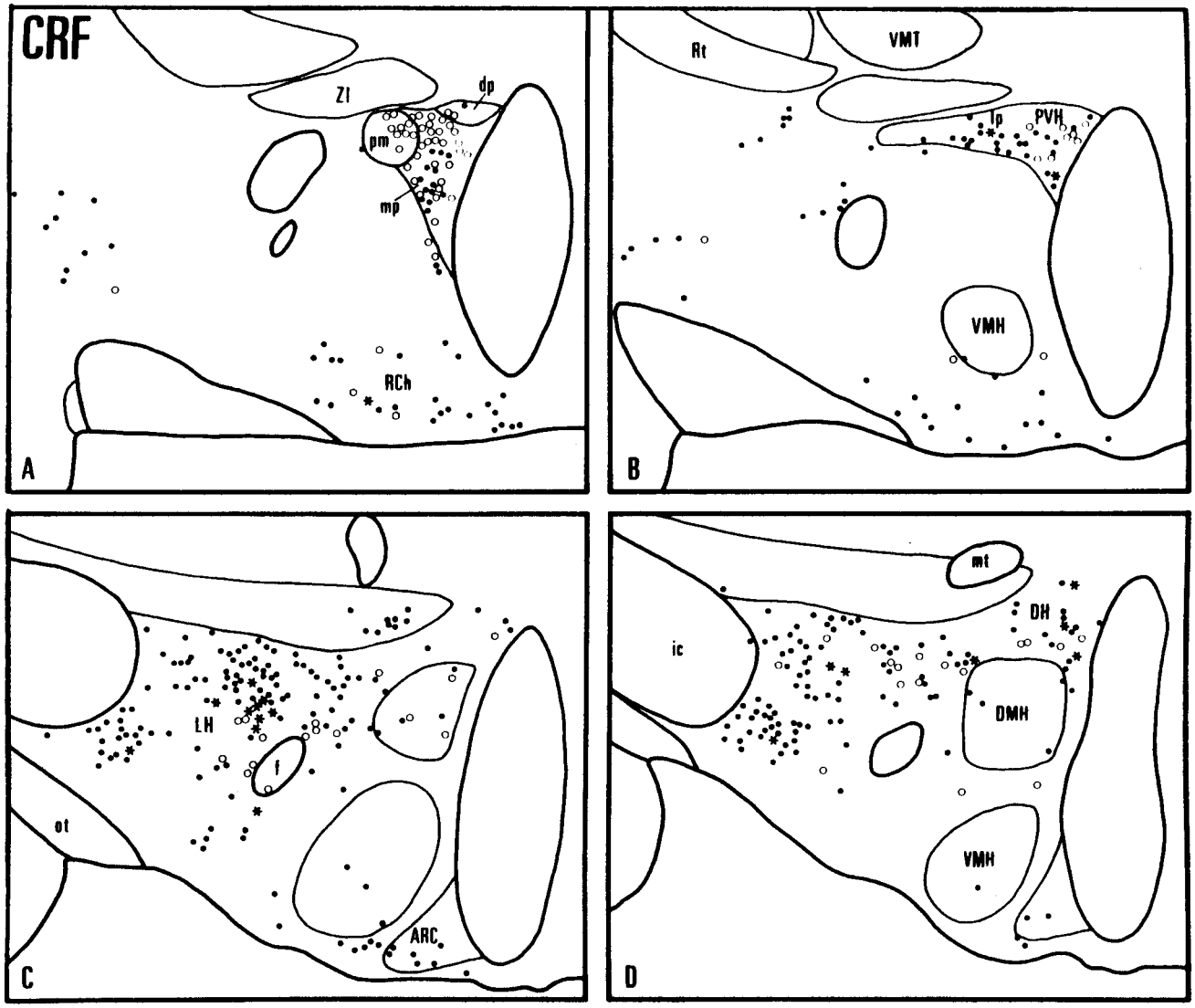
CRF
ZI
dp
pm
mp
RCh
A
Rt
VMT
Ip
PVH
VMH
B
LH
f
ot
ARC
C
mt
DH
ic
DMH
VMH
D

Figure 12. Line drawings of coronal sections through four levels of the hypothalamus (A-D, rostral to caudal) illustrating the distributions of Fast Blue (●), GAL-immunoreactive (○) and double-labeled (*) cells after Fast Blue injections into the PB.

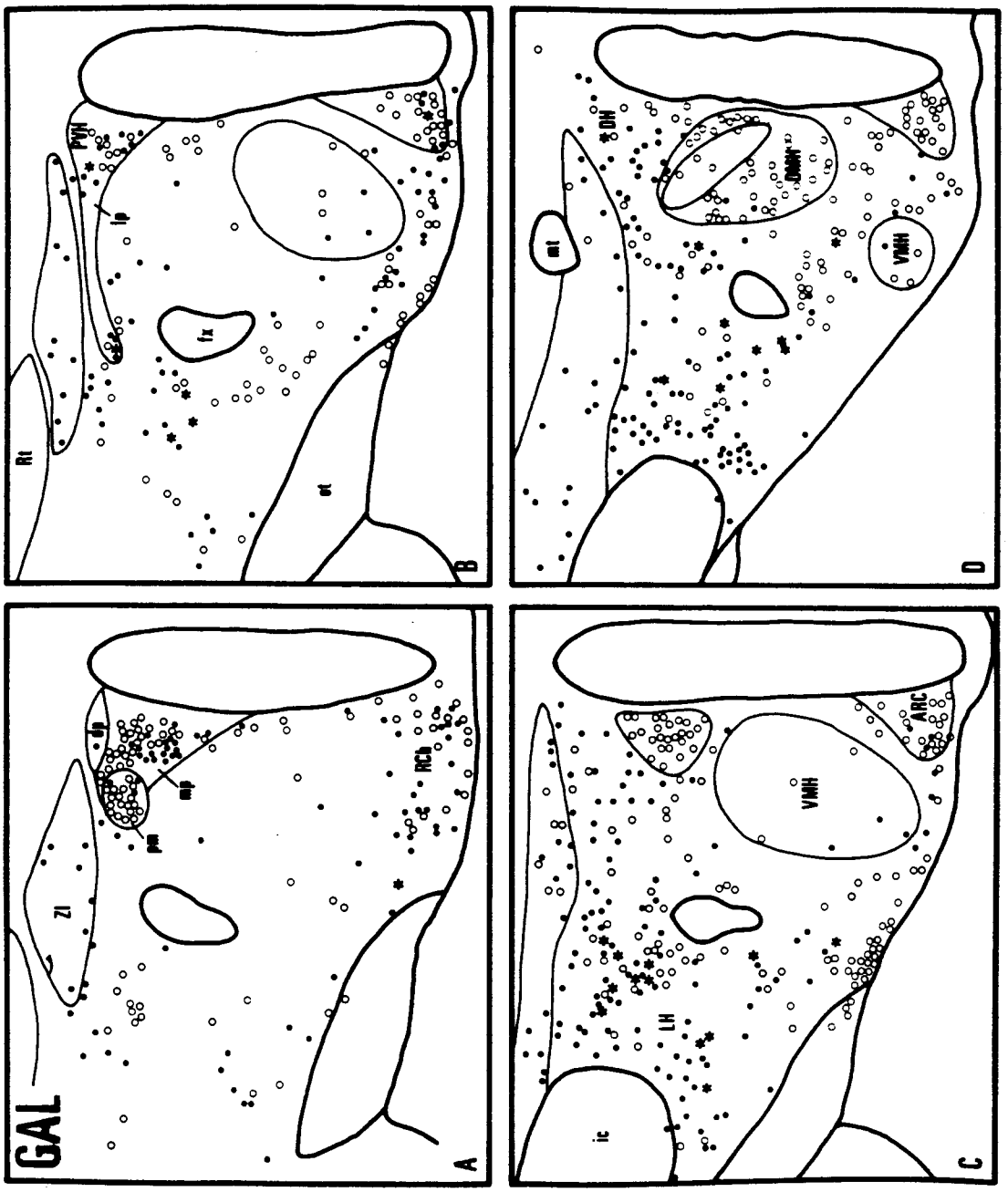
GAL
A
B
C
D
ZI
dp
mp
pm
RCh
Rt
PVH
lp
fx
ot
DMH
mt
VMH
ARC
LH
ic

Figure 13. Line drawings of coronal sections through four levels of the hypothalamus (A-D, rostral to caudal) illustrating the distributions of Fast Blue (●), SS-immunoreactive (o) and double-labeled (*) cells after Fast Blue injections into the PB.

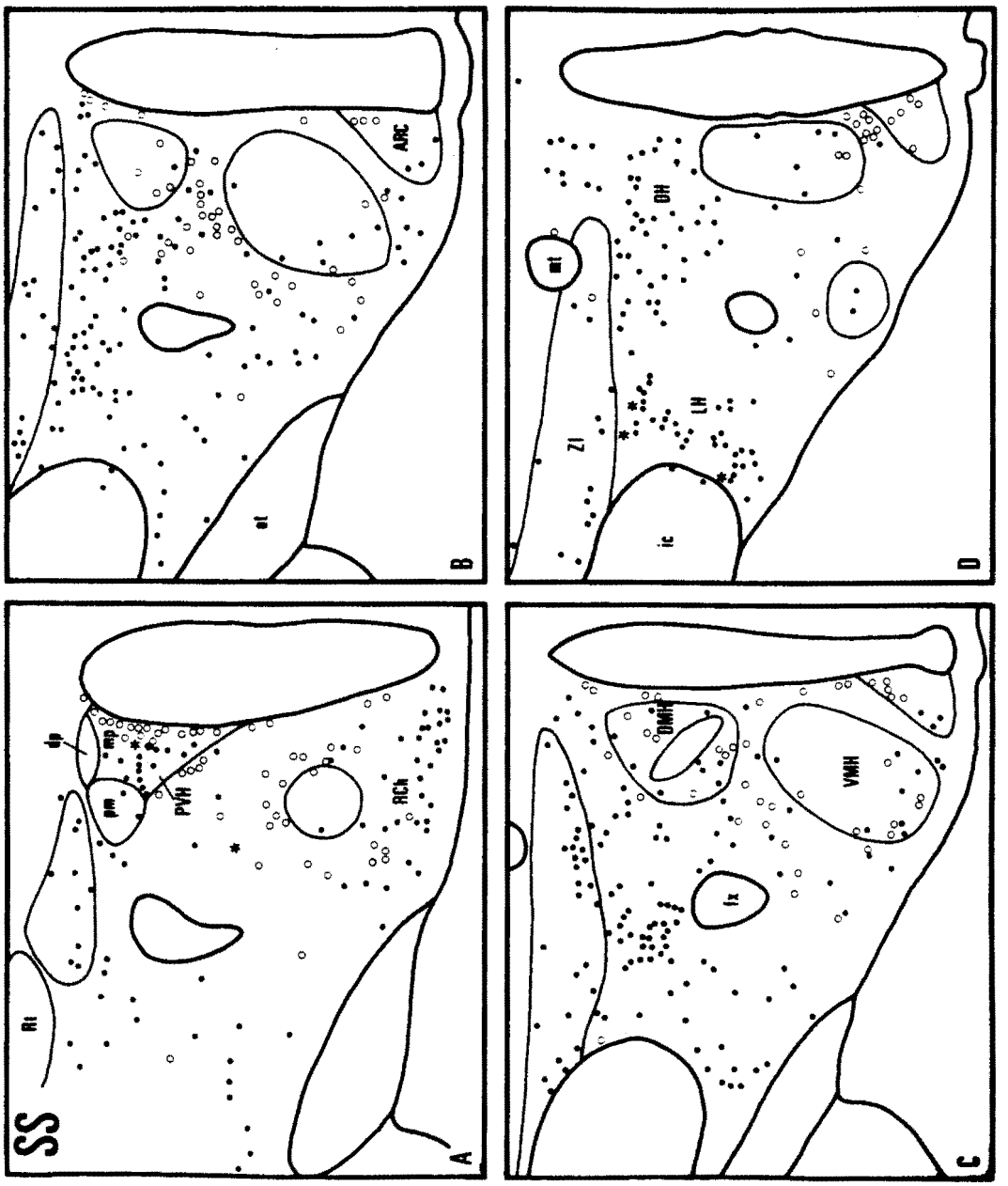
ARC
mt
B
DH
mt
ZI
LH
ic
D
SS
fp
mp
pm
PVH
RCh
Rt
A
DMH
VMH
fx
C

Figure 14. Line drawings of coronal sections through two levels of the paraventricular hypothalamus (A-B, rostral to caudal) illustrating the distributions of Fast Blue (●), OXY-immunoreactive (○) and double-labeled (*) cells after Fast Blue injections into the PB.

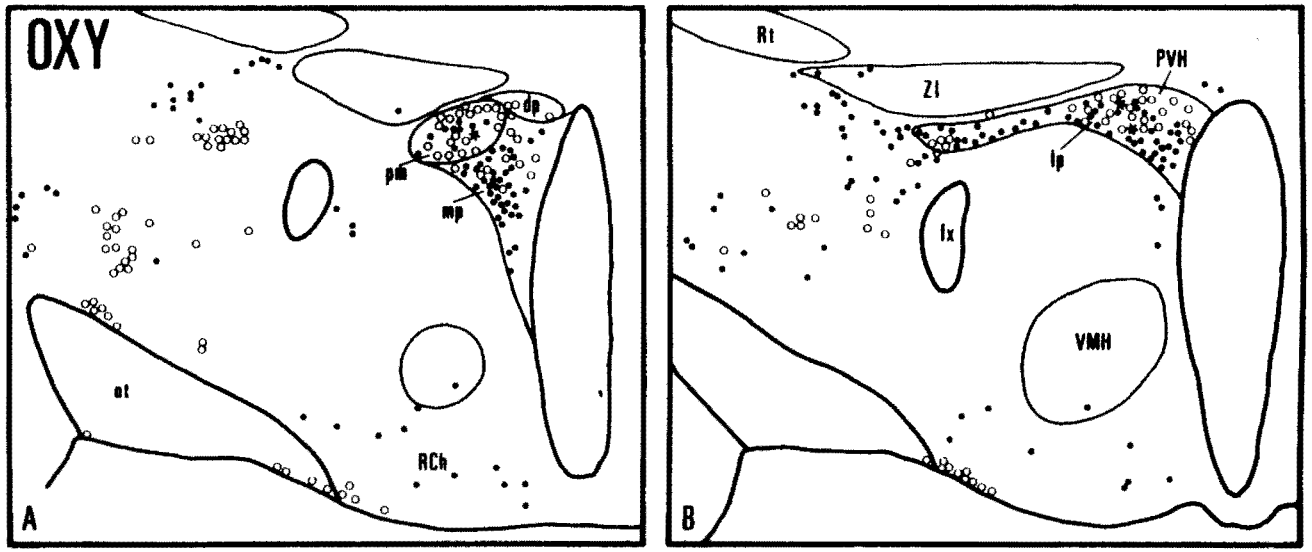
OXY
dp
pm
mp
at
RCh
A
Rt
ZI
PVH
lp
lx
VMH
B

Figure 15. Line drawings of coronal sections through two levels of the paraventricular hypothalamus (A-B, rostral to caudal) illustrating the distributions of Fast Blue (●), AVP-immunoreactive (o) and double-labeled (*) cells after Fast Blue injections into the PB.

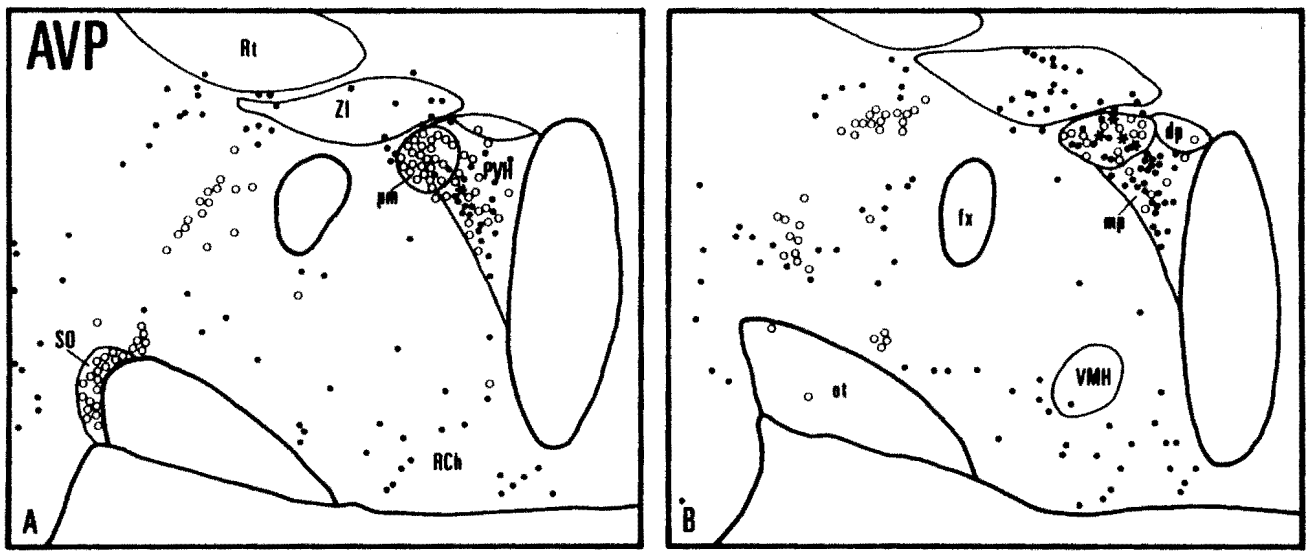
AVP
Rt
ZI
pm
PVH
SO
RCh
A
fx
mp
dp
VMH
ot
B

Figure 16. Line drawings of coronal sections through four levels of the hypothalamus (A-D, rostral to caudal) illustrating the distributions of Fast Blue (●), MSH-like immunoreactive (○) and double-labeled (*) cells after Fast Blue injections into the PB.

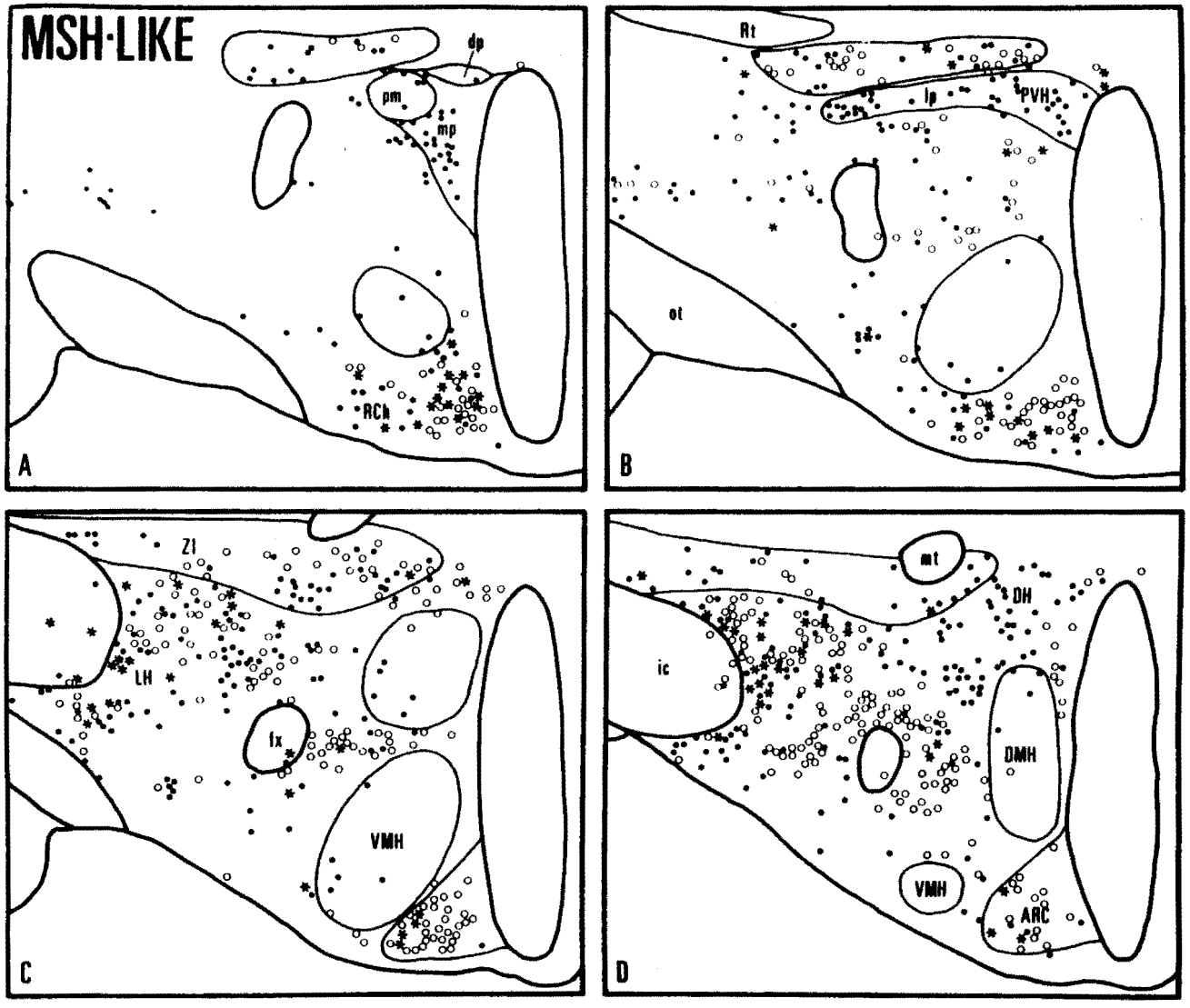
MSH-LIKE
dp
pm
mp
RCh
A
Rt
lp
PVH
ot
B
ZI
LH
fx
VMH
C
mt
DH
ic
DMH
VMH
ARC
D

Figure 17. Line drawings of coronal sections through four levels of the hypothalamus (A-D, rostral to caudal) illustrating the distributions of Fast Blue (●), ACTH-immunoreactive (o) and double-labeled (*) cells after Fast Blue injections into the PB.

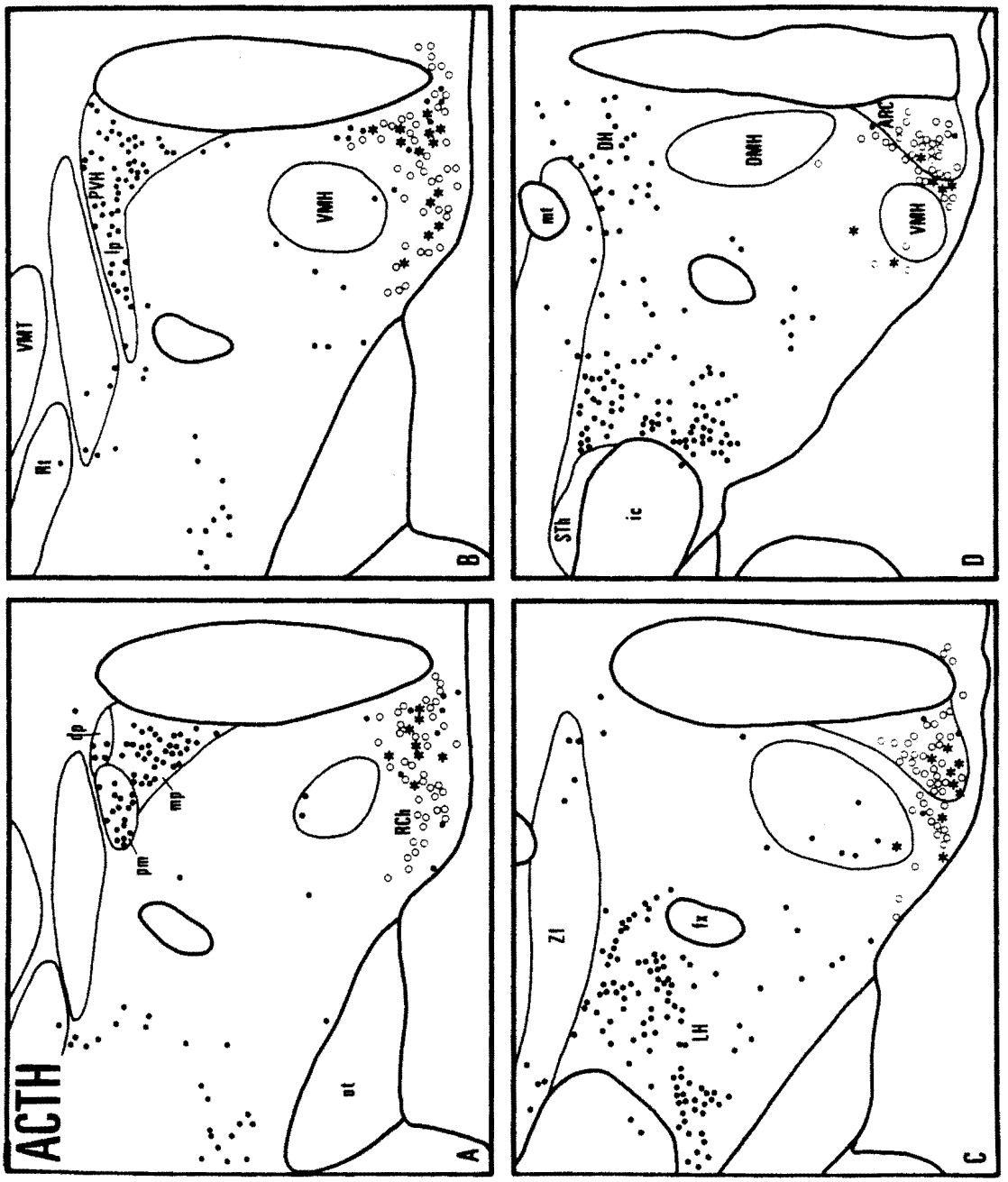
ACTH
A
dp
mp
pm
RCh
ot
B
VMT
Rt
PVH
lp
VMH
C
ZI
fx
LH
D
DH
mt
STh
ic
DMH
Arc
VMH

CHAPTER VI

GENERAL DISCUSSION

Descending pathways to the PB. Previously, a limited number of immunohistochemical studies had examined the forebrain projections to the PB for their neuropeptide content (Swanson, '77; Saper et al., '85; Milner and Pickel, '86a,b). The results from the present dissertation demonstrate that many neuropeptide-immunoreactive neurons in the amygdala, BST and hypothalamus project to the PB (Table 1). In the first two experiments, the PB afferent cell populations in the BST and CeA were found to stain for identical neuropeptides, that is, for CRF, NT and SS but not for ENK. Both of these peptidergic projections arise from largely circumscribed areas within the CeA and lateral BST, namely, the lateral subdivision of the CeA and the dorsal lateral subnucleus of the BST; and, both projections terminate predominantly in the external lateral subnucleus in the caudal half of the PB.

In the third experiment, the PB afferent cell populations in the hypothalamus were found to stain for a wide variety of neuropeptides, and each of these cell populations was found to contain a unique neuropeptide composition. Furthermore, the hypothalamic peptidergic projections to the PB were found to terminate predominantly in the rostral half of the PB. The neuropeptide-immunoreactive neurons in the hypothalamus that project to the PB are most numerous in the lateral hypothalamus (particularly in the perifornical area), the parvocellular

subdivisions of the PVH, the retrochiasmatic area and the arcuate nucleus. In a recent study examining the peptide content of hypothalamic pathways to the spinal cord using similar antisera, a different neuropeptide composition was found (Cechetto and Saper, '88), suggesting that peptidergic differences may, in addition to topographical differences, distinguish the hypothalamic descending pathways.

Historically, anterograde studies of the descending projections to the PB have reported diffuse labeling within the PB, suggesting a lack of topographical organization in the forebrain afferents (e.g., Conrad and Pfaff, '76; Hopkins and Holstege, '78; Swanson and Cowan, '79; Saper et al., '79). Contrary to this view, the results from this dissertation suggest that the forebrain afferents of the PB are topographically organized, although these data await further confirmation. For example, both the lateral CeA and dorsal lateral BST project almost exclusively to the external lateral PB subnucleus; in contrast, the medial CeA and posterior lateral BST project to a number of PB subnuclei, including the medial, central lateral and external lateral subnuclei (Chapters III, IV). These results further demonstrate the close anatomical ties between the CeA and lateral BST; in particular, the dorsal lateral BST may be homologous to the lateral CeA, and the posterior lateral BST, to the medial CeA.

Some degree of topographical organization within the hypothalamic projection to the PB was also observed (Chapter V). For example, retrogradely labeled cells in the caudal LH were most numerous after injections into the caudal waist area of the PB, while these same

injections produced few labeled cells in perifornical LH. Conversely, labeled cells in perifornical LH were more numerous, and cells in caudal LH less common, after rostral lateral PB injections.

Possible significance of neuropeptides. Neuropeptides are particularly abundant in autonomic structures such as the hypothalamus, CeA, BST, PB, NTS and midbrain central gray (for review, Pickel, '86). Possibly, neuropeptides may play a role in the visceral responses elicited from these autonomic nuclei. As evidence, relatively 'large' microinjections (i.e., 1-10 nanomoles) of neuropeptides, when bilaterally placed in autonomic nuclei, produce a variety of visceral effects. For example, microinjections of CCK into the NTS of awake cats produce an increase in respiratory frequency and a decrease in tidal volume (Denavit-Saubie et al., '85). Injections of NT into the CeA of rats increase their nociceptive threshold (Kalivas et al., '82). At physiological doses (i.e., picomoles), microiontophoresis of neuropeptides causes a variety of neuronal effects; these effects are dependent on the neuropeptide and its site of application within the CNS (Nicoll et al., '77; Henry, '82; Eberly et al., '83; Siggins et al., '85).

Few studies have specifically examined the role of neuropeptides in the PB. In one study, the application of the opioid agonists, FK-33824 and DADLE, to the rostral dorsal surface of the pons caused a significant decrease in respiratory frequency; this effect was attributed to opioid diffusion to the medial PB (Hurle et al., '85). More conclusively, Denavit-Saubie et al ('78) found that opioid agonists depress the spontaneous firing activity of respiratory-related

neurons in the medial PB. Clearly, more studies are needed before any conclusions can be drawn as to the role of neuropeptides in the PB.

Directions for future research. There are a number of possible experiments that would elucidate the role of these descending pathways, and their intrinsic neuropeptides, in central autonomic regulation. At a gross level, one could microinject (i.e., 10-6 M concentrations) bilaterally the neuropeptides examined here into the PB, and then observe what visceral responses (e.g., respiratory, cardiovascular) are elicited. The results from this study would suggest what PB visceral functions are associated with what neuropeptides. In addition, one could bilaterally inject neuropeptide antibodies into the PB to determine whether depletion of these neuropeptides produces any visceral effects.

At the cellular level, it would be interesting to inject "physiological" doses (i.e., picomoles) of the neuropeptides present in PB afferents, and then record single units in the PB for their responses (e.g., excitatory, inhibitory, biphasic). By marking the recording site, one could determine whether neurons in different PB subnuclei respond differently to a given neuropeptide.

Role of PB in visceral control. Early studies of the PB noted its importance as a relay for visceral afferent information from the NTS to the forebrain (Norgren and Leonard, '71,'73; Norgren, '74, '76; Saper and Loewy, '80). Recently, investigators have found that afferent information from different visceral organs converges onto individual PB neurons (Ogawa et al., '82; Hermann and Rogers, '85), suggesting that

the PB may 'integrate' diverse visceral sensory information rather than merely 'relay' that information to the forebrain.

As indicated in Chapter 1, physiological studies have implicated the PB in a diversity of visceral functions. As other central autonomic nuclei are also involved in these functions, what functions of the PB are unique? The position of the PB between, and its extensive connections with, autonomic nuclei in both forebrain and lower brainstem/spinal cord suggests a pivotal role for the PB in central autonomic regulation (Saper, '82). This role may involve adding both flexibility and safety to the central autonomic system. Specifically, the PB receives a heavier forebrain input than the NTS; thus, it could buffer the critical medullary reflexes from excess forebrain interference. At the same time, the PB projects heavily to a number of brainstem nuclei, including cranial motor nuclei and the reticular formation; these projections may provide a greater range of visceral responses and behaviors than could be found in a system without a nucleus at this level.

Table 1. Neuropeptide Immunoreactivity Detected in Afferent Cell Populations of the Parabrachial Nucleus.

Afferent	Neuropeptide										
	CRF	NT	SS	DYN	ENK	GAL	AII	aMSH	ACTH	AVP	OXY
CeA	++	++	++	-	-	+	nc	nc	nc	nc	nc
BST	++	++	++	-	-	+	nc	nc	nc	-	nc
LH	+++	+++	+	+++	-	+++	+++	+++	nc	nc	nc
RCh	+	+	-	+	-	+	+	++	++	nc	nc
PVH	+	+	+	+	+	+	+	nc	nc	+	+
ARC	-	+	-	+	-	-	-	+++	+++	nc	nc

nc No cell staining in this nucleus
\- No double-labeled cells found with this antisera
\+ Less than 4% of afferent cell population stains for this antisera
++ 5-14%
+++ 15-30%

BIBLIOGRAPHY

Abrahams, V.C., S.M. Hilton, and A.W. Zbrozyna (1960) Active muscle vasodilatation produced by stimulation of the brain stem: its significance in the defence reaction. J. Physiol. (Lond.) 154: 491-513.

Abrahams, V.C., S.M. Hilton, and A.W. Zbrozyna (1964) The role of active muscle vasodilatation in the alerting stage of the defence reaction. J. Physiol. (Lond.) 171: 189-202.

Allen, W.F. (1923) Origin and destination of the secondary visceral fibers in the guinea-pig. J. Comp. Neurol. 35: 275-311.

Allen, Y.S., G.W. Roberts, S.R. Bloom, T.J. Crow, and J.M. Polak (1984) Neuropeptide Y in the stria terminalis: evidence for an amygdalofugal projection. Brain Res. 321: 357-362.

Atweh, S.F., and M.J. Kuhar (1977) Autoradiographic localization of opiate receptors in rat brain. II. The brain stem. Brain Res. 129: 1-12.

Barnard, J.W. (1936) A phylogenetic study of the visceral afferent areas associated with the facial, glossopharyngeal, and vagus nerves, and their fiber connections. The efferent facial nucleus. J. Comp. Neurol. 65: 503-602.

Barrington, F.J.F. (1925) The effect of lesions of the hind- and midbrain on micturition in the cat. Quart. J. exp. Physiol. 15: 81-102.

Beitz, A.J. (1982) The organization of afferent projections to the midbrain periaqueductal gray of the rat. Neurosci. 7: 133-159.

Beitz, A.J. (1982) The sites of origin of brain stem neurotensin and serotonin projections to the rodent nucleus raphe magnus. J. Neurosci. 2: 829-843.

Beltramino, C., and S. Taleisnik (1978) Facilitatory and inhibitory effects of electrochemical stimulation of the amygdala on the release of luteinizing hormone. Brain Res. 144: 95-107.

Beltramino, C., and S. Taleisnik (1980) Dual action of electrochemical stimulation of the bed nucleus of the stria terminalis on the release of LH. Neuroendocrinol. 30: 238-242.

Berk, M.L., and J.A. Finkelstein (1982) Efferent connections of the lateral hypothalamic area of the rat: an autoradiographic investigation. Brain Res. Bull. 8: 511-526.

Bertrand, F., and A. Hugelin (1971) Respiratory synchronizing function of nucleus parabrachialis medialis: pneumotaxic mechanisms. J. Neurophysiol. 34: 189-207.

Block, C.H., and G.E. Hoffman (1987) Neuropeptide and monoamine components of the parabrachial pontine complex. Peptides 8: 267-283.

Block, C.H., G.E. Hoffman, and B.S. Kapp (1983) Peptide interactions of cells projecting to the central nucleus of the amygdala. Soc. Neurosci. Abstr. 134.7.

Block, C.H., R.E. Watson, J., and G. Hoffman-Small (1984) Neuropeptide connections of the lateral parabrachial nucleus (LPBN) with the anteroventral third ventricular area (AVEV). Soc. Neurosci. Abstr. 178.5.

Brennan, T.J., U.T. Oh, M.-N. Girardot, W.S. Ammons, and R.D. Foreman (1987) Inhibition of cardiopulmonary input to thoracic spinothalamic tract cells by stimulation of the subcoeruleus-parabrachial region in the primate. J. Auton. Nerv. Sys. 18: 61-72.

Brown, M.R., L.A. Fisher, J. Spiess, C. Rivier, J. Rivier, and W. Vale (1982) Corticotropin-releasing factor: actions on the sympathetic nervous system and metabolism. Endocrinology 111: 928-931.

Burton, H., and R.M. Benjamin (1971) Central projections of the gustatory system. In L.M. Beidler (ed.): Handbook of Sensory Physiology, Vol. IV, Chemical Senses, Part 2, Taste. New York: Springer-Verlag, pp. 148-164.

Cassell, M.D., T.S. Gray, and J.Z. Kiss (1986) Neuronal architecture in the rat central nucleus of the amygdala: a cytological, hodological and immunocytochemical study. J. Comp. Neurol. 246: 478-499.

Cechetto, D., and F.R. Calaresu (1983) Stimulation of buffer nerves and of the amygdala affects firing frequency of parabrachial neurons in the cat. Fed. Proc. 42: 1120.

Cechetto, D., and C.B. Saper (1988) Neurotransmitters in the hypothalamo-spinal projection in the rat. J. Comp. Neurol. accepted for publication.

Cechetto, D.F., D.G. Standaert, and C.B. Saper (1985) Spinal and trigeminal dorsal horn projections to the parabrachial nucleus in the rat. J. Comp. Neurol. 240: 153-160.

Chai, C.Y., and S.C. Wang (1962) Localization of central cardiovascular control mechanism in lower brain stem of cat. Amer. J. Physiol. 202: 25-30.

Chiba, T., and Y. Murata (1985) Afferent and efferent connections of the medial preoptic area in the rat: a WGA-HRP study. Brain Res. Bull. 14: 261-272.

Ciriello, J., D. Lawrence, and Q.J. Pittman (1984) Electrophysiological identification of neurons in the parabrachial nucleus projecting directly to the hypothalamus in the rat. Brain Res. 322: 388-392.

Cohen, M.I. (1971) Switching of the respiratory phases and evoked phrenic responses produced by rostral pontine electrical stimulation. J. Physiol. (Lond.) 217: 133-158.

Cohen, M.I., and S.C. Wang (1959) Respiratory neuronal activity in pons of cat. J. Neurophysiol. 22: 33-50.

Conrad, L.C.A., and D.W. Pfaff (1976) Efferents from medial basal forebrain and hypothalamus in the rat. I. An autoradiographic study of the medial preoptic area. J. Comp. Neurol. 169: 185-220.

Coote, J.H., S.M. Hilton, and A.W. Zbrozoyna (1973) The pontomedullary area integrating the defense reaction in the cat and its influence on muscle blood flow. J. Physiol. (Lond.) 229: 257-274.

deGroat, W.C. (1975) Nervous control of the urinary bladder of the cat. Brain Res. 87: 201-211.

Denavit-Saubie, M., J. Champagnat, and W. Zieglgansberger (1978) Effects of opiates and methionine-enkephalin on pontine and bulbar respiratory neurones of the cat. Brain Res. 155: 55-67.

Denavit-Saubie, M., M.A. Hurle, M.P. Morin-Surun, A.S. Foutz, and J. Champagnat (1982) The effects of cholecystokinin-8 in the nucleus tractus solitarius. Ann. N.Y. Acad. Sci. 448: 375-384.

DeOlmos, J., G.F. Alheid, and C.A. Beltramino (1985) Amygdala. In G. Paxinos (ed.): The Rat Nervous System, Vol. 1, Forebrain and Midbrain. Orlando: Academic Press, pp.223-334.

Deschepper, C.F., D.A. Crumrine, and W.F. Ganong (1986) Evidence that the gonadotrophs are the likely site of production of angiotensin II in the anterior pituitary of the rat. Endocrinol. 119: 36-43.

Dunn, J.D. (1987) Plasma corticosterone responses to electrical stimulation of the bed nucleus of the stria terminalis. Brain Res. 407: 327-331.

Dunn, J.D., and J. Whitener (1986) Plasma corticosterone responses to electrical stimulation of the amygdaloid complex: cytoarchitectural specificity. Neuroendocrinol. 42: 211-217.

Eberly, L.B., C.A. Dudley, and R.L. Moss (1983) Iontophoretic mapping of corticotropin-releasing factor (CRF) sensitive neurons in the rat forebrain. Peptides 4: 837-841.

Edwards, G.L., and R.C. Ritter (1981) Ablation of the area postrema causes exaggerated consumption of preferred foods in the rat. Brain Res. 216: 265-276.

Eiden, L.E., T. Hokfelt, M.J. Brownstein, and M. Palkovits (1985) Vasoactive intestinal polypeptide afferents to the bed nucleus of the stria terminalis in the rat: an immunohistochemical study. Neurosci. 15: 999-1013.

Emson, P.C., M. Goedert, B. Williams, M. Ninkovic, and S.P. Hunt (1982) Neurotensin: regional distribution, characterization and inactivation. Annals N.Y. Acad. Sci. 198-215.

Eng, R., and R.R. Miselis (1981) Polydipsia and abolition of angiotensin-induced drinking after transections of subfornical organ efferent projections in the rata. Brain Res. 225: 200-206.

Epstein, A.N., J.T. Fitzsimons, and B.J. Rolls (1970) Drinking induced by injection of angiotensin into the brain of the rat. J. Physiol. (Lond.) 210: 457-474.

Euler, C. von, and T. Trippenbach (1976) Excitability changes of the inspiratory 'off-switch' mechanism tested by electrical stimulation in nucleus parabrachialis in the cat. Acta Physiol. Scand. 97: 175-188.

Euler, C. von, I. Martilla, J.E. Remmers, and T. Trippenbach (1976) Effects of lesions in the parabrachial nucleus on the mechanisms for central and reflex termination of inspiration in the cat. Acta Physiol. Scand. 96: 324-337.

Faiers, A.A., F.R. Calaresu, and G.J. Mogenson (1976) Factors affecting cardiovascular responses to stimulation of hypothalamus in the rat. Exper. Neurol. 51: 188-206.

Feldman, J.L., and H. Gautier (1976) Interaction of pulmonary afferents and pneumotaxic center in control of respiratory pattern in cats. J. Neurophysiol. 39: 31-44.

Fields, H.L., and A.I. Basbaum (1978) Brainstem control of spinal pain-transmission neurons. Ann. Rev. Physiol. 40: 217-248.

Finley, J.C.W., J.L. Maderdrut, L.J. Roger, and P. Petrusz (1981) The immunocytochemical localization of somatostatin-containing neurons in the rat central nervous system. Neurosci. 6: 2173-2192.

Folkow, B., and E.H. Rubinstein (1965) Behavioral and autonomic patterns evoked by stimulation of the lateral hypothalamic area in the cat. Acta Physiol. Scand. 65: 292-299.

Frysinger, R.C., J.D. Marks, R.B. Trelease, V.L. Schechtman, and R.M. Harper (1984) Sleep states attenuate the pressor response to central amygdala stimulation. Exper. Neurol. 83: 604-617.

Fulwiler, C.E., and C.B. Saper (1984) Subnuclear organization of the efferent connections of the parabrachial nucleus in the rat. Brain Res. Rev. 7: 229-259.

Fulwiler, C.E., and C.B. Saper (1985) Cholecystokinin-immunoreactive innervation of the ventromedial hypothalamus in the rat: possible substrate for autonomic regulation of feeding. Neurosci. Lett. 53: 289-296.

Galeno, T.M., and M.J. Brody (1983) Hemodynamic responses to amygdaloid stimulation in spontaneously hypertensive rats. Amer. J. Phys. 245: R281-286.

Galeno, T.M., G.W. Van Hoesen, and M.J. Brody (1984) Central amygdaloid nucleus lesion attenuates exaggerated hemodynamic responses to noise stress in spontaneously hypertensive rat. Brain Res. 291: 249-259.

Gray, T.S., and D.J. Magnuson (1987) Neuropeptide neuronal efferents from the bed nucleus of the stria terminalis and central amygdaloid nucleus to the dorsal vagal complex in the rat. J. Comp. Neurol. 262: 365-374.

Grossman, S.P., D. Dacey, A.E. Halaris, T. Collier, and A. Routtenberg (1978) Aphagia and adipsia after preferential destruction of nerve cell bodies in hypothalamus. Science 202: 537-539.

Haber, S., and R.P. Elde (1982) The distribution of enkephalin immunoreactive fibers and terminals in the monkey central nervous system: an immunohistochemical study. Neurosci. 7: 1049-1095.

Hammond, D.L., and H.K. Proudfit (1980) Effects of locus coeruleus lesions on morphine-induced antinociception. Brain Res. 188: 79-91.

Harper, R.M., R.C. Frysinger, R.B. Trelease, and J.D. Marks (1984) State-dependent alteration of respiratory cycle timing by stimulation of the central nucleus of the amygdala. Brain Res. 306: 1-8.

Henke, P.G. (1982) The telencephalic limbic system and experimental gastric pathology: a review. Neurosci. Biobehav. Rev. 6: 381-390.

Henry, J.L. (1982) Electrophysiological studies on the neuroactive properties of neurotensin. Ann. N.Y. Acad. Sci. 400: 216-227.

Herbert, H., M.M. Moga, and C.B. Saper (1987) Peptidergic projections from the nucleus of the solitary tract to the parabrachial nucleus. Soc. Neurosci. Abstr. 203.2.

Hermann, G.E., and R.C. Rogers (1985) Convergence of vagal and gustatory afferent input within the parabrachial nucleus of the rat. J. Auton. Nerv. Sys. 13: 1-17.

Hernandez, D.E., C.B. Nemeroff, R.C. Orlando, and A.J. Prange, Jr. (1983) The effect of centrally administered neuropeptides on the development of stress-induced gastric ulcers in rats. J. Neurosci. Res. 9: 145-157.

Herrick, C.J. (1905) The central gustatory paths in the brains of bony fishes. J. Comp. Neurol. 15: 375-456.

Herrick, C.J. (1944) The fasciculus solitarius and its connections in amphibians and fishes. J. Comp. Neurol. 81: 307-331.

Herrick, C.J. (1948) The Brain of the Tiger Salamander, Ambystoma tigrinum. Chicago: University of Chicago Press.

Higgins, G.A., and J.S. Schwaber (1983) Somatostatinergic projections from the central nucleus of the amygdala to the vagal nuclei. Peptides 4: 657-662.

Hilton, S.M., and K.M. Spyer (1971) Participation of the anterior hypothalamus in the baroreceptor reflex. J. Physiol. (Lond.) 218: 271-293.

Hilton, S.M., and A.W. Zbrozyna (1963) Amygdaloid region for defence reactions and its efferent pathway to the brain stem. J. Physiol. (Lond.) 165: 160-173.

Hoebel, B.G. (1969) Feeding and self-stimulation. Ann. N.Y. Acad. Sci. 157: 758-778.

Hokfelt, T., L. Skirboll, J.F. Rehfeld, M. Goldstein, K. Markey, and O. Dann (1980) A subpopulation of mesencephalic dopamine neurons projecting to limbic areas contains a cholecystokinin-like peptide: evidence from immunohistochemistry combined with retrograde tracing. Neurosci. 5: 2093-2124.

Holstege, G., L. Meiners, and K. Tan (1985) Projections of the bed nucleus of the stria terminalis to the mesencephalon, pons, and medulla oblongata in the cat. Exp. Brain Res. 58: 379-391.

Hopkins, D.A., and G. Holstege (1978) Amygdaloid projections to the mesencephalon, pons and medulla oblongata in the cat. Exp. Brain Res. 32: 529-547.

Hosoya, Y., and M. Matsushita (1981) Brainstem projections from the lateral hypothalamic area in the rat, as studied with autoradiography. Neurosci. Lett. 24: 111-116.

Hubbard, J.W., R.A. Buchholz, T.K. Keeton, and M.A. Nathan (1987) Parabrachial lesions increase plasma norepinephrine concentration, plasma renin activity and enhance baroreflex sensitivity in the conscious rat. Brain Res. 421: 226-234.

Hurle, M.A., A. Mediavilla, and J. Florez (1985) Differential respiratory patterns induced by opioids applied to the ventral medullary and dorsal pontine surfaces of cats. Neuropharm. 24: 597-606.

Joseph, S.A., W.H. Pilcher, and C. Bennett-Clarke (1983) Immunocytochemical localization of ACTH-ir perikarya in nucleus tractus solitarius in the medulla: evidence for a second opicortin neuronal system. Neurosci. Lett. 38: 221-225.

Kaada, B.R. (1972) Stimulation and regional ablation of the amygdaloid complex with reference to functional representations. In Elftheriou, B.E. (ed): The Neurobiology of the Amygdala, New York: Plenum Press, pp. 205-281.

Kabat, H., H.W. Magoun, and S.W. Ranson (1935) Electrical stimulation of points in the forebrain and midbrain. Arch. Neurol. Psychiat. 34: 931-955.

Kalivas, P.W., B.A. Gau, C.B. Nemeroff, and A.J. Prange, Jr. (1982) Antinociception after microinjection of neurotensin into the central amygdaloid nucleus of the rat. Brain Res. 243: 279-286.

Kawai, Y., S. Inagaki, S. Shiosaka, E. Senba, Y. Hara, M. Sakanaka, K. Takatsuki, and M. Tohyama (1982) Long descending projections from amygdaloid somatostatin-containing cells to the lower brain stem. Brain Res. 239: 603-607.

Kawakami, F., K. Fukui, H. Okamura, N. Morimoto, N. Yanaihara, T. Nakajima, and Y. Ibata (1984) Influence of ascending noradrenergic fibers on the neurotensin-like immunoreactive perikarya and evidence of direct projection of ascending neurotensin-like immunoreactive fibers in the rat central nucleus of the amygdala. Neurosci. Lett. 51: 231-234.

Khachaturian, H., S.J. Watson, M.E. Lewis, D.Coy, A. Goldstein, and H. Akil (1982) Dynorphin immunocytochemistry in the rat central nervous system. Peptides 3: 941-954.

Khachaturian, H., M.E. Lewis, S.N. Haber, H. Akil, and S.J. Watson (1984) Proopiomelanocortin peptide immunocytochemistry in rhesus monkey brain. Brain Res. Bull. 13: 785-800.

Khachaturian, H., M.E. Lewis, M.K.-H. Schafer, and S.J. Watson (1985) Anatomy of the CNS opioid systems. Trends Neurosci. 8: 111-119.

Kohler, C., and V. Chan-Palay (1982) Somatostatin-like immunoreactive neurons in the hippocampus: an immunocytochemical study in the rat. Neurosci. Lett. 34: 259-264.

Kohler, C., L. Haglund, and L.W. Swanson (1984) A diffuse alpha-MSH-immunoreactive projection to the hippocampus and spinal cord from individual neurons in the lateral hypothalamic area and zona incerta. J. Comp. Neurol. 223: 501-514.

Krettek, J.E., and J.L. Price (1978) Amygdaloid projections to subcortical structures within the basal forebrain and brainstem in the rat and cat. J. Comp. Neurol. 178: 225-254.

Lalley, R.M., deGroat, W.C., and P.L. McLain (1972) Activation of the sacral parasympathetic pathway to the urinary bladder by brain stem stimulation. Fed. Proc. 31: 386.

Lappe, R.W., J.L. Dinish, F. Bex, K. Michalak, and R.L. Wendt (1986) Effects of atrial natriuretic factor on drinking responses to central angiotensin II. Pharmacol. Biochem. Behav. 24: 1573-1576.

Lawrence, D., and Q.J. Pittman (1985) Response of rat paraventricular neurones with central projections to suckling, haemorrhage or osmotic stimuli. Brain Res. 341: 176-183.

Leibowitz, S.F. (1978) Paraventricular nucleus: a primary site mediating adrenergic stimulation of feeding and drinking. Pharmacol. Biochem. Behav. 8: 163-175.

Leibowitz, S.F. (1980) Neurochemical systems of the hypothalamus: control of feeding and drinking behavior and water-electrolyte excretion. In P.J. Morgane and J. Panskepp (eds.): Handbook of the Hypothalamus, Vol. 3A. New York: Marcel Dekker, pp. 299-437.

Light, A.R., D.L. Trevino, and E.R. Perl (1979) Morphologic features of functionally defined neurons in the marginal zone and substantia gelatinosa of the spinal dorsal horn. J. Comp. Neurol. 186: 151-172.

Lind, R.W., and L.W. Swanson (1984) Evidence for corticotropin releasing factor and leu-enkephalin in the neuronal projection from the lateral parabrachial nucleus to the median preoptic nucleus: a retrograde transport, immunohistochemical double labeling study in the rat. Brain Res. 321: 217-224.

Lind, R.W., L.W. Swanson, and D. Ganten (1985) Organization of angiotensin II immunoreactive cells and fibers in the rat central nervous system. Neuroendocrinol. 40: 2-24.

Loewy, A.D. and S. McKellar (1980) The neuroanatomical basis of central cardiovascular control. Fed. Proc. 39: 2495-2503.

Loewy, A.D., J.H. Wallach, and S. McKellar (1981) Efferent connections of the ventral medulla oblongata in the rat. Brain Res. Rev. 3: 63-80.

Luiten, P.G.M., G.J. ter Horst, H. Karst, and A.B. Steffens (1985) The course of paraventricular hypothalamic efferents to autonomic structures in medulla and spinal cord. Brain Res. 329: 374-378.

Lumb, B.M., and J.F.B. Morrison (1987) An excitatory influence of dorsolateral pontine structures on urinary bladder motility in the rat. Brain Res. 435: 363-366.

Lumsden, T. (1923) Observations on the respiratory centres in the cat. J. Physiol. (Lond.) 57: 153-160.

Lundberg, J.M., L. Terenius, T. Hokfelt, and K. Tatemoto (1984) Comparative immunohistochemical and biochemical analysis of pancreatic polypeptide-like peptides with special reference to presence of neuropeptide Y in central and peripheral neurons. J. Neurosci. 4: 2376-2386.

Mantyh, P.W., and S.P. Hunt (1984) Neuropeptides are present in projection neurons at all levels in visceral and taste pathways: from periphery to sensory cortex. Brain Res. 299: 297-311.

Marley, P.D., P.C. Emson, S.P. Hunt, and J. Fahrenkrug (1981) A long ascending projection in the rat brain containing vasoactive intestinal polypeptide. Neurosci. Lett. 27: 261-266.

Mayer, D.J., and D.D. Price (1976) Central nervous system mechanisms of analgesia. Pain 2: 379-404.

McCaleb, M.L., and R.D. Myers (1980) Cholecystokinin acts on the hypothalamic 'noradrenergic system' involved in feeding. Peptides 1: 47-49.

McDonald, A.J. (1983) Neurons of the bed nucleus of the stria terminalis: a golgi study in the rat. Brain Res. Bull. 10: 111-120.

McDonald, A.J. (1987) Somatostatinergic projections from the amygdala to the bed nucleus of the stria terminalis and medial preoptic-hypothalamic region. Neurosci. Lett. 75: 271-277.

Micco, D.J. Jr. (1974) Complex behaviors elicited by stimulation of the dorsal pontine tegmentum. Brain Res. 75: 172-176.

Milner, T.A., and V.M. Pickel (1986a) Neurotensin in the rat parabrachial region: ultrastructural localization and extrinsic sources of immunoreactivity. J. Comp. Neurol. 247: 326-343.

Milner, T.A., and V.M. Pickel (1986b) Ultrastructural localization and afferent sources of substance P in the rat parabrachial region. Neurosci. 17: 687-707.

Milner, T.A., T.H. Joh, R. J. Miller, and V.M. Pickel (1984) Substance P, neurotensin, enkephalin, and catecholamine-synthesizing enzymes: light microscopic localizations compared with autoradiographic label in solitary efferents to the rat parabrachial region. J. Comp. Neur. 226: 434-437.

Mitchell, R.A., and A.J. Berger (1981) Neural regulation of respiration. In: Neurogenesis of Central Respiratory Rhythm, pp. 191-197, A.L. Bianchi and M. Denavit-Saubie, eds. Lancaster: MTP Press Limited.

Miura, M., and D.J. Reis (1969) Cerebellum: a pressor response elicited from the fastigial nucleus and its efferent pathway in brain stem. Brain Res. 13: 595-599.

Moga, M.M., and T.S. Gray (1984) Neuropeptide neuronal efferents from the central nucleus of the amygdala to the parabrachial nuclei. Soc. Neurosci. Abstr. 8:128.

Moga, M.M., and T.S. Gray (1985a) Neuropeptide neuronal efferents from the bed nucleus of the stria terminalis to the parabrachial nuclei. Anat. Rec. 211: 131A.

Moga, M.M., and T.S. Gray (1985b) Evidence for corticotropin releasing factor, neurotensin, and somatostatin in the neural pathway from the central nucleus of the amygdala to the parabrachial nucleus. J. Comp. Neurol. 241: 275-284.

Moga, M.M., and T.S. Gray (1985c) Peptidergic efferents from the intercalated nuclei of the amygdala to the parabrachial nucleus. Neurosci. Lett. 61: 13-18.

Moga, M.M., and T.S. Gray (1985d) Hypothalamic peptidergic efferents to the parabrachial nucleus in the rat. Soc. Neurosci. Abstr. 204.9.

Moga, M.M., K.M. Hurley-Gius, D.F. Cechetto, T.S. Gray, and C.B. Saper (1986) Distribution of forebrain afferents to the parabrachial nucleus in the rat. Soc. Neurosci. Abstr. 289.6.

Moga, M.M., T.S. Gray, and C.B. Saper (1987) Subnuclear organization of the bed nucleus of the stria terminalis: a cytoarchitectural, connectional and immunocytochemical study. Soc. Neurosci. Abstr. 125.3.

Mogenson, G.J., and J.A.F. Stevenson (1967) Drinking elicited by electrical stimulation of the lateral hypothalamus. Exper. Neurol. 17: 119-127.

Mraovitch, S., M. Kumada, and D.J. Reis (1982) Role of the nucleus parabrachialis in cardiovascular regulation in cat. Brain Res. 232: 57-75.

Nicoll, R.A., G.R. Siggins, N. Ling, F.E. Bloom, and R. Guillemin (1977) Neuronal actions of endorphins and enkephalins among brain regions: a comparative microiontophoretic study. Proc. Natl. Acad. Sci. 74: 2584-2588.

Norgren, R. (1974) Gustatory afferents to ventral forebrain. Brain Res. 81: 285-295.

Norgren, R. (1976) Taste pathways to hypothalamus and amygdala. J. Comp. Neurol. 166: 17-30.

Norgren, R. (1978) Projections from the nucleus of the solitary tract in the rat. Neurosci. 3: 207-218.

Norgren, R., and C.M. Leonard (1971) Taste pathways in rat brainstem. Science 173: 1136-1139.

Norgren, R., and C.M. Leonard (1973) Ascending central gustatory pathways. J. Comp. Neurol. 150: 217-238.

Norgren, R., and C. Pfaffmann (1975) The pontine taste area in the rat. Brain Res. 91: 99-117.

O'Donohue, T.L., R.L. Miller, and D.M. Jacobowitz (1979) Identification, characterization and stereotaxic mapping of intraneuronal alpha-melanocyte-stimulating hormone-like immunoreactive peptides in discrete regions of the rat brain. Brain Res. 176: 101-123.

Ogawa, H., T. Hayama, and S. Ito (1982) Convergence of input from tongue and palate to the parabrachial nucleus neurons of rats. Neurosci. Lett. 28: 9-14.

Ohman, L.E., and A.K. Johnson (1986) Lesions in lateral parabrachial nucleus enhance drinking to angiotensin II and isoproterenol. Amer. J. Physiol. 251: R504-509.

Olschowka, J.A., T.L. O'Donohue, G.P. Mueller, and D.M. Jacobowitz (1982) Hypothalamic and extrahypothalamic distribution of CRF-like immunoreactive neurons in the rat brain. Neuroendocrinol. 35: 305-308.

Ottersen, O.P. (1981) The afferent connections of the amygdala of the rat as studied with retrograde transport of horeseradish peroxidase. In Y. Ben Ari (Ed.): The Amygdaloid Complex. Amsterdam: Elsevier/North Holland Biomedical press, pp.91-104.

Paxinos, G., and C. Watson (1982) The Rat Brain in Stereotaxic Coordinates. Academic Press, New York.

Pfaff, D.W. (1980) Estrogen and Brain Function. New York: Springer.

Pickel, V.M. (1985) General morphologic features of peptidergic neurons. In: Handbook of Chemical Neuroanatomy, Vol. 4, GABA and Neuropeptides in the CNS, A. Bjorklund, T. Hokfelt, eds., Amsterdam: Elsevier, pp. 72-92.

Powley, T.L. (1977) The ventromedial hypothalamic syndrome, satiety and acephalic phase hypothesis. Psychol. Rev. 34: 809-826.

Price, J.L., and D.G. Amaral (1981) An autoradiographic study of the projections of the central nucleus of the monkey amygdala. J. Neurosci. 1: 1242-1259.

Raisman, G., and P.M. Field (1973) Sexual dimorphism in the neuropil of the preoptic area of the rat and its dependence on neonatal androgen. Brain Res. 54: 1-29.

Randich, A., and W. Maixner (1984) Interactions between cardiovascular and pain regulatory systems. Neurosci. Biobehav. Rev. 8: 343-367.

Ranson, S.W. (1936) The Anatomy of the Nervous System, p. 175, Philadelphia: W.C. Saunders Company.

Rao, Z.R., M. Yamano, S. Shiosaka, A. Shinohara, and M. Tohyama (1987) Origin of leucine-enkephalin fibers and their two main afferent pathways in the bed nucleus of the stria terminalis in the rat. Exp. Brain Res. 65: 411-420.

Ricardo, J.A., and E.T. Koh (1978) Anatomical evidence of direct projections from the nucleus of the solitary tract to the hypothalamus, amygdala, and other forebrain structures in the rat. Brain Res. 153: 1-26.

Roberts, W.W. (1980) [^{14}C] deoxyglucose mapping of first-order projections activated by stimulation of lateral hypothalamic sites eliciting gnawing, eating, and drinking in rats. J. Comp. Neurol. 194: 617-638.

Roberts, G.W., P.L. Woodhams, J.M. Polak, and T.J. Crow (1980a) Distribution of neuropeptides in the limbic system of the rat: The amygdaloid complex. Neurosci. 7: 99-131.

Roberts, G.W., P.L. Woodhams, M.G. Bryant, T.J. Crow, S.R. Bloom, and J.M. Polak (1980b) VIP in the rat brain: evidence for a major pathway linking the amygdala and hypothalamus via the stria terminalis. Histochem. 65: 103-119.

Robinson, M.M., and M.D. Evered (1987) Pressor action of intravenous angiotensin II reduces drinking response in rats. Amer. J. Physiol. R754-759.

Rogers, R.C., and D.O. Nelson (1984) Neurons of the vagal division of the solitary nucleus activated by the paraventricular nucleus of the hypothalamus. J. Auton. Nerv. Sys. 10: 193-197.

Rokaeus, A., T. Melander, T. Hokfelt, J.M. Lundberg, K.Tatemoto, M. Carlquist and V. Mutt (1984) A galanin-like peptide in the central nervous system and intestine of the rat. Neurosci. Lett. 47: 161-166.

St. John, W.M., R.L. Glasser, and R. King (1972) Rhythmic respiration in awake vagotomized cats with chronic pneumotaxic lesions. Respir. Physiol. 15: 204-210.

Sakai, K., M. Touret, D. Salvert, L. Leger, and M. Jouvet (1977) Afferent connections of the nucleus raphe dorsalis in the cat as visualized by the horseradish peroxidase technique. Brain Res. 137: 11-35.

Sakanaka, M., S. Shiosaka, K. Takatsuki, S. Inagaki, H. Takagi, E. Senba, Y. Kawai, T. Matsuzaki, and M. Tohyama (1981) Experimental immunohistochemical studies on the amygdalofugal peptidergic (substance P and somatostatin) fibers in the stria terminalis of the rat. Brain Res. 221: 231-242.

Saper, C.B. (1978) Anatomical substrates for the hypothalamic control of the autonomic nervous system. In: Integrative Functions of the Autonomic Nervous System, C.McC. Brooks, K. Koizumi, and A. Sato, eds. Amsterdam: Elsevier/North-Holland Biomedical Press, pp.333-341.

Saper, C.B. (1982) Reciprocal parabrachial-cortical connections in the rat. Brain Res. 242: 33-40.

Saper, C.B., and D. Levisohn (1983) Afferent connections of the median preoptic nucleus in the rat: anatomical evidence for a cardiovascular integrative mechanism in the anteroventral third ventricular (AV3V) region. Brain Res. 288: 21-31.

Saper, C.B., and A.D. Loewy (1980) Efferent connections of the parabrachial nucleus in the rat. Brain Res. 197: 291-317.

Saper, C.B., L.W. Swanson, and W.M. Cowan (1976) The efferent connections of the ventromedial nucleus of the hypothalamus of the rat. J. Comp. Neurol. 169: 409-422.

Saper, C.B., L.W. Swanson, and W.M. Cowan (1979) An autoradiographic study of the efferent connections of the lateral hypothalamic area in the rat. J. Comp. Neurol. 183: 689-706.

Saper, C.B., D.G. Standaert, M.G. Currie, D. Schwartz, D.M. Geller, and P. Needleman (1985) Atriopeptin-immunoreactive neurons in the brain: presence in cardiovascular regulatory areas. Science 227: 1047-1049.

Satoh, K., N. Shimizu, M. Tohyama, and T. Maeda (1978) Localization of the micturition reflex center at dorsolateral pontine tegmentum of the rat. Neurosci. Lett. 8: 27-33.

Sawchenko, P.E., and L.W. Swanson (1981) A method for tracing biochemically defined pathways in the central nervous system using combined fluorescence retrograde ransport and immunohistochemical techniques. Brain Res. 210: 31-51.

Sawchenko, P.E., and L.W. Swanson (1982) Immunohistochemical identification of neurons in the paraventricular nucleus of the hypothalamus that project to the medulla or to the spinal cord in the rat. J. Comp. Neurol. 205: 260-272.

Schreiner, L., and A. Kling (1953) Behavioral changes following rhinencephalic injury in cat. J. Neurophysiol. 16: 643-659.

Schwaber, J.S., B.S. Kapp, G.A. Higgins, and P.R. Rapp (1982) Amygdaloid and basal forebrain direct connections with the nucleus of the solitary tract and the dorsal motor nucleus. J. Neurosci. 2: 1424-1438.

Schwartzbaum, J.S. (1983) Electrophysiology of taste-mediated functions in parabrachial nuclei of behaving rabbit. Brain Res. Bull. 11: 61-89.

Shapiro, R.E., and R.R. Miselis (1985) The central neural connections of the area postrema of the rat. J. Comp. Neurol. 234: 344-364.

Shimada, S., S. Shiosaka, P.C. Emson, C.J. Hillyard, S. Girgis, I. MacIntyre, and M. Tohyama (1985) Calcitonin gene-related peptidergic projection from the parabrachial area to the forebrain and diencephalon in the rat: an immunohistochemical analysis. Neurosci. 16: 607-616.

Shipley, M.T., and M.S. Sanders (1982) Special senses are really special: evidence for a reciprocal, bilateral pathway between insular cortex and nucleus parabrachialis. Brain Res. Bull. 8: 493-501.

Shiosaka, S., Y. Kawai, T. Shibasaki, and M. Tohyama (1985) The descending alpha-MSHergic (alpha-melanocyte-stimulating hormone-ergic) projections from the zona incerta and lateral hypothalamic area to the inferior colliculus and spinal cord in the rat. Brain Res. 338: 371-375.

Sieck, G.C., and R.M. Harper (1980a) Discharge of neurons in the parabrachial pons related to the cardiac cycle: changes during different sleep-waking states. Brain Res. 199: 385-399.

Sieck, G.C., and R.M. Harper (1980b) Pneumotaxic area neuronal discharge during sleep-waking states in the cat. Exper. Neurol. 67: 79-102.

Siggins, G.R., D. Gruol, J. Aldenhoff, and Q. Pittman (1985) Electrophysiological actions of corticotropin-releasing factor in the central nervous system. Fed. Proc. 44: 237-242.

Simantov, R., M.J. Kuhar, G.R. Uhl, and S.H. Snyder (1977) Opioid peptide enkephalin: immunohistochemical mapping in rat central nervous system. Proc. Natl. Acad. Sci. 74: 2167-2171.

Simerly, R.B., L.W. Swanson, and R.A. Gorski (1984) Demonstration of a sexual dimorphism in the distribution of serotonin-immunoreactive fibers in the medial preoptic nucleus of the rat. J. Comp. Neurol. 225: 151-166.

Simpson, J.B. (1981) The circumventricular organs and the central actions of angiotensin. Neuroendocrinol. 32: 248-256.

Skirboll, L., T. Hokfelt, G. Norell, O. Phillipson, H.G.J.M. Kuypers, M. Bentivoglio, C.E. Catsman-Berrevoets, T.J. Visser, H. Steinbusch, A.D. Verhofstad, A.C. Cuello, M. Goldstein, and M. Brownstein (1984) A method for specific transmitter identification of retrogradely labeled neurons: immunofluorescence combined with fluorescence tracing. Brain Res. Rev. 8: 99-127.

Skofitsch, G., and D.M. Jacobowitz (1985) Immunohistochemical mapping of galanin-like neurons in the rat central nervous system. Peptides 6: 509-546.

Smith, O.A., and J.L. DeVito (1984) Central integration for the control of autonomic responses associated with emotion. Ann. Rev. Neurosci. 7: 43-65.

Sofroniew, M.V. (1979) Immunoreactive beta-endorphin and ACTH in the same neurons of the hypothalamic arcuate nucleus in the rat. Am. J. Anat. 154: 283-289.

Sofroniew, M.V. (1985) Vasopressin, oxytocin and their related neurophysins. In: Handbook of Chemical Neuroanatomy, Vol. 4, GABA and Neuropeptides in the CNS, Part 1, A. Bjorklund, T. Hokfelt, eds. Amsterdam: Elsevier, pp. 93-165.

Standaert, D.G., S.J. Watson, R.A. Houghten, and C.B. Saper (1986b) Opioid peptide immunoreactivity in spinal and trigeminal dorsal horn neurons projecting to the parabrachial nucleus in the rat. J. Neurosci. 6: 1220-1226.

Standaert, D.G., P. Needleman, and C.B. Saper (1986) Organization of atriopeptin-like immunoreactive neurons in the central nervous of the rat. J. Comp. Neurol. 253: 315-341.

Stern, J.J., C.A. Cudillo, and J. Kruper (1976) Ventromedial hypothalamus and short-term feeding suppression in male rats. J. Comp. Physiol. Psychol. 90: 484-490.

Stuesse, S.L., and S.E. Fish (1984) Projections to the cardioinhibitory region of the nucleus ambiguus of rat. J. Comp. Neurol. 229: 271-278.

Sutton, R.E., G.F. Koob, M. LeMoal, J. Rivier, and W. Vale (1982) Corticotropin releasing factor produces behavioral activation in rats. Nature 297: 331-333.

Sved, A.F. (1986) Pontine pressor sites which release vasopressin. Brain Res. 369: 143-150.

Swanson, L.W. (1976) An autoradiographic study of the efferent connections of the preoptic region in the rat. J. Comp. Neurol. 167: 227-256.

Swanson, L.W. (1977) Immunohistochemical evidence for a neurophysin-containing autonomic pathway arising in the paraventricular nucleus of the hypothalamus. Brain Res. 128: 346-353.

Swanson, L.W., and H.G.J.M. Kuypers (1980) A direct projection from the ventromedial nucleus and retrochiasmatic area of the hypothalamus to the medulla and spinal cord of the rat.

Swanson, L.W., and W.M. Cowan (1979) The connections of the septal region in the rat. J. Comp. Neurol. 186: 621-656.

Swanson, L.W., and L.G. Sharpe (1973) Centrally induced drinking: comparison of angiotensin II- and carbachol-sensitive sites in rats. Amer. J. Physiol. 225: 566-573.

Swanson, L.W., P.E. Sawchenko, J. Rivier, and W.W. Vale (1983) Organization of ovine corticotropin-releasing factor immunoreactive cells and fibers in the rat brain: an immunohistochemical study. Neuroendocrinol. 36: 165-186.

Swanson, L.W., G.J. Mogenson, R.B. Simerly, and M. Wu (1987) Anatomical and electrophysiological evidence for a projection from the medial preoptic area to the 'mesencephalic and subthalamic locomotor regions' in the rat. Brain Res. 405: 108-122.

Takeuchi, Y., and D.A. Hopkins (1984) Light and electron microscopic demonstration of hypothalamic projections to the parabrachial nuclei in the cat. Neurosci. Lett. 46: 53-58.

Takeuchi, Y., M. Uemura, K. Matsuda, R. Matsushima, and N. Mizuno (1980) Parabrachial nucleus neurons projecting to the lower brain stem and the spinal cord. A study in the cat by the Fink-Heimer and the horseradish peroxidase methods. Exper. Neurol. 70: 403-413.

Takeuchi, Y., J.H. McLean, and D.A. Hopkins (1982) Reciprocal connections between the amygdala and parabrachial nuclei: ultrastructural demonstration by degeneration and axonal transport of horseradish peroxidase in the cat. Brain Res. 239: 583-588.

Travers, J.B., and R. Norgren (1983) Afferent projections to the oral motor nuclei in the rat. J. Comp. Neurol. 220: 280-298.

Turner, B.H. (1981) The cortical sequence and terminal distribution of sensory related afferents to the amygdaloid complex of the rat and monkey. In Y. Ben-Ari (Ed.): The Amygdaloid Complex. Amsterdam: Elsevier/North Holland Biomedical Press, pp. 51-62.

Uhl, G.R., and S.H. Snyder (1981) Neurotensin. In: Martin, J.B., S. Reichlin, and K.L. Bick (eds.): Neurosecretion and Brain Peptides. New York: Raven Press, pp. 87-106.

Uhl, G.R., R.R. Goodman, M.J. Kuhar, and S.H. Snyder (1978) Enkephalin and neurotensin: immunocytochemical localization and identification of an amygdalofugal pathway. In Costa, E., and M. Trabuchi (eds): Advances in Biochemical Psychopharmacology, vol. 18, New York: Raven Press, pp. 71-87.

Van der Kooy, D. (1979) An analysis of the behavior elicited by stimulation of the dorsal pons in rat. Physiol. Behav. 23: 427-432.

Van der Kooy, D., L.Y. Koda, J.F. McGinty, C.R. Gerfen, and F.E. Bloom (1984) The organization of projections from the cortex, amygdala, and hypothalamus to the nucleus of the solitary tract in rat.

Veening, J.G., L.W. Swanson, and P.E. Sawchenko (1984) The organization of projections from the central nucleus of the amygdala to brainstem sites involved in central autonomic regulation: a combined retrograde transport-immunohistochemical study. Brain Res. 303: 337-357.

Veening, J.G., S. Te Lie, P. Posthuma, L.M.G. Geeraedts, and R. Nieuwenhuys (1987) A topographical analysis of the origin of some efferent projections from the lateral hypothalamic area in the rat. Neurosci. 22: 537-551.

Wang, S.C., and S.W. Ranson (1939) Autonomic responses to electrical stimulation of the lower brain stem. J. Comp. Neurol. 71: 437-455.

Ward, D.G., W.E. Grizzle, and D.S. Gann (1976) Inhibitory and facilitatory areas of the rostral pons mediating ACTH release in the cat. Endocrinol. 99: 1220-1228.

Watson, S.J., and H. Akil (1980) alpha-MSH in rat brain: occurrence within and outside brain beta-endorphin neurons. Brain Res. 182: 217-223.

Watson, S.J., C.W. Richard, J.D. Barchas (1978a) Adrenocorticotropin in rat brain: immunocytochemical localization in the cells and axons. Science 200: 1180-1182.

Watson, S.J., H. Akil, C.W. Richard, and J.D. Barchas (1978b) Evidence for two separate opiate peptide neuronal systems and the coexistence of beta-lipotropin, beta-endorphin and ACTH immunoreactivities in the same hypothalamic neurons. Nature 275: 226-228.

Watson, S.J., H. Akil, A. Fischli, A. Goldstein, E. Zimmerman, G. Nilaver, T.B. van Wimersma Greidanus (1982) Dynorphin and vasopressin: common localization in magnocellular neurons. Science 216: 85-87.

Weiss, G.F., and S.F. Leibowitz (1985) Efferent projections from the paraventricular nucleus mediating alpha$_2$-noradrenergic feeding. Brain Res. 347: 225-238.

Weller, K.L., and D.A. Smith (1982) Afferent connections to the bed nucleus of the stria terminalis. Brain Res. 232: 255-270.

Williams, R.G., and G.J. Dockray (1983) Distribution of enkephalin-related peptides in rat brain: immunohistochemical studies using antisera to met-enkephalin and met-enkephalin-Arg^6-Phe^7. Neurosci. 9: 563-586.

Woodhams, P.L., G.W. Roberts, J.M. Polak, and T.J. Crow (1983) Distribution of neuropeptides in the limbic system of the rat: the bed nucleus of the stria terminalis, septum and preoptic area. Neurosci. 8: 677-703.

Woods, S.C., G.J. Taborsky, Jr., and D. Porte, Jr. (1986) Central nervous system control of nutrient homeostasis. In V.B. Mountcastle, F.E. Bloom, and S.R. Geiger (eds.): Handbook of Physiology, Section 1, The Nervous System, Vol. IV, Intrinsic Regulatory Systems of the Brain. Baltimore: Waverly Press, Inc., pp. 365-412.

Wray, S., and G.W. Hoffman (1983) Organization and interrelationship of neuropeptides in the central amygdaloid nucleus of the rat. Peptides 4: 525-541.

Yardley, C.P., and S.M. Hilton (1986) The hypothalamic and brainstem areas from which the cardiovascular and behavioral components of the defense reaction are elicited in the rat. J. Auton. Nerv. Sys. 15: 227-244.

Yasui, Y., K. Itoh, M. Takada, A. Mitani, T. Kaneko, and N. Mizuno (1985) Direct cortical projections to the parabrachial nucleus in the cat. J. Comp. Neurol. 234: 77-86.

Zaborszky, L., M.C. Beinfeld, M. Palkovits, and L. Heimer (1984) Brainstem projection to the hypothalamic ventromedial nucleus in the rat: a CCK-containing long ascending pathway. Brain Res. 303: 225-231.

Zarbin, M.A., R.B. Innis, J.K. Wamsley, S.H. Snyder, and M.J. Kuhar (1983) Autoradiographic localization of cholecystokinin receptors in rodent brain. J. Neurosci. 3: 877-906.

Zardetto-Smith, A.M., and T.S. Gray (1986) Peptidergic efferents from the parabrachial nucleus to the central nucleus of the amygdala in the rat. Soc. Neurosci. Abstr. 289.7.

Zardetto-Smith, A.M., M. Moga, D. Magnuson, S.J. Watson, and T.S. Gray (1985) Dynorphin cells in the lateral hypothalamus innervate the amygdala, central gray, parabrachial nucleus and dorsal vagal complex. Soc. Neurosci. Abstr. 336.6.

Zeman, W., and J.R.M. Innes (1963) Craigie's Neuroanatomy of the Rat. pp.69-70. New York: Academic Press.

Zerihun, L., and M. Harris (1983) An electrophysiological analysis of caudally-projecting neurones from the hypothalamic paraventricular nucleus in the rat. Brain Res. 261: 13-20.

APPROVAL SHEET

The dissertation submitted by Margaret M. Moga has been read and approved by the following committee:

Dr. Thackery S. Gray, Director
Associate Professor, Anatomy, Loyola University

Dr. Edward J. Neafsey
Associate Professor, Anatomy, Loyola University

Dr. Anthony J. Castro
Professor, Anatomy, Loyola University

Dr. Robert D. Wurster
Professor, Physiology, Loyola University

Dr. Clifford B. Saper
Associate Professor, Pharmacological and
Physiological Sciences and Neurology,
University of Chicago

The final copies have been examined by the director of the dissertation and the signature which appears below verifies the fact that any necessary changes have been incorporated and that the dissertation is now given final approval by the Committee with reference to content and form.

The dissertation is therefore accepted in partial fulfillment of the requirements for the degree of Doctor of Philosophy.

4-19-88
Date

Director's Signature